THESIS

ESTABLISHMENT AND SYSTEMATIC CHARACTERIZATION OF *MYCOBACTERIUM TUBERCULOSIS* IN BIOREACTORS

Submitted by

Phillip Knabenbauer

Department of Microbiology, Immunology and Pathology

In partial fulfillment of the requirements

For the Degree of Master of Science

Colorado State University

Fort Collins, Colorado

Fall 2016

Master's Committee:

Advisor: Karen Dobos

Richard Slayden
Michael McNeil
Christie Peebles

ABSTRACT

ESTABLISHMENT AND SYSTEMATIC CHARACTERIZATION OF *MYCOBACTERIUM TUBERCULOSIS* IN BIOREACTORS

Mycobacterium tuberculosis infection is characterized by active and latent disease states. Granuloma-induced oxygen tension may shift bacteria into bacteriostatic persistence. Current models of hypoxia-induced mycobacteria have limitations, requiring establishment of novel culturing methods. Here, *M. tuberculosis* was propagated under defined oxygen concentration in bioreactors. Initial analyses confirmed mycobacterial non-replicating persistence. This study will provide insight into core physiological adaptations of *M. tuberculosis* while reducing bias from the contaminants during adaptation into dormancy. Here we describe a novel method of propagation using defined oxygen concentrations, then enrich the final culture for viability to remove transcriptional bias, and finally interrogate the presence of viable but non-culturable tubercle bacilli in order to obtain a greater sense of true viability. The current study will further contribute to our understanding of the physical adaptation of *Mtb* during growth and dormancy, by removing bias from the contaminating transcriptome gradient generated by the temporal adaptation of *M. tuberculosis* into dormancy. This will enhance the accuracy of downstream structural and transcriptomic analyses as well as give rise to a novel high throughput approach to *M. tuberculosis* propagation for research materials.

ACKNOWLEDGEMENTS

My upmost gratitude goes to my mentor Dr. Karen Dobos. I have been imprinted with her dedication to quality science and innovation that will have a lasting effect. Without her enthusiasm and drive for excellence, the work presented here would not have been possible. Her drive and encouragement has enabled me to push myself and thrive not only academically, but professionally as well. I am forever fortunate for the opportunities given to me by Dr. Dobos and CSU. I would also like to thank the personnel of the Dobos and Izzo laboratories, giving special thanks to Dr. Carolina Mehaffy, Dr. Linda Izzo and Anne Simpson for their substantial support and guidance.

I would also like to give my final acknowledgements to the American Type Culture Collection for the valuable funding needed to conduct this body of work. ATCC funding #2010-0516-0005.

TABLE OF CONTENTS

ABSTRACT ii
ACKNOWLEDGEMENTS iii
1.0 Ch.1 Introduction; literature review 1
1.1 Background 1
1.2 Pathogenesis 4
1.3 Latency 6
1.4 Models of Hypoxia 9
1.4.1 The Wayne model of hypoxia. 9
1.4.2 The modified Wayne model of hypoxia 10
1.4.3 A multiple-stress model of hypoxia. 11
2.0 Ch.2 Aim 1 Establishment of *M. tuberculosis* propagation in bioreactors 14
2.1 Introduction 14
2.2 Materials and Methods 16
2.2.1 Inoculation and system parameters 16
2.2.2 Preparation of cellular material 17
2.2.3 Analysis 18
2.2.4 Lipid extraction method 19
2.3 Results 20
2.3.1 Establishment of the propagation system 20
2.3.2 Establishment of Normoxic system 20
2.3.3 Establishment of Hypoxic system 22
2.3.4 Abundance of Acr as a marker of hypoxia 24
2.3.5 Total lipid analysis 26
2.4 Discussion 27
3.0 Ch.3 Aim 2 Viability enrichment 31
3.1 Introduction 31
3.2 Materials and Methods 32
3.2.1 Establishment of separation conditions 32
3.2.2 Discontinuous density gradient centrifugation of the test cultures 32
3.2.3 Discontinuous density gradient centrifugation of normoxic and hypoxic paired cultures. 34
3.3 Results 34
3.3.1 Viability of the viable-enriched separation test culture 34
3.3.2 Viability of viable-enriched normoxic and hypoxic paired cultures 37
3.4 Discussion 39
4.0 Ch.4 Aim 3 Viability assessment and Viable but Non-Culturable cells 44
4.1 Introduction 44

4.2 Materials and methods 45
4.2.1 Generation of standard curve control 45
4.2.2 Preparation of standard curve Alamar Blue assay 46
4.2.3 Preparation of Alamar Blue assay of bioreactor paired cultures 46
4.3 Results 46
4.3.1 Standard rate of respiration 46
4.3.2 Relationship between standard rate of respiration and expected CFUs 48
4.3.3 Respiration rate of bioreactor pairs enriched for viability 49
4.3.4 Estimation of VBNC population 50
4.4 Discussion 52
5.0 Ch. 5 Discussion 55
6.0 References 61
7.0 Appendix I 69
7.1 Continuous density gradient centrifugation of normoxic and hypoxic cultures 69
7.2 Volatile organic compound analysis 72
8.0 Supplemental Material 81

1.0 Ch.1 Introduction; literature review

1.1 Background

1.2 Pathogenesis

1.3 Latency

1.4 Hypoxia

1.1 Background

Mycobacterium tuberculosis is the causative agent of tuberculosis (TB) and currently the leading cause of death by an infectious agent worldwide, overtaking the human immunodeficiency virus (HIV) in 2014. It is estimated that two to three billion individuals are infected with *M. tuberculosis (Mtb)* and according to the World Health Organization, 2014 was reported to have 9.6 million new cases of tuberculosis and 1.5 million deaths [1] (Figure 1.1).

Even though tuberculosis is treatable, with the current diagnostic procedures and drugs available, it still requires a degree of infrastructure to maintain a dent in the number of cases per global region. The global burden of *Mtb* is contributed to poor diagnostic procedures and treatment, especially in developing countries. A review of the compliance to anti-tuberculosis treatment was conducted to identify risk factors associated with treatment default in sub-Saharan Africa. The study was done by meta-analysis of Medline articles and found that distance from the hospital and use of public transportation were major contributors to non-compliance. Regional infrastructure is key to the treatment regimen of *Mtb* and most developing countries are lacking in sufficient health care to provide the support and knowledge of TB treatment. Another major risk factor identified was the lack of family support. Often those of the highest risk of TB infections are of the poorest economic status where family homes are overcrowded with poor ventilation, poor hygiene and malnutrition [2]. HIV and acquired immunodeficiency syndrome (AIDS) also contributes to a higher incidence of TB cases in low-income countries. Tuberculosis is one of the deadliest opportunistic infections that a person with HIV or AIDS can acquire due to the individuals compromised immune system. Without proper treatment, almost half of HIV-negative individuals will die on average and nearly all HIV-positive individuals will die of TB. People who are infected with HIV are twenty to thirty times more likely to develop active TB and continue the spread of the disease [3]. With this, it is understood

that our current methods of attrition toward the disease is simply not sufficient enough. The cost of TB treatment and diagnostics needs to become more economical for lower income countries to be able to hold their own against

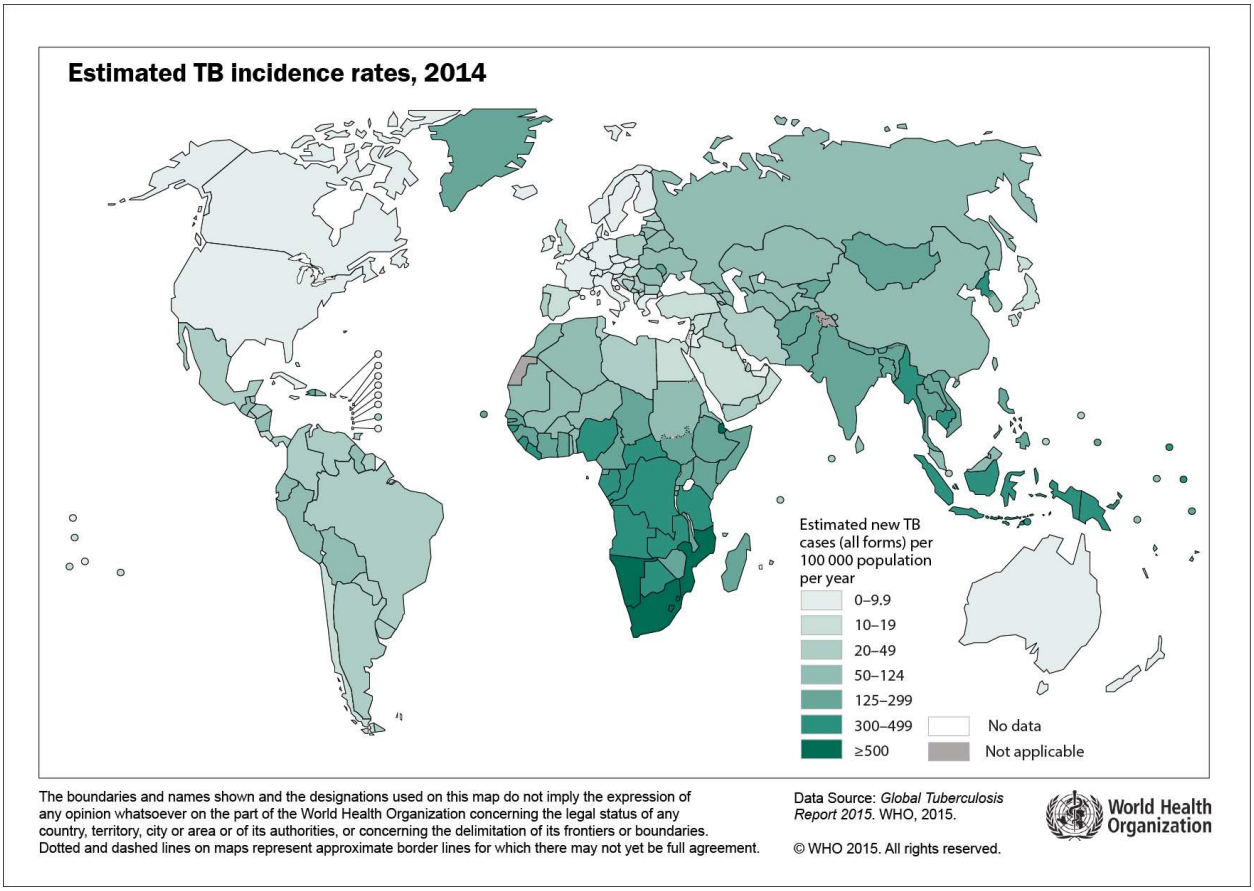

Figure 1.1

The World Health Organization estimates the global burden tuberculosis infection. Endemic regions include much of Africa, with southern Africa having the greatest prevalence, and southeast Asia, eastern Europe, and Russia. Adapted from WHO World TB Report (2015). (CC BY)

the disease. In order to develop new and improved, cost effective methods to battle the global burden of TB and rid our population of its prevalence, novel methods must be interrogated to develop more accurate research materials for the use of treatment and diagnostic research.

The current drug regiment to treat active tuberculosis infection is costly and quite toxic and unbearable to the individual, the drugs alone can have very severe side effects as well as requiring administration over a period of six months or more. The recommended treatment of active *Mtb* infection involves administering daily doses of three or four of the first-line anti TB drugs Isoniazid, Rifampin, Pyrazinamide, Ethambutol or Streptomycin during

the first two months. This is then followed by Isoniazid and Rifampin for an additional four to seven months. A study conducted in 2005 focused on the side effects of the most commonly used first-line anti-TB drugs. The most common side effect was shown to be liver damage, however others ranged from rashes, flu-like symptoms, abscesses, fever, loss of vision and even peripheral nerve damage [4]. Treatment for latent TB infection (LTBI) is typically done by a twelve-month regiment of Isoniazid or four months of Rifampicin (or rifabutin if used with protease inhibitors for HIV coinfections). This treatment for LTBI has shown to give 30 to 100% protection against the development of active TB [5]. The communal lack of infrastructure and aberrant toxicity of drug treatment induces difficulties in promoting adherence to tuberculosis treatment in its own right due to socioeconomics and health education in developing countries. These obstacles in local infrastructure as noted previously can lead to incomplete treatment duration and also creates challenges of TB surveillance in regions where health care is poor and under developed [6]. This lack of treatment or treatment default is contributing to induce the continued prevalence of multiple and extensively drug resistant phenotypes of *Mtb*.

As stated before, billions of individuals are estimated to be infected with *Mtb*, leading to millions succumbing to the disease every year while the current Bacillus Calmette-Guerin (BCG) vaccines are hardly efficient enough to curb its prevalence. BCG vaccines are live vaccines derived from attenuated *Mycobacterium bovis* with the ability to induce an immune response to tuberculin and is the most widely used vaccine in the world. The BCG vaccine is given at birth and does have its benefits, about 86% protection to early childhood tuberculosis infections such as tuberculous meningitis and military TB. However, it has an extremely broad range of efficacy, from 0 to 80%, that wanes into early adulthood for the protection against pulmonary TB [7]. Wide spread use of the BCG vaccine also has its limitations against diagnosis of the disease. The Purified protein derivative (PPD) skin test is an inexpensive way to test if an individual has an acquired immune response against *Mtb*, suggesting that the individual has come in contact with the pathogen. A small amount of PPD, generated from heat killed *Mtb* and filtered for sterility, is injected into the intradermal layer of the skin. After two to three days the injection site is observed for induration and redness from a type 4 hypersensitivity immune reaction to the PPD, indicating exposure. However, the PPD test is very non-specific and can give a false-positive to other *mycobacterium* species including BCG. Thus the QuantiFERON-TB (QFT) Gold was developed more recently in respect to PPD which was the standard diagnostic method along with chest x-ray since the 1940's. QFT is based on

interferon-γ *ex-vivo* assays involving gene products in the *Mtb* genome that are absent in BCG and most environmental mycobacteria. QFT is far more specific than PPD, especially in diagnosis of LTBI in immunocompromised patients, however the assay requires a higher degree of health care infrastructure to perform properly and thus not as cost effective in low-income developing countries [8]. What is truly desired is novel diagnostic methods to not only distinguish between active and latent disease, but be cost effective and require little to no specialized infrastructure and training.

1.2 Pathogenesis

Tuberculosis is characterized by an active and an asymptomatic latent disease state. Not every individual that comes in contact with the bacilli will show signs of disease. At the center of the immunopathogenesis of TB is the granuloma. Granulomas are lesions of blood derived infected and uninfected macrophages, foamy macrophages, epithelioid cells, and multinucleated giant cells (Langerhans cells), B and T lymphocytes, and fibroblasts, all well-organized in a dynamic structure, as an effort to control the *Mtb* invasion (Figure 1.2) [9].

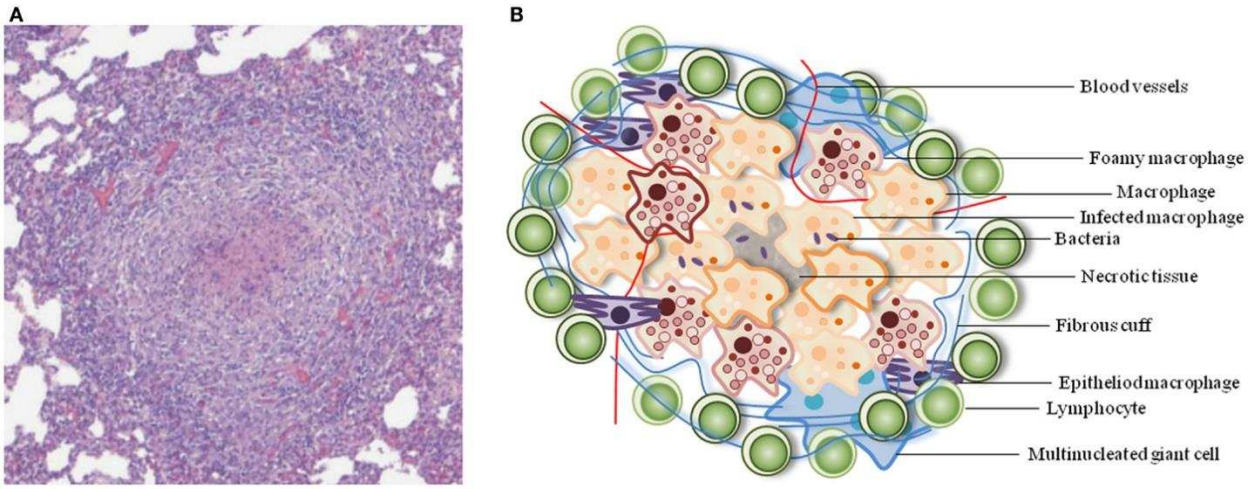

Figure 1.2

Typical architecture of a TB granuloma. (A) Representative granuloma with central necrosis from minipig lung tissue. Histological samples were formalin-fixed, cut, and stained with hematoxylin-eosin. Adapted from Gil et al. (2010). (B) Schematic of the cellular constituents of a TB granuloma. Adapted from Guirado *et al.* Frontiers in Immunology (2013) vol. 4, article 98. [5] (CC BY)

Upon initial exposure to the pathogen through respiratory droplets, the bacilli are engulfed by alveolar macrophages which initiates a pro and anti-inflammatory response. The production of cytokines leads to the

recruitment of additional mononuclear leukocytes to the site of infection within the lung and this accumulation of immune cells leads to the formation of the macrophage-rich granuloma. The inability of the immune response to control the proliferation of the bacilli furthers lesion progression, causing the center to become caseous and with time evolve to necrotic tissue as the granuloma breaks down. Active virulent *Mtb* is released into the airway of the lungs and may then go to infect other individuals [9].

In humans, TB infected lungs generally show a heterogeneity of lung lesions, often with necrosis in the center and surrounded by peripheral fibrosis [10]. To better understand tuberculosis lesion pathogenesis, animal models are essential. Little is still known on the complicated *in vivo* conditions of the bacteria in human lung lesions and *Mtb* has been described to exist as multiple populations in *in vitro* and *in vivo* conditions within relatively single microenvironments [11]. We must rely on animal or novel propagation models to elucidate critical information on the mechanisms of the pathogen [12]. Hoff *et al.* (2011) provided a comprehensive microscopic and histopathologic analysis of the disease progression of the mouse and guinea pig models and focused on the location of the bacilli within the lungs and primary granulomas. They were able to show that *Mtb* exist both intra and extracellularly by fluorescent staining methods. Their work described that with aerosol infected guinea pigs, during the first few weeks of infection, the bacilli stayed roughly equally intra and extracellularly, evenly dispersed throughout the primary lesion. However, after a month, they were seen to be predominantly extracellular within the core of the necrotic granulomatous lesions. Using immunofluorescence of tubulin, the lack of fluorescence in the necrotic region indicates loss of the host cell and thus the bacilli remain in a persistent extracellular state. Using GKO immunocompromised mice, Hoff and colleagues (2011) described similar results to the guinea pig model. Again the bacilli stayed mostly intracellular in epithelioid macrophages until late stage of infection where the lesions became necrotic and the bacilli progress to an extracellular state within the core of the necrotic region [13]. This progression of the granuloma to a necrotic lesion with calcification and fibrosis in the guinea pig model has been described to be consistent with what has been indicated in the human lung disease, which gives strong evidence that the progression of *Mtb* from an intracellular state to an extracellular state is most likely consistent as well [14].

To determine the regions of hypoxia, which is an environment of extreme oxygen tension, in the infected guinea pig lungs, the animals were treated intraperitoneally with the hypoxia marker pimonidizole, 2-

nitroimidazole shortly before sacrifice. This hypoxic marker forms covalent bonds when subjected to a hypoxic environment. Cells in regions of hypoxia stained with pimonidizole will develop with a light brown color. Staining for hypoxic regions was seen beginning one-month post infection, in the periphery of the necrotic center of the primary granuloma [15]. This study gave strong evidence that the core of the evolved granuloma, around the necrotic center, is an environment high in oxygen tension. This also gives evidence the very center region is also hypoxic even though staining was only observed in the periphery, thus where the lesion is hypocellular with central necrosis and in the early stages of dystrophic mineralization.

Animal models have been routinely employed to study the micro-environment the bacilli are exposed to during infection. *In vivo* models to study the physiology of *Mtb*, especially in relations to active infection and LTBI, can be very tedious. Animal models are very expensive and carry a high level of regulation in order to promote even a small study. Also, retrieving the bacilli from animal tissue results in low yields as much processing is required with heavy solvents [16]. Thus, it is beneficial to explore novel *in vitro* culture methods to attempt to mimic these *in vivo* environments for the study of *Mtb* and LTBI.

1.3 Latency

Mtb latency is the ability of the pathogen to enter into a dormant state where is can survive asymptomatic in the host and reactivate at a later time due to immunological pressures. Upon infection, the innate immune response may or may not be able to eliminate the *Mtb* bacteria. The adaptive immune response will activate with the recruitment of macrophages, and again may or may not be able to clear the bacteria. During the host immune response, the tuberculosis bacilli are phagocytized by host macrophages where an attempt is made to subject them to degradation within the macrophages lysosome. *Mtb* is able to prevent lysosome/phagosome fusion and can escape to the cytosol of the macrophage where it can survive. The granulomas restrict access to oxygen and nutrients while exposing the bacilli to acidic pH and reactive nitric oxide species in order to eliminate the pathogen. The enzyme isocitrate lyase (Icl) has been shown to be highly upregulated in macrophage models and is a key enzyme in the glyoxylate shunt pathway and utilizes fatty acids as an energy source. The expression of *acr* (Rv2031), which encodes the small heat shock protein α-crystallin (Acr, also known as hspX), is also dramatically increased during hypoxia. Acr is essential for growth of the pathogen in macrophages and localizes to

the inner surface of the inner membrane and has chaperone activity to assist in the re-folding of damaged proteins due to environmental stress. A large transcriptional adaptation takes place as the Dormancy Survival Regulon (DosR) is induced during phagocytosis as a result to oxygen tension, in which anaerobic respiration is upregulated and results in the activation of the stringent response. This response is mediated by RelA and down regulates components necessary in protein translation and conserves the needed resources for survival in the harsh environment. The thick, waxy cell wall of *Mtb* increases in thickness as lipid metabolism is increased and assists as a physical barrier to the acidic stress and can also inhibit phagosomal maturation and phagosome/lysosome fusion, further resisting toxic protons. Other enzymes upregulated early in infection serve to detoxify oxidative damage from nitric oxide radicals such as superoxide dismutase (SOD) and KatG which both serve as catalases to rectify the free radicals. *Mtb* also possesses 88 toxin-antitoxin systems, where four of them have been shown to be activated by phagocytosis or low oxygen availability. Some of these systems seem to provide a mechanism that allows the bacilli to alter its growth rate in response to an environmental stress. When the toxin is released from an unstable anti-toxin interaction, it may function to cleave mRNA and thus inhibit translation, halting the growth of the bacterium. *Mtb* bacilli can then enter into a bacteriostatic state and persist within the granuloma and reactivate at a future time, allowing for continued persistence of the reservoir of latency [17].

One of the most accepted *in vivo* models of latent TB infection was developed in the 1950s and 1960s at Cornell University by Dr. Walsh McDermott and colleagues. What is now referred to as the Cornell Model of dormancy, outbred mice were infected with *Mtb* H_{37}Rv and immediately treated with antimicrobial drugs for 12 weeks. For about six weeks after the drugs were ceased, Mccune (1966) termed this period a sterile state as no cultivable bacilli were found. About 12 weeks after the drug treatments were ceased, one third of the mice developed active TB. Their work showed that homogenates of mouse tissue were ‘sterile’ by bacteriological culture techniques of the time, however by microscopy they determined that there was up to 4 logs of acid-fast bacilli per milliliter of tissue homogenate [18]. In these early times of *Mtb* research, the phenomenon of viable but non-culturable (VBNC) cells was hypothesized but really not well understood. Accurate culture methods to model LTBI did not exist *in vitro*, thus relying on *in vivo* studies. In order to further our understanding of the alternate physiological states of *Mtb* during infection, adequate materials and reagents are required for modern high throughput methods of investigation. Producing adequate amounts *in vivo* has thus far been limiting.

The latent disease of *Mtb* has long been associated to *Mtb* in a dormant state. Kell *et al.* (1998) defined cellular dormancy in their review as a reversible state of low metabolic activity, where the dormant cells are not capable of forming colonies on solid media but are not considered dead because they can regain colony forming units after appropriate resuscitation [19]. Early reports of total cell counts determined microscopically of *Mtb* extracted from human monocyte derived macrophages, when compared to colony forming units (CFU) showed evidence that a large proportion (70 to 90%) of the bacilli were unable to form colonies [20]. Biketov *et al.* (2000) sought to investigate this further and found that from over a dozen experimental replicates of macrophage derived *Mtb* contained a relatively uniform total cell number of 10^6 organisms per milliliter. However, the CFUs ranged greatly from 0 to 10^4 CFUs/ml. More extensive microscopy was employed and they described that successive passages of the bacilli *in vivo* started with a normal rod shaped morphology, but began to convert to an ovoid form of short rods, and even to a smaller coccoid morphology during the later passages. These findings indicate that during infection, a large population of the bacteria are converted to a dormant state due to the *in vivo* environmental stress and lose the ability to grow on traditional mycobacteria solid media, however Biketov and colleagues (2000) were also able to recover the dormant phenotype with the addition of a proteinaceous growth factor Rpf in liquid media to a viable replicating state [21]. With this, cells in a dormant state can be termed viable but non-culturable (VBNC) in a sense that they still carry out basal levels of metabolic activity but are unable to grow and be quantitated by direct methods such as plating for CFUs, thus giving an under estimated enumeration of bacterial load [22]. Furthermore, attempts were made to quantitate this phenomenon in a much more sensitive manner *in vivo*. In one study, quantitative PCR and dot blot hybridization was employed from tissue homogenates of BALB/C mice initially intravenously infected with $2.7x10^6$ CFU of *M. tuberculosis* $H_{37}Rv$. This study showed by quantitative PCR and culture methods that the homogenates resulted in approximately 10^7 organisms per organ, however rapidly declined after fourteen weeks to culture negative. During this period the quantitative PCR of the tissue homogenates resulted in about 5.5 logs of bacilli equivalents, even though no detectable CFUs were observed [23]. A major drawback to this method is, however, that this quantitative PCR method was unable to distinguish between dead bacilli, free *mycobacterium* DNA, or dormant viable bacilli. Even though early *in vitro* models, such as Wayne *et al.* (1977) discussed here later, were able to use sensitive molecular methods to

interrogate the presence of VBNC bacilli via ATP production. It is important to investigate the presence of a VBNC population *in vivo* to propagate our understanding to further treatment discoveries of LTBI.

1.4 Models of Hypoxia

Hypoxia is defined as a key host induced stress that limits the growth of the bacteria *in vivo* within the granuloma. Oxygen tension has been shown to be intimately associated with the outcome of *Mtb* infection and induce the adaptation of the bacilli to bacteriostatic persistence inside the granuloma. The shift into dormancy is no easy task for the bacterium, it requires a degree of fitness where only few bacteria are able to fully adapt into a non-replicating persistent state [24]. The adaptive shift has been shown to involve a huge genomic shift in the transcriptome that upregulates lipid generation and metabolism as energy stores are required for survival in a nutrient barren environment inside the granuloma and reflect discrete metabolic and drug-susceptibility states as compared to log phase growth. *Mtb* growth, metabolic activity, and transcriptional profile are acutely sensitive to varying levels of oxygen *in vitro* and *in vivo*. Alternative sigma factors SigB, SigE and SigF are upregulated, which promote broad changes in the transcriptome. The two-component transcriptional regulatory system, DosR/DosS, is one of the induced loci. DosR has been identified to form a DNA binding tetramer, phosphorylated to its active state by DosS and DosT. DosS binds to ferrous iron and senses the shift to ferric iron as a redox indicator within the cell, while DosT senses the oxygen tension by directly binding to heme bound oxygen [25].

1.4.1 The Wayne model of hypoxia.

The traditional model of hypoxia, the Wayne model, involves the growth of *Mtb* in a sealed, standing flask or tube where it relies on a self-generated oxygen gradient. The bacilli are allowed to naturally deplete the available oxygen in the media until the culture becomes progressively hypoxic. It was observed that the majority of the cells tended to settle to the bottom of the tube as growth ensued over time. When the sediment was extracted and plated for viable units, very few bacilli were observed. However, when the sediment was passaged through fresh oxygenated media, log phase growth was observed indicative of a much greater inoculum than what the original plated viable sediment demonstrated. These finding suggested that oxygen availability seemed to induce a shift of the *Mtb* tubercle to a dormant state, with no detectable active replication, but were able to resuscitate cellular division upon treatment with fresh media. [26]

1.4.2 The modified Wayne model of hypoxia

In later years, with the improvement of scientific techniques, Wayne *et al.* (1996) was able to improve on the model of hypoxia. Here, a sealed culture flask is used with light agitation. The addition of a port through a septum was used to lightly introduce oxygen to the head space of the flask in order to slowly reduce the oxygen concentration to hypoxic conditions. The depletion of dissolved oxygen (DO) in slowly stirred, 0.5-head space to culture ratio flasks of *Mtb* cultures, during growth and subsequent shift, was directly related to utilization and propagation of the bacilli. The oxygen concentration is expressed as a percent saturation of the medium with oxygen in terms of when inoculation was initiated. Visualizing this trend graphically would look much like two halves of a bell curve negatively correlated (Figure 1.3). At the start of propagation, DO concentration is very high

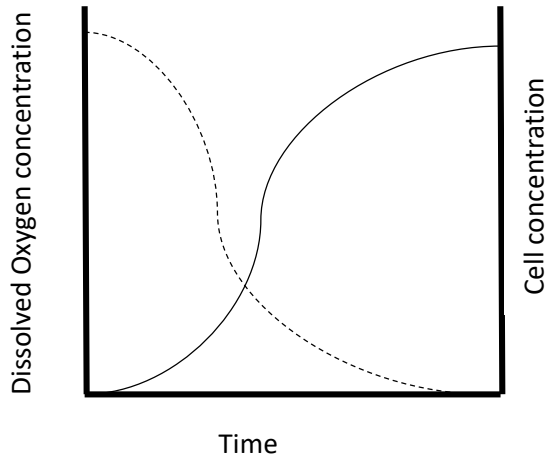

Figure 1.3

The relationship of cellular growth and oxygen utilization. *Mycobacterium tuberculosis* utilize the available oxygen via respiration. The cell density increases inversely to oxygen concentration within a culture environment, beginning with the lag phase and progressing through the log phase of exponential growth. As oxygen concentration is depleted to minimal levels the stationary growth phase progresses and persists as cell replication slows to a steady state.

while bacterial abundance is very low from initial inoculation. As the *Mtb* progress through the lag phase, the rate of oxygen utilization increases and DO is depleted at an exponential rate relative to the log phase of growing bacteria. When the DO concentration is depleted to hypoxic levels, the rate of utilization slows along with the rate of growth of the *Mtb* as they enter into the stationary phase. However, *Mtb* does not begin to show a distinct

trend of die off. Spectrophotometric absorbance of the turbidity of the culture in hypoxic conditions persists over time, and thus indicate a non-replicating persistent phenotype. At that point the bacteria undergo an adaptive shift into dormancy. Hypoxic conditions are described to be at a concentration of one percent or less dissolved oxygen concentration of the growth media. The first stage of non-replicating persistence (NRP1) was seen as the oxygen concentration of the media approached one percent. This microaerophilic state was characterized by a low increase in turbidity without the corresponding increase in viable units on solid media, while still maintaining a steady ATP concentration. When the oxygen concentration dropped below 0.06%, it was observed that an abrupt shift occurred to an anaerobic stage, termed NRP2, in which no further increase in turbidity was observed. It was also observed that during NRP2, the effect of antimicrobial agents on the bacilli was greatly hindered as the bacteria was able to regain log phase growth during periods of re-aeration. Wayne and colleagues (1996) concluded that turbidimetric measurements at an absorbance of 580nm, colony forming units, and ATP contents of cultures grown under hypoxia have shown that as the temporal shift further into hypoxia takes place, there is very little change in optical density of the culture. However, after approximately one hundred hours, well into oxygen tension, the number of CFUs and ATP utilization decreases contradictory to turbidity. Thus indicating a metabolically altered state of dormancy. Furthermore, they gave no evidence of active DNA replication but were readily able to undergo cell division during periods of re-aeration. Wayne *et al.* (1996) was able to show this using the uptake of radiolabel from [3H]uracil into total RNA and DNA during growth and shift of *M. tuberculosis* as well as synchronous replication of *Mtb* after dilution of non-replicating persistent cultures into fresh, oxygen-rich medium. [24]

1.4.3 A multiple-stress model of hypoxia.

The Wayne model of hypoxia paved the way for a new understanding of the complex mechanisms of *Mtb*. This led to further interrogation of hypoxic models to attempt to mimic *in vitro* the environment the pathogen may encounter *in vivo*. Deb and colleagues (2009) attempted a novel method to subject *Mtb* to multiple stresses in order to investigate the lipid stores used by the bacilli during dormancy. After growing *Mtb* on complete Dubos medium at aerobic conditions, the cells were transferred to a low-nutrient medium at acidic pH (pH 5.0) in an atmosphere of high CO_2 (10%) and low oxygen (5%) in a sealed roller bottle culture container. The roller bottles

were incubated in a roller bottle incubator apparatus for 18 days. They found that this method not only induced a state of bacteriostatic persistence, but the environment of multiple stressors led to the accumulation of high levels of triacyglycerol and wax esters as compared to the aerobic control cultures. With this, they sought to determine if the lipid accumulation would reflect changes in cellular buoyant density. A continuous density gradient was used with isotonic Percoll solution. The fractionated cell populations were separated at different density levels at different time periods during multiple stress treatment (Figure 1.4). With increasing time under hypoxia, the cells band and shift towards a higher buoyancy. Further treatment with Nile Red staining of the gradient fractions showed that the lighter fractions were more enriched in lipid-loaded cells [27]. Thus, this study indicates that during periods of multiple stress, including hypoxia, an increase in the cell wall lipids occurs causing the bacilli to become more buoyant.

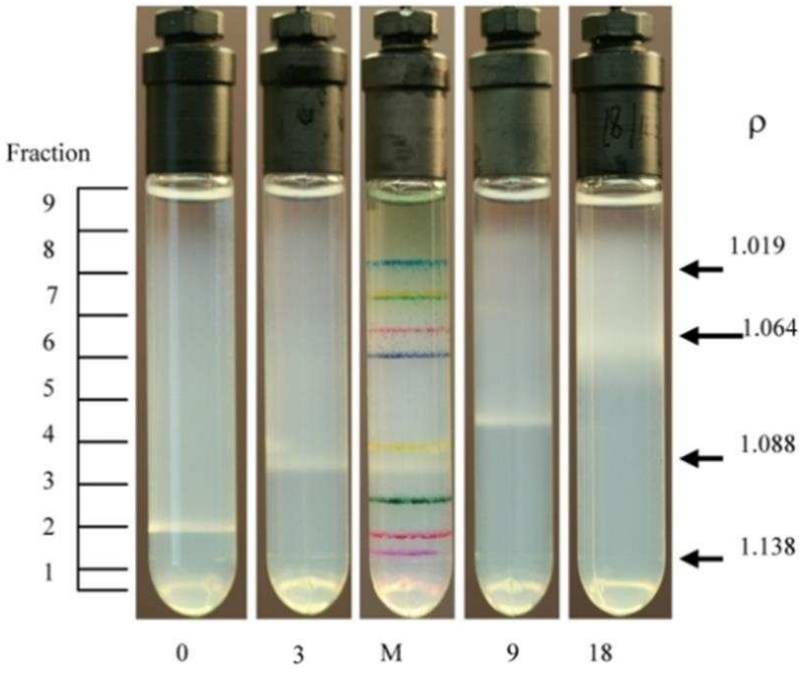

Figure 1.4

Decrease in density of *Mtb* cells subjected to multiple stress. The center tube is a three day cell sample mixed with density marker (M) beads. The densities of selected bead layers are given on the right, and the positions of 1ml fractions collected for analyses are at the left. Numbers below the tubes indicate the number of days under multiple stress. Adapted from Deb *et al.* PLos ONE (2009) vol. 4, issue 6 [27]. (CC BY)

In the last few decades, research to address novel drugs, drug toxicities, new vaccine candidates, etc. has led to new discoveries and understandings about mycobacterial physiology. However, culture techniques as well as

new *in vitro* models to help mimic our observations *in vivo* have not made the same progress. Methods of propagation of *Mtb* has remained relatively untouched. *Mtb* is a biosafety level 3 (BSL-3) organism due to its infectious nature. BSL-3 laboratories are incredibly expensive to build, maintain, and operate. These specialized laboratories require highly trained researchers to conduct the experiments as well as carry high regulations in order maintain the safety of the work. With that said, not all research entities can afford an establishment of that caliber. Developing a large scale novel *in vitro* propagation system that is capable of producing phenotypes of *Mtb* to mimic active and latent cellular states, and do it with accuracy and quality, will benefit the global research effort tremendously. Distributing this information, and providing quality reagents and materials for research, thus allowing more entities, large and small, to conduct TB research safely will increase our understanding of the disease exponentially.

2.0 Ch.2 Aim 1 Establishment of *M. tuberculosis* propagation in bioreactors

2.1 Introduction

2.2 Methods

2.3 Results

2.4 Discussion

2.1 Introduction

Tuberculosis infections have been described to be associated with the most oxygenated regions of the lungs, such as the upper respiratory lobes of the lungs in humans [28] and in the dorsal regions of the lungs in canines and other quadrupedal animals [28]. In the mid 1930's, animal testing was performed to determine the link between TB localization and oxygenation. TB-infected rabbits were maintained in an upright position for 11 hours a day and found that the TB lesions were predominantly in the apical zones of the lungs [29]. In humans, oxygen concentration varies significantly between tissues. The lung parenchyma of the human organ typically comprises of 4% to 14% oxygen concentration [30]. This gave strong evidence that reduced oxygen levels limit growth *in vivo.* These early observations led investigators to use hypoxic culture conditions to generate non-replicating persistent mycobacteria as an *in vitro* model of the metabolic state of latent TB *in vivo* [27]. The small heat shock protein, α-crystallin (Acr), is essential for the growth of the pathogen in macrophages [31]. As discussed previously, the expression of *acr* (Rv2031) is dramatically increased during hypoxia [32]. The Wayne model of hypoxia is an *in vitro* system that relies on a self-generated oxygen gradient in a static culture system [26]. As the bacilli naturally deplete the available oxygen within the media through respiration, over time when relatively all oxygen is depleted, the stationary phase begins to level out and persist. This was termed as the non-replicating persistent phenotype. The disease manifestation of latent TB is still poorly understood and difficult to replicate in model systems. One of the challenges in targeting the differential metabolic state of the latent disease is the inability of existing experimental models to capture the full range of observed phenotypes [33].

For over half a century, scientists have used cell cultivation in shake flasks for propagation and process development due to the inexpensiveness and process variation capabilities. Furthermore, shaker flask cultures are greatly unaffected by most mechanical complications. However, a major limitation to shake flasks is their reliance

on surface aeration, leading to reduced oxygen transfer relative to stirred tank reactors. Even baffled shake flasks can lead to splashing at high shaking speeds and can cause blockage of oxygen transfer through the gas-permeable plug of the flask via liquid saturation. By providing agitation and actively aerating the bioreactor, mass transfer rates of oxygenation can be optimally maintained and controlled [34].

The basic process of fermentation has been used for centuries for food production. Fermentation involves the breakdown of complex organic compounds to produce energy anaerobically. The need for bioreactors came during the first half of the 20th century when large scale production vessels capable of producing anaerobic conditions were warranted for the manufacture of fermentation alcohol bi-products for synthetic rubber synthesis during World War I. By the 1960's, bioreactors were a vital role in antibiotic manufacturing using bacteria, most notably *Escherichia coli* [35]. This method of using sealed reactor vessels has also proven advantageous in other pharmaceutical applications using mammalian cells. By the 1980's, disposable devices such as filters, tubing, bags, bottles and syringes entered the biotechnological manufacturing environment. In 1989, the recombinant glycoprotein Erythropoietin from Amgen Inc. was approved by the FDA for treatment of anemia. The production process was based on cultivating CHO (Chinese hamster ovary) cells in large numbers of roller bottles. However, this was not enough to keep up with demand. The first mammalian recombinant protein produced in hollow fiber bioreactors was approved by the FDA in 1996, called capromab pendetide by Cytogen Corp. In 1998, the commercially available WAVE bioreactor system was introduced and became an instant success in pharmaceutical manufacturing. These systems relied on a large rocking bag as the vessel. Even due to the popularity of the WAVE system, there was a higher utilization rate of the bag size as cultivation space was limited. This was realized by the development of single-use stirred-tank bioreactors as they came on the scene by HyClone in 2006 [36].

The adaptation of bioreactors has been developed for large scale plant production as well, for regeneration systems that are free of physiological disorders [37]. Using paddle agitators have been described to cause tangential flow as well as radial flow to provide proper mixing in the vessel culture [38] and maintain non-shearing forces against the rigid plant cells. Bioreactors have a great advantage in terms of their effectiveness in mixing. When used in tangent with a gas sparger, the impeller design of the agitator breaks up the sparging gas bubble, increasing bubble surface areas to increase oxygen diffusion into the media [39].

Bioreactors have been previously used to cultivate *mycobacterium*. Dietrich and colleagues (2002) published in the Journal of Biotechnology a detailed characterization of *Mycobacterium bovis* BCG propagated in bioreactors. They sought to devise a method of BCG cultivation that was highly reproducible and generated a high degree of viable bacilli. Using a Braun Biostat-E bioreactor system, BCG was grown in Sautons media. Their vessel was saturated to 100% DO concentration prior to inoculation and the temperature kept constant at 37°C with a stirring rate of 360 RPM. The DO was maintained at 35% by agitation. The growth parameters were recorded over a period of seven days where the system was halted. During this time a 52% increase in turbidity was measured by OD_{600} absorbance. These experiments showed to be highly reproducible through numerous replicates as the bioreactor cultivation process was started with approximately $5x10^7$ CFU/ml and reaching approximately $1.0x10^9$ CFU/ml. Acid-fast bacilli (AFB) staining and fluorescent microscopy was used along with CFU counts to determine culture viability, and Dietrich *et al.* (2002) reported their product to be 97% viable, as compared to an estimated 30% of BCG cultivated by traditional pellicle [40].

It is also equally important to bring the major disadvantage to the table in regards to bioreactor systems. These systems require a substantial initial investment for equipment, as well as repair, replacement parts and upkeep. Also if contamination is introduced into the batch, the cost and time loss can be devastating [41]. However, this drawback has not refrained scientists from perusing these advanced systems [37].

Use of a bioreactor system would be the ideal system to maintain direct control and monitoring of the growth environment *in vitro*. This notion also leads to such a system being ideal to induce differential metabolic phenotypes not unlike what is observed with a dormant persistent phenotype of *Mtb*. Here, the Eppindorf Bioflo 115 bioreactor system was used to produce pared cultures of *Mtb* grown both in normoxic and in hypoxic culture conditions to generate large scale research materials to foster research aimed at improving our understanding of active and latent TB.

2.2 Materials and Methods

2.2.1 Inoculation and system parameters

Growth of *Mtb* was performed in a batch bioreactor system using two conditions of oxygen tension. The Eppindorf Bioflo 115 system with one time use CelliGen Blu 5L reactor vessels (Eppindorf) was used to culture *Mtb*

H_{37}Rv (acquired from ATCC) in Glycerol-Alanine-Salt (GAS) media. First, large 7H11 agar plates (150mmx15mm plates) were inoculated with glycerol stocks of *Mycobacterium tuberculosis* H_{37}Rv cells and incubated at 37°C for three to four weeks until a full lawn was formed, one plate per vessel. The plates were scraped into 250ml of GAS media in an Erlenmeyer flask and incubated for one week on an orbital shaker at 37°C. The cell culture from the flask was then aspirated by pipetting and the cells dispensed into the bioreactor vessel containing 3.75 L of GAS media through the invasive pH probe port. The vessel was then sealed by insertion of the pH probe and connected to the BioFlo 115 control unit. Temperature and DO non-invasive probes were also connected to the control units and inserted into their respective ports on the vessel. The gas flow addition line was connected to a 0.2um filter and attached to the gas inlet port of the vessel, and the heating jacket wrapped tightly around the reactor to maintain temperature. Propagation was then initiated using the following parameters: Agitation set range between 25 and 65 RPM; Temperature set to 37°C; pH set to 6.6, maintained through the addition of CO_2 gas; Dissolved oxygen levels set to 40% saturation, maintained through cascade control with the addition of breathing air or nitrogen gas through a 0.2um filter; Gas flow set range between 0 and 1 vvm, maintained through cascade control with dissolved oxygen levels as the source.

The first two days of the propagation was used as an acclimation period for the cells. The DO concentration at the point of inoculation begins at 100% saturation of the GAS media at 37°C. This is due to probe calibration prior to inoculation. By the second day of growth, the oxygen levels have depleted to the initial set point of 40%, at which the cascade control begins to increase the agitation speed in an effort to maintain oxygenation. When the agitation reached its max limit of 65 RPM, breathing air was then sparged into the vessel at an increasing flow which mirrors the increasing cell density. At day four of propagation, the DO set point on the normoxic vessel was then lowered to 35% where it was maintained for the remainder of the growth period. The dissolved oxygen set point for the hypoxic vessel was lowered to 1%, where nitrogen gas was slowly sparged into the vessel to help coax the depletion of oxygen within the media. Both vessels were maintained in their respective oxygen conditions for ten days, corresponding to a late-mid log phase.

2.2.2 Preparation of cellular material

After the ten days of propagation was complete, all vessel parameters were shut down via the control unit and all gas and probe lines removed, leaving the invasive pH probe still attached to the vessel. The exhaust

line was closed using a tube clamp and the harvest port of the vessel was attached to a harvest line running into an adjacent biosafety cabinet. Using a small compressor pump filtered through a 0.2um filter attached to the gas addition port, the vessel was slowly pressurized and the culture was pushed into a fernbach collection flask inside the biosafety cabinet where the cell pellet and culture filtrate protein (CFP) could be harvested by pipetting (Figure 2.1C and D). The final cell pellets harvested from the bioreactors were briefly washed with phosphate buffered saline (PBS), centrifuged at 3.75k RPM for 10 minutes in a table top centrifuge and re-suspended in 100ml GAS media containing 20% glycerol, then immediately frozen at -80C for storage.

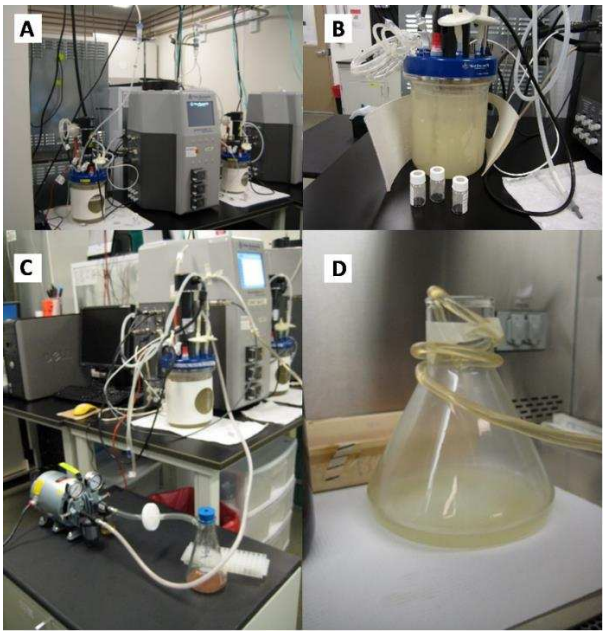

Figure 2.1

The Bioflo 115 Celligen Blu system of propagation. A; system set up for paired Normoxic/Hypoxic cultures. B; single vessel containing high biomass of *M. tuberculosis*. C; system preparation for harvesting. D; culture is purged into a 3.8L fernbach flask where the culture filtrate protein (CFP) and cells are harvested via pipetting.

2.2.3 Analysis

To determine the efficiency of the system to induce a morphological shift to a dormant, bacteriostatic phenotype of *Mtb* via oxygen tension, western blot analysis was performed using cells extracted at two-day time points produced from the normoxic and hypoxic vessels. Samples from normoxic and hypoxic vessels were taken at 48-hour time points using a 60ml laurel lock syringe attached to the sample port of the reactor. Without disturbing the agitation of the vessel, 50ml of culture was taken and dispensed into a 50ml conical tube. The conical was then

centrifuged in a table top centrifuge at 3.75K RPM for ten minutes. The supernatant was discarded and the pellet frozen at -80°C until inactivation. The time point samples of *Mtb* H_{37}Rv were gamma irradiated to inactivate the cells. The cells were analyzed for viability using the Alamar Blue assay (Alamar Blue Cell Viability Assay, ThermoFisher Scientific). The inactivated cells were transferred out of the BSL-3 facility for analysis. Cell pastes were suspended in 3ml of breaking buffer and lysed via French press as described previously [42]. The lysed cell suspension was collected in a 15ml conical tube and centrifuged at 3.75K RPM for ten minutes on a tabletop centrifuge and the supernatant containing total protein was quantitated by bicinchoninic acid (BCA) assay (Pierce BCA Protein Assay kit, ThermoFisher Scientific). For each of the two-day time point samples, 4ug of total protein was loaded and subject to SDS-PAGE and transferred to nitrocellulose for western blot analysis using anti-Acr mouse primary antibody (The following reagent was obtained through the NIH Biodefense and Emerging Infections Research Resources Repository, NIAID, NIH: Monoclonal Anti-Mycobacterium tuberculosis HspX (Gene Rv2031c), Clone CS-49 (produced in vitro), NR-13814) for hybridization and anti-mouse goat conjugated secondary anti-body (Sigma) for development.

2.2.4 Lipid extraction method

Approximately 1g of cell paste from each of the 3 replicate pairs' final harvested biomass was transferred to a glass tube, in triplicate. 3ml of 10:10:3 (chloroform:methanol:water) was added to each and the tubes were incubated overnight on a shaker table at 37°C. The tubes were then centrifuged at 3.5K RPM for 10 minutes in a table top centrifuge and the organic layer was removed from the delipidated cells and transferred to a new glass storage vial. The storage vials were placed in a nitrogen bath to dry overnight. The dried total lipid samples were then resuspended in 750ul of 2:1 (chloroform:methanol) and briefly sonicated in a high frequency sonication bath and the organic layer was again removed from the aqueous layer and transferred to a new tared glass storage vial and dried for approximately 4 hours in a nitrogen bath. 10:10:3 was then added to each sample to bring the concentration to 50 mg/ml total lipid. 50ug of each sample was analyzed by analytical thin layer chromatography (TLC) using a 65:25:4 (chloroform:methanol:water) solvent system. Two analytical TLC

plates were done, one plate was sprayed with $CuSO_4$ charring developer and the other plate was sprayed with α-naphthol developer.

2.3 Results

2.3.1 Establishment of the propagation system

The self-contained vessel allows for direct control and monitoring of the growth environment via the control units (Figure 2.1A), most importantly the control over the dissolved oxygen (DO) concentration. By maintaining consistent oxygen levels, the vessels are able to produce *Mtb* cultures to a very high cell density (Figure 2.1B). Here, the bioreactor system was shown to be able to produce an average of about 6.63 g/L and 5.29 g/L of wet weight biomass for normoxic and hypoxic cultures (n=5 each), respectively, with the highest normoxic yield of 14.8 g/L and the highest hypoxic yield of 8.8 g/L. This is compared to 4.26 g/L wet weight biomass from traditional propagation methods (n=25) using 1L GAS media in fernbach culture flasks in tandem with 400ml GAS media in roller bottles (data not shown). The results of the BCA analysis show the starting abundance of total whole cell lysate protein at 48-hours post inoculation to be 107.4 mg/ml for the normoxic vessel and 158.8 mg/ml for the hypoxic vessel. Both vessel conditions steadily increased consistently with each other to 175.3 mg/ml and 197.2 mg/ml by 96-hours post inoculation for the normoxia and hypoxia cultures, respectively. Between day 4 and 6 of incubation the normoxic culture overtook the hypoxic culture, showing a higher rate in total whole cell lysate protein production as the hypoxic rate in total whole cell lysate protein production began to slow in regards to the shift into oxygen starvation (Figure 2.2). The increase in total whole cell lysate protein production over time also indicates an increase in biomass as the cultures grow in their respective environments.

2.3.2 Establishment of Normoxic system

The normoxic vessels, N1, N2, and N3, and their paired hypoxic vessels, H1, H2, and H3 were monitored using BioCommand Track and Trend software. At the start of the incubation period the DO concentration is initially 100% saturation. Agitation begins low at 25 RPM and temperature along with pH are initiated at 37°C and 6.6, respectively. For the first approximately 90 hours, agitation, pH and temperature remain constant at their respective set points, while the DO steadily decreases at an observably consistent rate. After approximately 90 hours, the DO reached its initial set point of 40%, at which the agitation can be seen increasing rapidly over the

following approximately ten hours where it reached its maximum set point of 65 RPM and the DO is maintained at 40% for approximately 24 hours. About 140 hours into incubation, the set point for DO was lowered to 35%

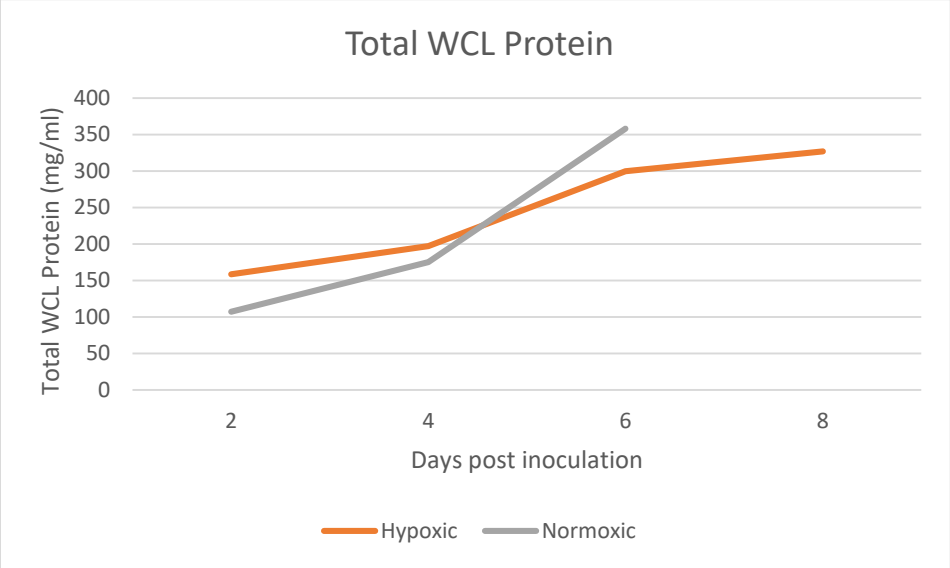

Figure 2.2

Total whole cell lysate protein abundance over time in incubation via BCA analysis. The time point samples were taken at 48 hour intervals of *Mtb* H_{37}Rv grown in bioreactors under normoxic and hypoxic conditions. Each cell sample was gamma irradiated for inactivation and lysed via French press and analyzed by BCA analysis. The normoxic vessel, gray line, begins at day 2 with 107.4 mg/ml, increasing to 175.3 mg/ml by day 4, and 357.9 mg/ml by day 6, with a rate increase of 91 mg/ml per day between day 4 and 6. The hypoxic vessel, orange line, begins at day 2 with 158.8 mg/ml, increasing to 197.2 mg/ml by day 4 and 299.7 mg/ml by day 6. Finally ending at 326.9 mg/ml by day 8. This shows a rate increase of 51.25 mg/ml per day between day 4 and 6, and 13.6 mg/ml per day between days 6 and 8.

saturation where it was maintained for the remaining six days, giving a total of ten days under normoxic propagation conditions. Over the 250 hours of monitoring, the temperature and pH levels remained consistent and unwavering. The parameter trend over the 250 hours of incubation for the normoxic vessels is shown in Figure 2.3.

The DO of the normoxic vessels were initially maintained via agitation alone, up until approximately 125 hours from which the agitation reached its maximum set point and was then unable to maintain oxygenation. At that point the gas flow was activated by sparging filtered breathing air into the vessel (Figure 2.4). For the remaining 125 hours, the gas flow gradually increases in order to maintain oxygen levels of the vessels, peaking at approximately 0.3 to 0.4 SLPM by the end of the incubation period.

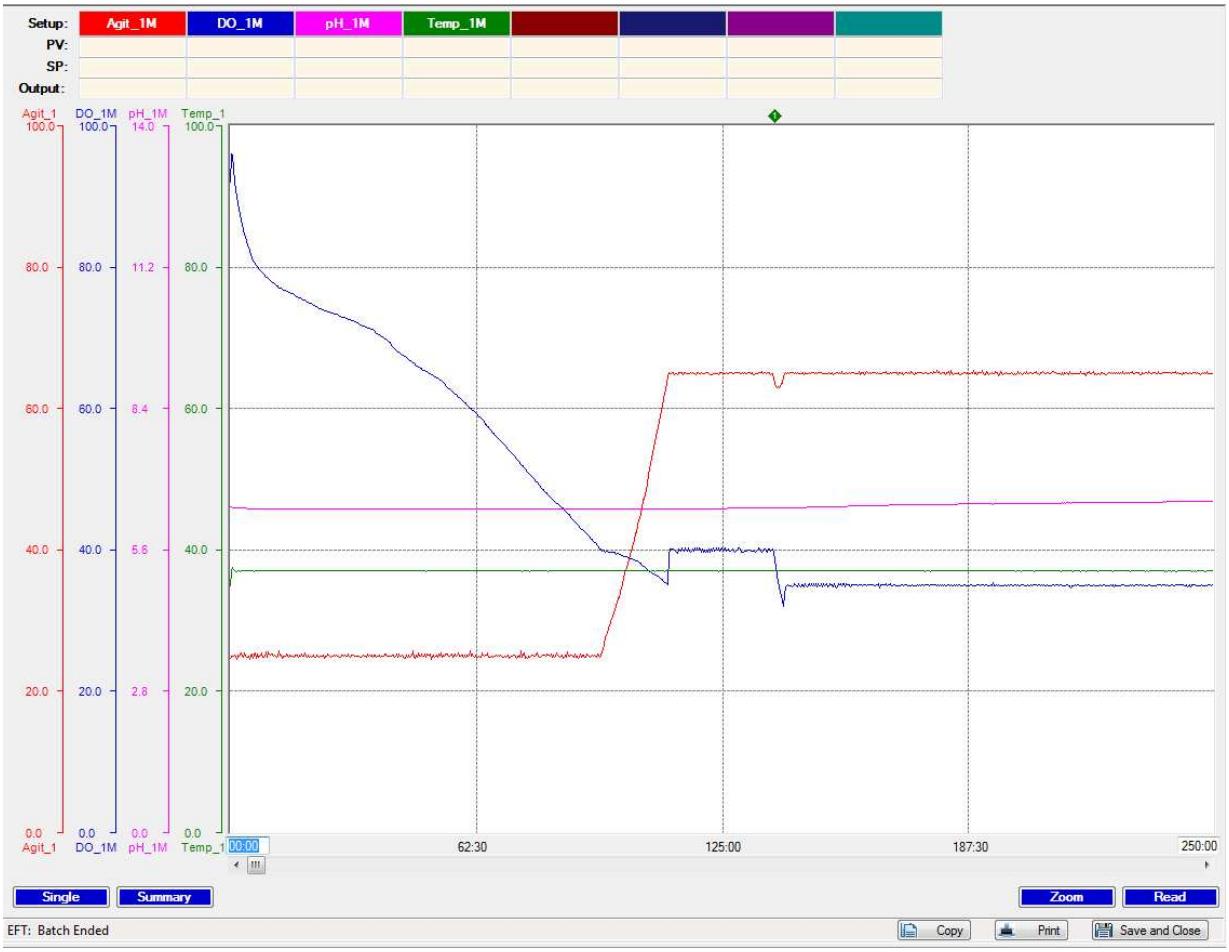

Figure 2.3

Vessel N3, Normoxic culture conditions. Trend lines monitored throughout the course of incubation for approximately 250 hours. Red, blue, pink and green trends represent agitation, DO, pH and temperature, respectively.

2.3.3 Establishment of Hypoxic system

In order for the hypoxic vessels to be congruent to the normoxic vessel and subject the culture to hypoxic conditions for a total of ten days, the incubation period was carried out over a longer period of time. However, similarly to the normoxic trend, incubation was initiated with a starting DO of 100%, where over a period of approximately 180 hours, steadily decreased through normal respiration. At approximately 200 hours, the DO rapidly decreases to about 5% and then slowly continues to decrease to levels reaching below 1% DO concentration for the remainder of the incubation. The Temperature and pH both remained static at 37°C and 6.6,

respectively, over the 360 hours of incubation. Agitation remained consistent at 25 RPM where only after approximately 290 hours a slight increase in agitation can be seen to about 27 RPM (Figure 2.5).

No increase in agitation was needed to maintain oxygen levels over the initial acclimation period while the bacilli naturally depleted the available oxygen through natural respiration. However, after approximately 190

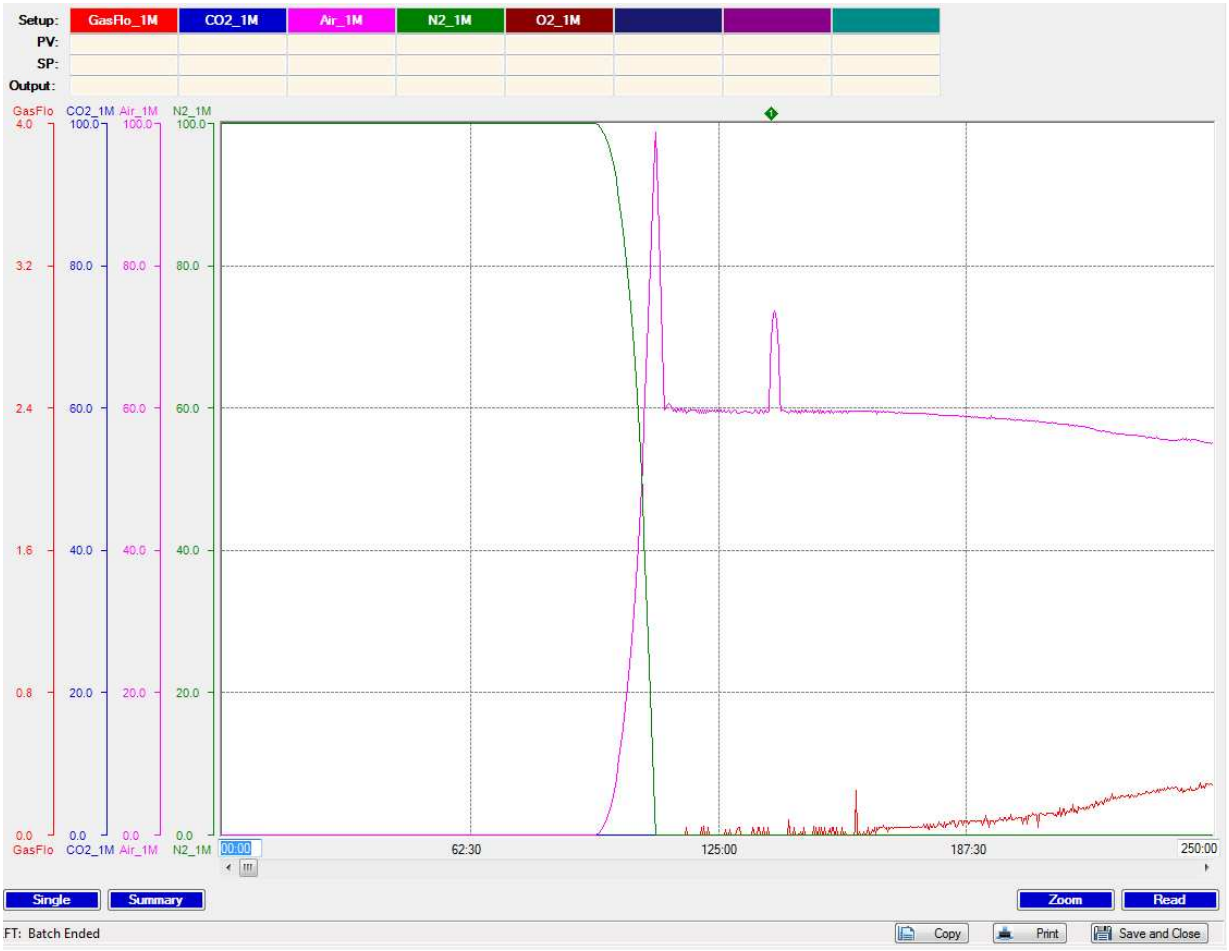

Figure 2.4

Vessel N3, Normoxic culture conditions. Trend lines monitored throughout the course of incubation for approximately 250 hours. Red, blue, pink and green trends represent gas flow, CO_2, air and nitrogen, respectively.

hours, gas flow was initiated to about 0.2 SLPM with the introduction of nitrogen gas to maintain hypoxic conditions of 1% or less for the remainder of the incubation period (Figure 2.6).

Additional trend line Figures for vessels N1, N2, H1 and H2 are provided below in the supplemental material.

2.3.4 Abundance of Acr as a marker of hypoxia

Using Western blot analysis and anti-Acr primary antibody, the beginning accumulation of Acr was observed by day six of the cell culture in the hypoxic vessel, two days after induction to hypoxia. By day eight, Acr stays observably consistent for the remainder of the run at day fourteen (Figure 2.7).

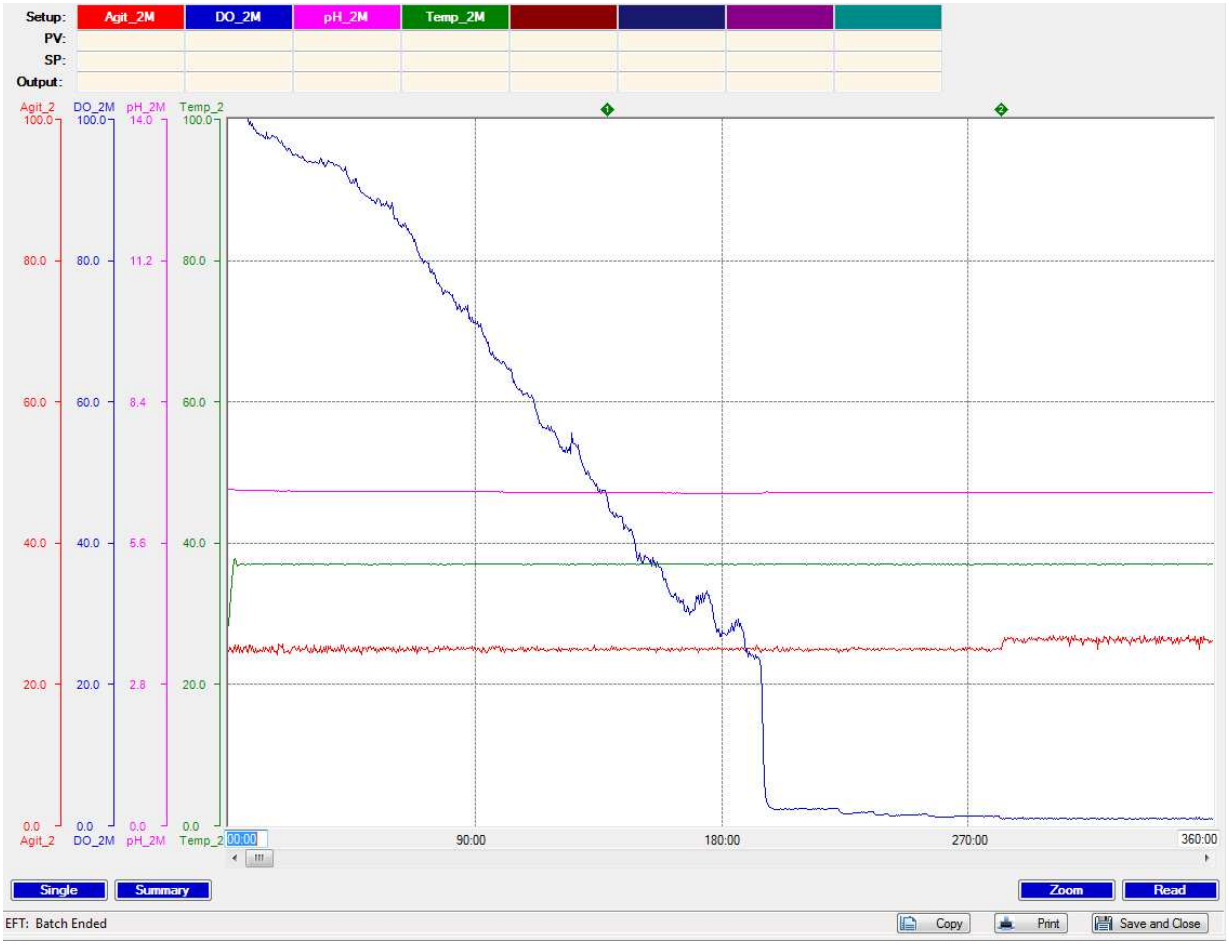

Figure 2.5

Vessel H3, Hypoxic culture conditions. Trend lines monitored throughout the course of incubation for approximately 360 hours. Red, blue, pink and green trends represent agitation, DO, pH and temperature, respectively.

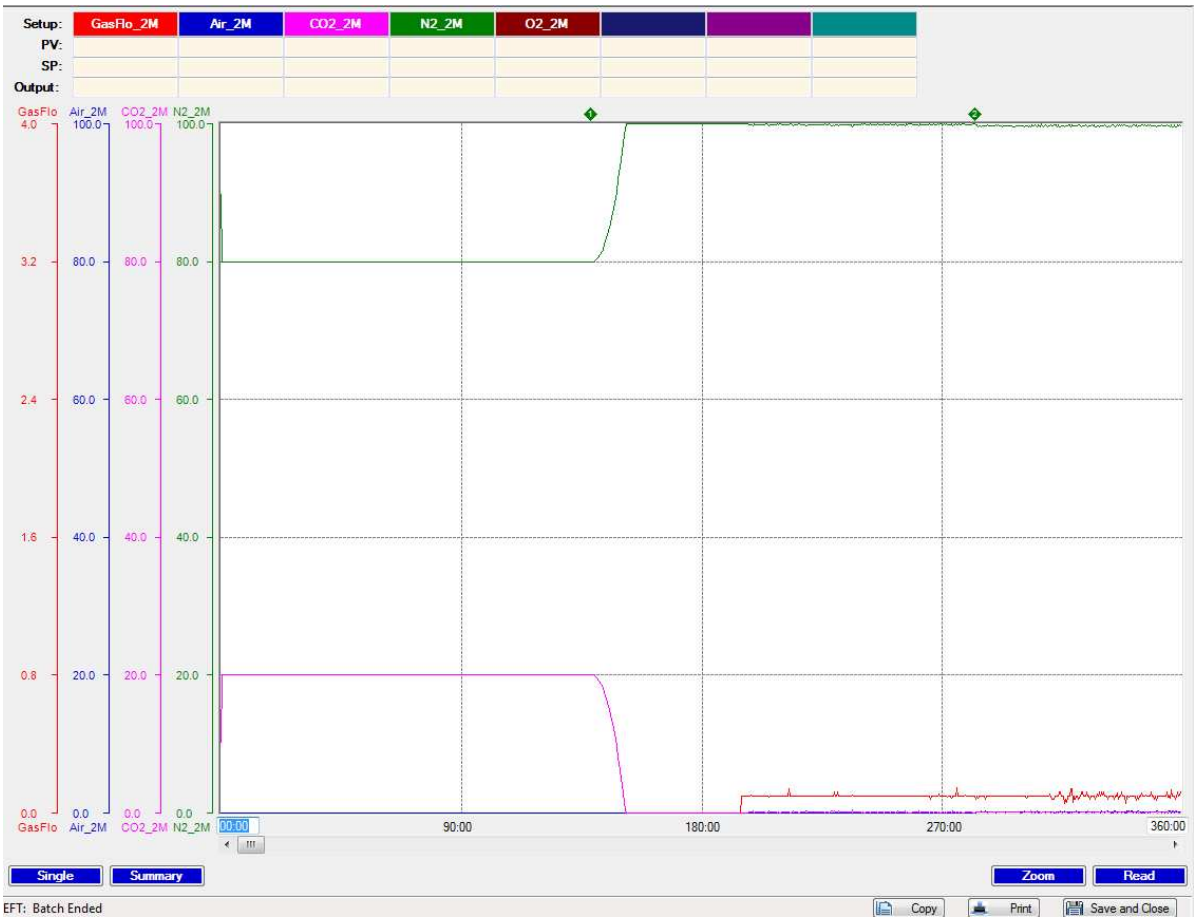

Figure 2.6

Vessel H3, Hypoxic culture conditions. Trend lines monitored throughout the course of incubation for approximately 360 hours. Red, blue, pink and green trends represent gas flow, CO_2, air and nitrogen, respectively.

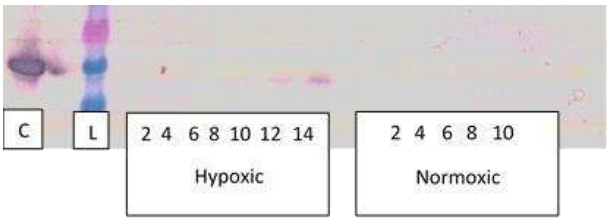

Figure 2.7

Western blot analysis of the accumulation of Acr during hypoxia. Using anti-Acr primary antibody, day four signifies the start of hypoxia. The beginning accumulation of Acr is observed at day six, in this figure a prominent band can be observed starting at day ten, increasing in relative abundance through day ten where it stays relatively consistent until harvesting at day fourteen. The early time point samples starting with day 2 through day 14 for the hypoxic culture, and day 2 through day 10 for the normoxic culture, is detailed in the box under the lanes. The accumulation of Acr can be detected in the hypoxic culture as propagation continued further into hypoxia, whereas no detectable Acr was developed in the normoxic culture. C; recombinant HspX control. L; protein ladder (Invitrogen).

2.3.5 Total lipid analysis

The results from the TLC analysis (Figure 2.8) show to be quite consistent between the normoxic and hypoxic culture conditions and between replicates, except for replicates N1 and H1 in which no development by charring spray can be detected and only two bands are detected by α-naphthol in comparison to replicates N2, N3, H2 and H3. This is believed to be due to experimental error. However, in both the $CuSO_4$ TLC (Figure 2.8A) and α-naphthol TLC (Figure 2.8B), very subtle differences can be seen near the non-polar base of the TLC plate between the normoxic and the hypoxic cultures.

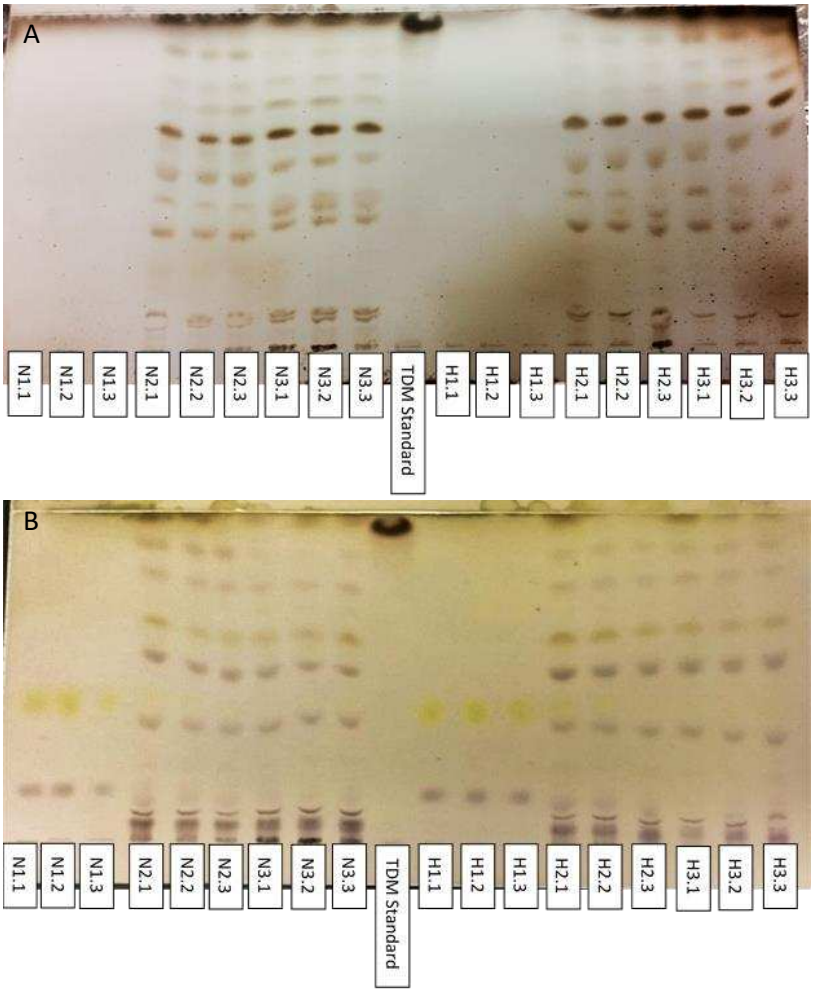

Figure 2.8

Thin layer chromatography of total lipid extracts. 10:10:3 soluble total lipid extracts of *Mtb* $H_{37}Rv$ propagated under normoxic and hypoxic conditions in bioreactors were analyzed via TLC with a 65:25:4 solvent system. 50ug of each sample loaded. N1, N2 and N3, in triplicate, correspond to normoxic cultures; H1, H2 and H3, in triplicate, correspond to hypoxic cultures. A) $CuSO_4$ charring developer. B) α-naphthol developer.

Total lipid extracts from the normoxic and hypoxic bioreactor replicate three was again analyzed by TLC, however 200ug, instead of 50ug, of each sample was loaded onto the plate in order to better visualize lipid differences in the lower non-polar region of the 65:25:4 solvent system (Figure 2.9). Here, outlined in red, very subtle lipid differences can be detected between the normoxic and hypoxic bioreactor cultures. The TLC plate developed with charring spray shows a slight lipid band in the lower non-polar region of the normoxic total lipid extracts that is absent in the same region of the hypoxic total lipid extracts. Additionally, the hypoxic total lipid extracts show a light band slightly higher in the region that is absent in the normoxic total lipid extracts. Furthermore, the TLC plate developed with α-naphthol shows a band in the same non-polar region in the hypoxic total lipid extracts that is absent in the normoxic total lipid extracts (Figure 2.9).

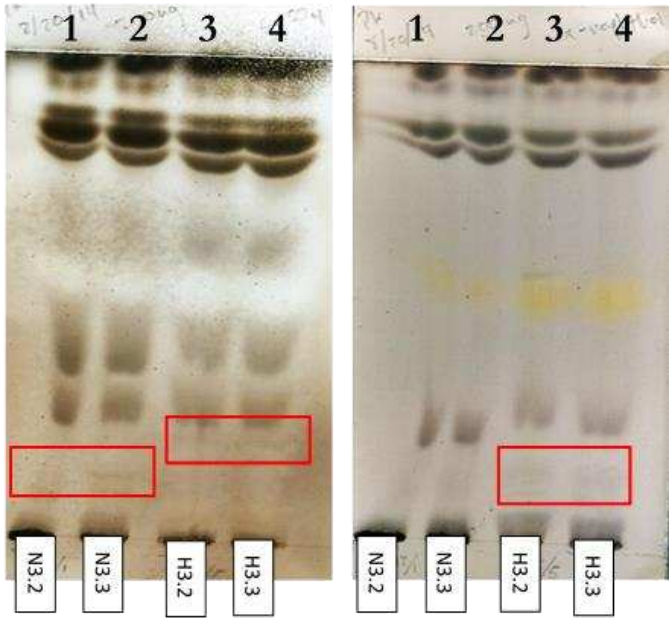

Figure 2.9

Thin layer chromatography of total lipid extracts. 10:10:3 soluble total lipid extracts from *Mtb* $H_{37}Rv$ of the normoxic and hypoxic bioreactor replicate three were analyzed via TLC in a 65:25:4 solvent system with 200ug of each sample loaded. Left; $CuSO_4$ charring developer. Right; α-naphthol developer. Red boxes indicate slight differences between normoxic and hypoxic total lipid extracts.

2.4 Discussion

Methods of propagation for *Mtb* have been around for decades, but have remained relatively unchanged. Common techniques using culture flasks with defined head space ratios, with and without agitation, are stricken with variability in cell concentration as well as viability [43]. Furthermore, *Mtb* has a doubling time of roughly 20 to

24 hours, requiring long incubation periods as well as an inability to target different metabolic states and observed phenotypes effectively [30]. Consistency is key when developing research materials for the use of vaccine, drug and diagnostic purposes.

Dietrich et. a. (2002) was able to show both high viability and consistent bacterial loads using BCG propagated in bioreactors [33]. Here, we used the Bioflo 115 bioreactor system with a CelliGen Blu 5L vessel to propagate *Mtb* H_{37}Rv in GAS media (Figure 2.1). The controlled environment of the bioreactor system can deliver optimal conditions to induce multiple metabolic phenotypes indicative of dormant *Mtb* with consistency. Furthermore, direct and consistent control over the growth environment will aid in the quality deduction of the metabolic phenotype being induced by the culture environment.

Three replicates of paired cultures of *Mtb* H_{37}Rv propagated with and without oxygen tension were generated using the bioreactor system described here. Using the systems cascade control, respective DO concentrations were maintained for ten days each, N1, N2 and N3 for normoxic conditions of 35% oxygenation (Figure 2.3 and 2.4) and H1, H2 and H3 for hypoxic conditions of 1% or less (Figure 2.5 and 2.6). The cascade control over the agitation and gas flow was able to deliver consistency of oxygen tension between the three replicates, corroborating with the methods proposed by Dietrich (2002). Interrogation of bacillary load and viability are interrogated later in this study in chapter 3.

The rate at which the oxygen was utilized by each vessel was not consistent however. High variability of oxygen consumption was observed between each of the six vessels (Supplemental Material). Even though this phenomenon was observed during the initial acclimation period, the cascade control was able to maintain appropriate normoxic and hypoxic levels for the remaining ten-day incubation period with high accuracy and sensitivity.

To qualify the system and determine if said hypoxic conditions using the bioreactor control were able to induce a perceived dormant state, western blot analysis of Acr was employed. The heat shock protein Acr is rapidly induced during oxygen tension and is often used as an indicator of hypoxia, as elucidated by both *in vitro* and *in vivo* studies [44]. Here we observed a marked increase in the relative abundance of Acr from total protein lysate as shown from the western blot analysis (Figure 2.7) in hypoxic cultures. This indicates that the system is able to

achieve hypoxic conditions suitable for persistence due to the increased production of Acr as time progresses under hypoxic stress.

As proposed by Wayne (1996), the adaptation to a non-replicating dormant state requires time. Contradictory to what is shown here, they stated that a rapid reduction of oxygen in the culture media resulted in a massive die off where as a slower temporal decrease to hypoxia will lead to NRP stage 2 where no further replication is observed [24]. Here we observed variability in the time it took to go from the acclimation period of 35% DO concentration and the abrupt depletion of oxygen to hypoxia. The final depletion of oxygen described here ranged from a matter of hours to up to 48 hours, with roughly a relative average of about 24 hours to reach hypoxic condition. This is contradictory to the experiments conducted by Wayne *et al.* (1996). However, Rustad *et al.* (2008) did not observe significant killing by rapid oxygen depletion as described by Wayne and colleagues. Furthermore, they showed an increase in fold induction of Acr relative to a DosR mutant strain also subjected their cultures to rapid oxygen depletion [45], similar to our system.

Aside from potential viability issues, the question still remains as to whether or not the system proposed in this study is inducing hypoxia too rapidly. This could potentially give inaccurate results to downstream applications concerning certain modifications that would be naturally seen *in vivo* or over a more gradual oxygen depletion *in vitro*. Rustad (2008) also addressed this by comparing the temporal transcriptional adaptation of the DosR regulon from both *in vitro* and *in vivo* conditions. Their findings indicated that, using microarray analysis, oxygen starved cultures displayed induction of the regulon within hours and nearly half of those genes returning to baseline within 24 hours. In addition to this, a larger set of genes were induced and sustained following the DosR-mediated initial response. Rustad (2008) termed this the Enduring Hypoxic Response (EHR) and consisted of over 230 genes greatly induced at four to seven days' post hypoxia [45]. With this, it seems that there is evidence that the transcriptional shift to dormancy occurred early and rapidly after initial exposure to oxygen tension, thus supporting a ten-day incubation period under hypoxic culture conditions to fully induce the transcriptional modifications associated with a chronic hypoxic environment.

In the presence of this study, GAS media was used as the culture media and thus causes difficulty when attempting to accurately quantitate bacillary load and viability downstream. This is due to the characteristic cording of the pathogen to not fully suspend in culture media, but clump together and fall out of solution [46]. The

clumping of *Mtb in vitro* causes inaccuracy when attempting to quantitate the cellular concentrations, giving an under-estimation of the number of cells present by means of CFU or microscopy. Traditionally Tween 80 can be supplemented to culture media at a concentration of 0.05%. Tween is utilized as a carbon source and disrupts the cording of the bacilli and allows a more confluent cellular suspension. However, Tween has been shown to perhaps have some inhibitory effects of the growth and morphology of mycobacteria. Observations of *Mycobacterium avium* complex grown in varying concentrations of Tween 80 supplemented to the media were interrogated and found that higher concentrations of Tween resulted in a bacteriostatic effect, reduced glycolipids of the cell membrane as well as a morphological elongation of the rod shape as seen by SEM [47]. Thus in order to develop a system to generate mycobacterial biomass suitable for multiple downstream applications, a more minimal media would be warranted, regardless of the difficulties in quantification. With that said, a future examination of the proposed bioreactor system using GAS media supplemented with Tween 80 would be beneficial to elucidate accurate quantification of the capabilities of such a system in terms of biomass generation.

3.0 Ch.3 Aim 2 Viability enrichment

3.1 Introduction

3.2 Methods

3.3 Results

3.4 Discussion

3.1 Introduction

Adapting to hypoxia takes a degree of fitness by the bacilli, where only the “strongest” population will be able to survive the shift into bacteriostatic persistence [24]. During this shift, aerobic respiration decreases the concentration of oxygen available. As a result, the bacteria begin to die off. For example, the bacilli that die at an early time point will have a different transcriptional profile than the bacilli that die at a later time point (Figure 3.1). This is because the later bacilli were able to survive longer through the temporal adaptation to dormancy. This litter of transcriptomes from dead bacteria skew downstream analysis and creates a bias from a gradient of transcriptional profiles when the goal is to only interrogate the live bacteria in true bacteriostasis.

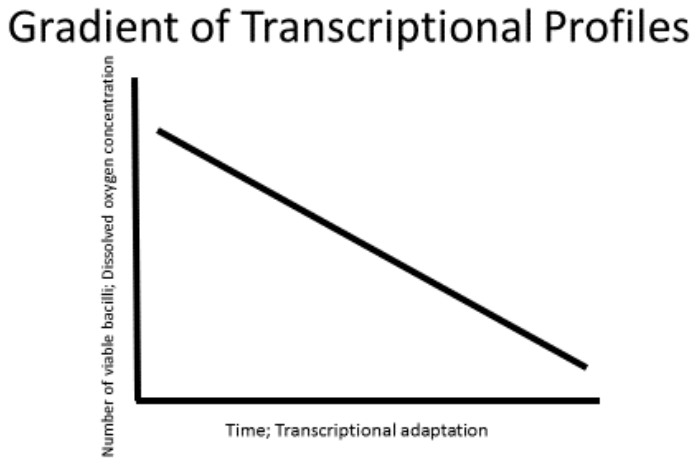

Figure 3.1

Gradient of transcriptional profiles. The number of viable bacilli is dependent on the concentration of available oxygen within the culture medium. Thus the number of viable bacilli and DO concentration have a negative correlation over time. As time increases, the transcriptional profiles of the viable bacilli must change and reflect the adaptation for the bacilli to survive in the decreasing oxygen environment.

Previous work has shown that there are distinct physiological differences between active and dormant *Mtb*. Cunningham *et al.* (1998) provided much evidence that there is a degree of cell wall thickening, up to 4 nm, by *Mtb* cells grown under hypoxic conditions as compared to normoxic conditions, as shown via scanning electron microscopy (SEM) [48]. This is further corroborated by Galagan *et al.* (2013) in their work to show the transcriptional change during hypoxia and subsequent re-aeration. In their study they provided evidence of an increase in lipid metabolism and catabolism, particularly in the abundance of mycolic acids. The increase in lipid synthesis suggests that these energy stores are necessary for survival in the nutrient depleted environment that the bacilli would encounter during hypoxia [49]. These findings led to the prospect as described previously, where a measurable increase in buoyancy as time increases under hypoxic conditions are observed [27].

Here, we sought out to determine if a density based gradient would separate *Mtb* grown in bioreactors, as described in chapter 2, not only by state of metabolic stress, but also filter out non-viable cells [50]. Using a density gradient centrifugation method to enrich the final cell product could prove useful by removing the transcriptional bias from dead bacilli. Current culture methods for *Mtb* provide a high degree of variability for viability [43] and the transcriptional profiles from the abundant dead bacteria could mask or deliver bias to the true transcriptional profile of the dormant phenotype of *Mtb*. Removing some of that transcriptional bias could shed some light to more accurate downstream analysis such as transcriptomics and systems biology approaches.

3.2 Materials and Methods

3.2.1 Establishment of separation conditions

First, to interrogate the bioreactor propagation system of *Mtb*, the proper controls must be taken into account. Two test cultures of *Mycobacterium tuberculosis* H_{37}Rv were grown in 100ml of 7H9 media supplemented with oleic acid, albumin, dextrose, and catalase (OADC) enrichment media and 0.05% Tween in a sealed Erlenmeyer flask. One test culture was incubated at 37°C on an orbital shaker for three months, while the other was incubated for twelve days. One milliliter of each culture was extracted, serially diluted, and plated in triplicate on 7H11 agar and incubated for 16 days at 37°C for colony forming unit (CFU) counts, and analyzed via microscopy for Petroff-Hausser (P-H) counts via a hemocytometer.

3.2.2 Discontinuous density gradient centrifugation of the test cultures

Based on previous work, with the prospect of separating different phenotypes of *Mtb* based on their density, it should also be possible to separate live and dead cells based on the same principle. Thus a density based discontinuous Percoll gradient was used to separate and enrich the cell product for viability. First, a standard isopycnic (SIP) solution was generated by a 1:10 dilution of Percoll stock solution (Sigma) at 1.130 g/ml with 1.5M saline. Then two density phases were generated by diluting the Percoll SIP solution with 0.15M saline to a final concentration of 1.088 g/ml and 1.067 g/ml Percoll solution. The separation column then comprised of 3ml of each density phase that was carefully pipetted, starting with the phase with the highest density and working toward the least dense, into a 15ml glass tube. One milliliter of each culture was extracted, serially diluted, plated in triplicate on 7H11 agar and incubated for 16 days at 37°C for CFU counts, and analyzed via microscopy for P-H counts via a hemocytometer.

Finally, 1ml of the cell suspension from each test culture was layered on the top of the density column (Figure 3.2). The glass tube was centrifuged on a table top centrifuged at 400xg for 15 minutes and the banded cell fractions extracted by pipetting and transferred to a 1.7ml microcentrifuge tube and spun down to pellet at 14K RPM for 10 minutes in a microcentrifuge. The supernatant was decanted and the pellet was washed with 1ml of PBS media and spun down to pellet at 14K RPM for 10 minutes in a microcentrifuge. The supernatant was

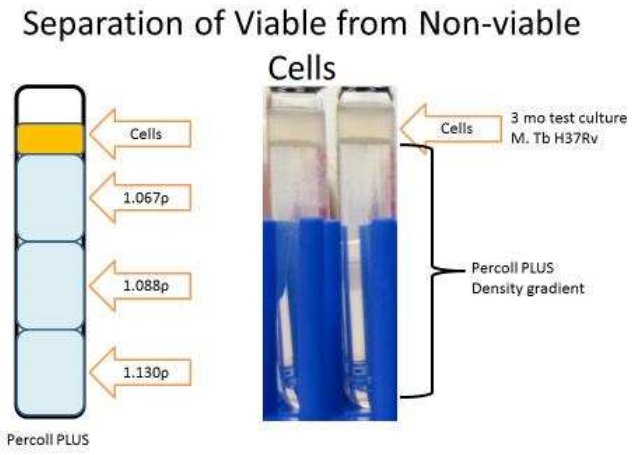

Figure 3.2

The Percoll density separation column. The separation column comprises of 1ml of *Mtb* $H_{37}Rv$ culture grown in 7H9 media supplemented with OADC and 0.05% Tween and incubated in a sealed Erlenmeyer flask with gentle shaking for three months, overlaid onto a Percoll gradient of 1.067g/ml Percoll solution, followed by 1.088g/ml Percoll solution and 1.130g/ml Percoll solution, respectively.

decanted and the washed pellet was re-suspended in 1ml of GAS media, serially diluted and plated in triplicate for CFU and counted via the P-H method. Based on the total number of cells from the Petroff-Hauser counts and the number of viable cells based on the CFU counts, a percent viability was determined.

3.2.3 Discontinuous density gradient centrifugation of normoxic and hypoxic paired cultures

To perform the gradient separation using the hypoxic and normoxic paired replicates, three density phases were generated by diluting the Percoll SIP solution with 0.15M saline. Briefly, a 90% Percoll SIP was used to produce a final concentration of 1.120 g/ml in 1.5M saline, a 65% Percoll SIP for a final concentration of 1.08 g/ml in 1.5M saline, and a 40% Percoll SIP for a final concentration of 1.05 g/ml in 1.5M saline. The separation column then comprises of 3ml of each density phase carefully pipetted, starting with the phase with the highest density and working toward the least dense, into a 15ml conical tube. Finally, 1ml of the normoxic and hypoxic culture cell suspension is layered on the top of the density column. The conical tube is centrifuged at 400xg for 15 minutes in a table top centrifuge and the banded cell fractions extracted by pipetting and transferred to a 1.7ml microcentrifuge tube and spun down to pellet at 14K RPM for 10 minutes in a microcentrifuge. The supernatant was decanted and the pellet was washed with 1ml of PBS media and spun down to pellet at 14K RPM for 10 minutes in a microcentrifuge. The supernatant was decanted and the washed pellet was re-suspended in 1ml of GAS media, serially diluted and plated in triplicate for CFU and counted via the P-H method. Based on the total number of cells from the P-H counts and the number of viable cells based on the CFU counts, a percent viability was determined.

3.3 Results

3.3.1 Viability of the viable-enriched separation test culture

The test culture of *Mtb* H_{37}Rv grown for three months with gentle shaking produced three very distinct bands of cells at each interphase of the separation density gradient after a soft centrifugation of 400xg for 15 minutes (Figure 3.3). At the top of the column, a very tight and even band was formed at the interface between the GAS media and the least dense phase of 1.067 g/ml Percoll solution. This band was carefully extracted by pipetting as Fraction A. Continuing further into the column, another irregular, globular layer formed surrounded by a light cellular haze at or just above the interphase between the lightest 1.067 g/ml phase and the 1.088 g/ml

Percoll solution phase. Here, only the globular cell material, not the surrounding haze, was carefully extracted via pipetting as Fraction B. Finally, at the interphase between 1.088 g/ml and the densest 1.130 g/ml Percoll solution

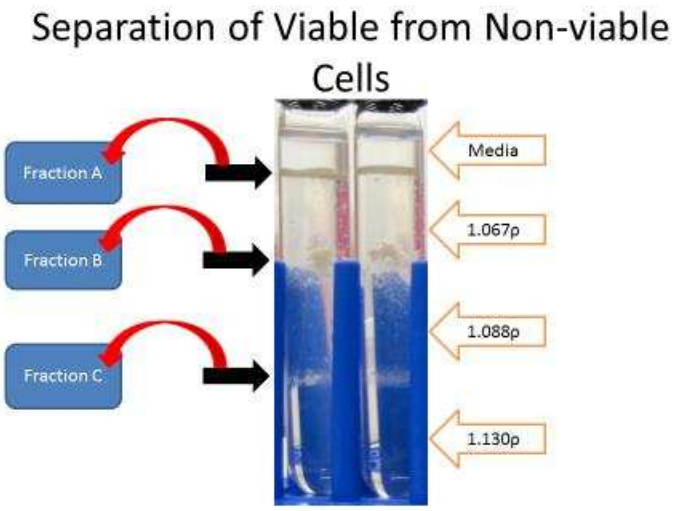

Figure 3.3

Discontinuous density separation of the separation test culture. A separation test culture of *Mtb* H_{37}Rv was grown for three months with gentle shaking in 7H9 media supplemented with OADC and 0.05% Tween. A 1ml sample of the test culture was overlaid onto the gradient and centrifuged to separation, producing three separate fractions. The fractions were extracted via pipetting for viability analysis.

phase was a third, even band of slightly more dispersed cells. This region was also carefully extracted by pipetting as Fraction C.

Each fraction extracted from the test culture was washed with 1ml PBS media and then resuspended to 1ml GAS media. P-H counting was performed using a cell counting hemocytometer and 100x oil immersion light microscopy. The upper neat Fraction A was shown to contain $2.17x10^8$ cells/ml, while the middle globular Fraction B and lower hazy Fraction C was shown to contain $2.33x10^7$ cells/ml and $3.35x10^6$ cells/ml, respectively. The unseparated control from the separation test culture was shown to contain $6.22x10^6$ cells/ml (Table 3.1). CFU counting was performed after 16 days of incubation on 7H11 agar at 37°C. Fraction A of the separation test culture contained $7.2x10^7$ CFU/ml, which gives 33.13% viability for Fraction A with a 3.02-fold difference between the total number of cells per milliliter and the viable number of cells per milliliter. Fraction B of the separation test culture contained $5.43x10^6$ CFU/ml, which gives 23.29% viability for Fraction B with a 4.29-fold difference. Fraction C of the separation test culture contained $4.83x10^4$ CFU/ml, which gives 1.44% viability for Fraction C with a 69.3-fold

difference. Finally, the unseparated control from the separation test culture contained $1.97x10^5$ CFU/ml, which gives 3.17% viability for the unseparated control with a 31.5-fold difference between the total number of cells per milliliter and the viable number of cells per milliliter, while the unseparated late mid-log phase control grown with shaking at 37°C, was shown to contain $2.6x10^8$ CFU/ml, which gives 23.30% viability with a 4.29-fild difference (Table 3.1).

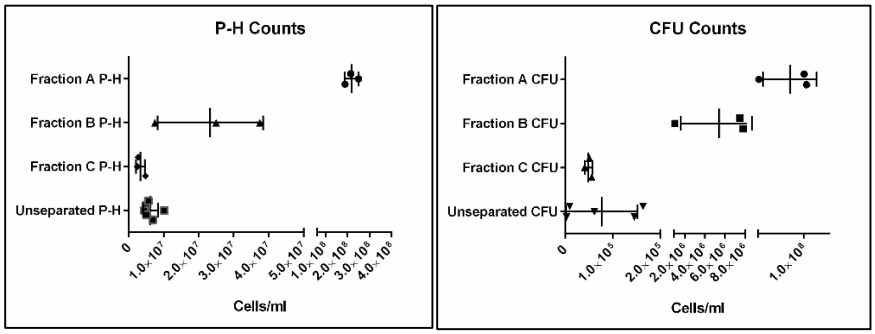

Figure 3.4

The standard deviations of the P-H cells/ml for fraction A, fraction C and the unseparated control were more narrow (within a tenth of a log) as compared to the broad standard deviation (spanning almost half a log) of fraction B. The standard deviations of the CFU cells/ml for fraction A, fraction B and the unseparated control were consistent with each other whereas fraction C contained the lowest deviation. The averages of the replicates increase in viability are summarized in Table 3.1. For these counts: raw values presented as diamonds, circles, squares and triangles; vertical bars indicate average; horizontal bars indicate standard deviation.

Table 3.1

Viability of fractions obtained through discontinuous density centrifugation of *Mtb* $H_{37}Rv$ grown for three months with gentle shaking in 7H9 media supplemented with OADC and 0.05% Tween in an Erlenmeyer flask at 37°C. Fraction A was extracted at the biphase of the culture media and 1.067 g/ml Percoll solution. Fraction B was extracted from the biphase of 1.067 g/ml and 1.088 g/ml Percoll solution. Fraction C was extracted from the biphase of 1.088 g/ml and 1.130 g/ml Percoll solution.

Table 3.1 Viability of separation test culture			
Fraction	Petroff-Hausser (cells/ml)	Colony Forming Units (CFU/ml)	Percent Viability
Fraction A	$2.17x10^8$	$7.20x10^7$	33.18%
Fraction B	$2.33x10^7$	$5.43x10^6$	23.30%
Fraction C	$3.35x10^6$	$4.83x10^4$	1.44%
Unseparated Control	$6.22x10^6$	$1.97x10^5$	3.17%

3.3.2 Viability of viable-enriched normoxic and hypoxic paired cultures

The separation performed using 1ml extracts from the normoxic and hypoxic paired cultures grown using the bioreactor formed quite uniform bands between the two growth conditions. Replicates N1, N2 and N3 of the normoxic vessels banded right at the interface between Percoll density solutions 1.08 g/ml and 1.12 g/ml, aligned at the 3ml mark of the 15ml conical tube; with the exception of N3 being slightly lower at the 2ml mark of the 15ml conical. Alternatively, replicates H1, H2, and H3 of the hypoxic vessels banded slightly above the mid and higher density interface, aligned at approximately the 4ml marker of the 15ml conical tube; with the exception of H3 being slightly lower at the 3ml marker of the 15ml conical (Figure 3.5). Each cell fraction was carefully extracted and washed with PBS and resuspended in 1ml GAS media and plated for CFUs and counted via P-H methods.

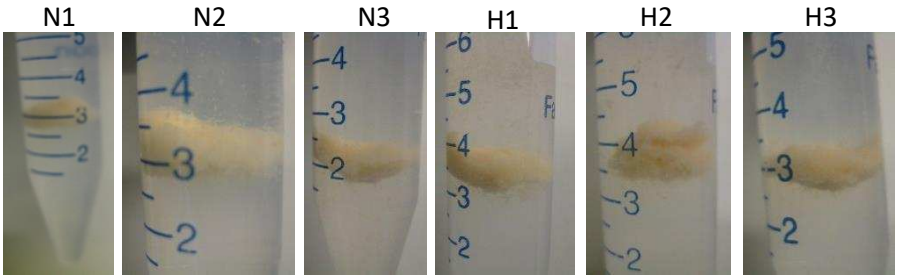

Figure 3.5

Discontinuous density separation of *Mtb* $H_{37}Rv$ produced in bioreactors with and without oxygen tension. Replicates N1, N2, and N3 represent cultures of normoxic conditions, and their respective pairs H1, H2 and H3 represent culture condition under hypoxia. The 3ml mark of the 15ml conical tube represents the biphase of 1.08 g/ml and 1.12 g/ml Percoll solution.

Each fraction extracted from the separation of each of the bioreactor replicates were washed with PBS and resuspended in 1ml of GAS media. P-H counting was performed using a cell counting hemocytometer and 100x oil immersion light microscopy. CFU counting was performed after 16 days of incubation on 7H11 agar at 37°C. The first normoxic replicate was shown to be 17.00% viable with a fold difference of 5.88 between total cell number and CFUs. The second and third normoxic vessel replicate were shown to be 0.81% and 18.15% viable with fold differences of 123.76 and 5.51, respectively (Table 3.2). The first hypoxic replicate was shown to be 13.19% viable with a fold difference of 7.59 between total cell number and CFUs. The second and third hypoxic vessel replicates were shown to be 1.24% and 10.86% viable with fold differences of 80.46 and 9.21, respectively (Table 3.2). For this experiment, the unseparated bioreactor control was propagated as described in chapter 2.

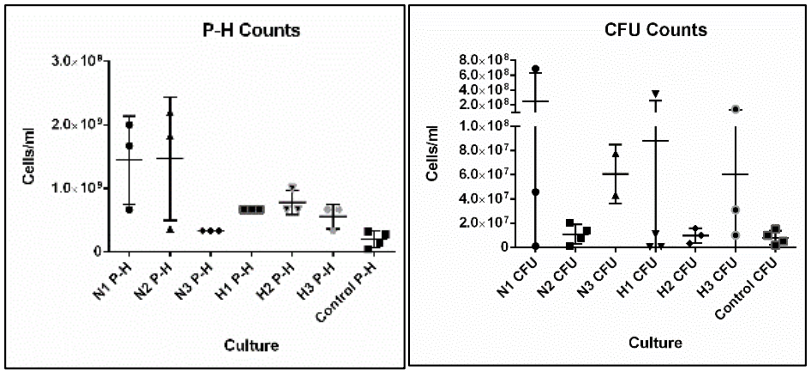

Figure 3.6

The standard deviations for the Control P-H and Control CFU is the pool of cells/ml of both the normoxic (n=3) and hypoxic (n=1) for the unseparated control counts. The P-H standard deviations are all very low for the hypoxic cultures as compared to the normoxic cultures which N1 and N2 have very high standard deviations. The CFU standard deviations are all quite variable, however, the culture pairs do share in their level of deviation. Bioreactor replicate pairs 1 and 3 both have high standard deviations whereas replicate pair 2 has a low standard deviation. The averages of the replicates increase in viability are summarized in the Table 3.2. For these counts: raw values presented as diamonds, circles, squares and triangles; horizontal bars indicate average; vertical bars indicate standard deviation.

Table 3.2

Viability of fractions obtained through discontinuous density centrifugation of *Mtb* $H_{37}Rv$ propagated in bioreactors with and without oxygen tension. N1 (n=3), N2 (n=4) and N3 (n=2) represent P-H and CFU counts from the three bioreactor cultures under normoxic condition. H1 (n=4), H2 (n=3), and H3 (n=3) represent P-H and CFU counts from the three bioreactor cultures under hypoxic conditions.

Table 3.2 Viability of Bioreactor replicates			
Replicate	Petroff-Hausser (cells/ml)	Colony Forming Units (CFU/ml)	Percent Viability
N1	$1.44x10^9$	$2.46x10^8$	17.00%
N2	$1.33x10^9$	$1.08x10^7$	0.81%
N3	$3.33x10^8$	$6.05x10^7$	18.15%
H1	$6.67x10^8$	$8.79x10^7$	13.19%
H2	$7.78x10^8$	$9.67x10^6$	1.24%
H3	$5.56x10^8$	$6.03x10^7$	10.86%
Unseparated Normoxic Control	$4.29x10^7$	$1.80x10^6$	4.20%
Unseparated Hypoxic Control	$3.25x10^8$	$1.50x10^7$	4.61%

3.4 Discussion

Here, a density based gradient centrifugation was able to separate *Mtb* grown in bioreactors, propagated as described in chapter 2, not only by state of metabolic stress, but also seemed to enrich the final cell extract for viable cells. However, consistencies as well as inconsistencies were observed that almost propose more questions than answers.

The test culture, grown in 7H9 media with OADC and Tween in a sealed flask with gentle shaking at 37°C for three months, was fractionated into three distinct bands at the interface between density layers (Figure 3.3) which is in agreement to what was observed as shown in Figure 1.4 [27]. In their study, a continuous density gradient was used with isotonic Percoll solution with a density range from 1.13 g/ml to 1.01 g/ml. Cells under multiple stress were extracted at progressive time points and overlaid onto the density gradient at a ratio of 1:10, cells to Percoll gradient. The tubes were then centrifuged at 400xg for 16 minutes. The fractionated cell populations were separated at different levels at different time periods during multiple stress treatment. With increasing time under hypoxia, the cells band and shift towards a higher buoyancy. At day zero, the cells seem to band at a high density between 1.138 g/ml and 1.088 g/ml. By day three the cell band has shifted slightly higher to a lower density right about 1.088 g/ml and even banding higher between 1.088 g/ml and 1.064 g/ml by day nine. This was taken much further and by day 18 the cells formed a hazy region within the gradient tube at about 1.064 g/ml and 1.019 g/ml. Further treatment with Nile Red staining of the gradient fractions showed that the lighter fractions were more enriched in lipid-loaded cells [27]. Similarly, here, the three populations separated from the separation test culture fell to the density biphases between the densities of 1.13 g/ml, 1.088 g/ml and 1.067 g/ml which is consistent with what was observed by previous work [27]. As previously stated, *Mtb* can exist in multiple phenotypes within the same culture [11]. Described here, three separate populations were able to be fractionated via their buoyancies, all from the same culture.

The unseparated control extracted from the separation test culture revealed to be merely 3.13% viable by culture and microscopy methods. Comparing the unseparated control viability to the two upper separated fractions of 33.13% and 23.29% viability, this indicates a marked increase in fraction viability. Observing low fold differences between the number of viable cells over the total number of cells leads to the evidence that a viability

enrichment was achieved to a certain degree (Table 3.1). Finally, it would be expected that the lower fractions only showed to be 1.44% viable as the majority of the cells are dead and thus should have a higher density. This is corroborated by the work done by Lewis *et al.* (2014) where they used a suspended microchannel resonator (SMR), which is a cantilever sensor suspended in a vacuum cavity that measures the buoyant mass of individual particles such as single cells, nanoparticles or biomolecules. They described that dead cells have a lower buoyant mass as compared to live cells, and thus have a higher density [50].

The fact that each bioreactor replicate was consistent in the banding within their respective culture conditions (Figure 3.5) is quite desirable and gives affirmation that the reactor system may be ideal to produce single phenotypic populations in culture. The observation that the third replicate pair showing congruent banding only 1ml lower than the first and second replicate pairs could be attributed to human error. One possibility for this could be that only 2ml of the densest Percoll solution was added instead of 3ml during the preparation of the gradient column.

In this study, a late-mid log phase control of *Mtb* was used to compare to the late-mid log phase of the normoxic cultures and the hypoxic cultures grown in bioreactors as described in chapter 2. The control culture not subject to treatment by density gradient centrifugation and was shown to be 23.20% viable by culture and microscopy methods (Table 3.1). Unsurprisingly, the normoxic cultures of replicates one and three showed higher viability than their paired hypoxic cultures, giving 17% and 18% compared to 13% and 10.86%, respectively (Table 3.2). This is a good sign as the normoxic cultures harvested at late-mid log phase should understandably be more viable as the bacilli were still actively dividing as compared to the hypoxic cultures where the bacilli have induced an adaptation to bacteriostasis. However, comparing the bioreactor cultures to the unseparated late-mid log phase control grown in an Erlenmeyer flask on an orbital shaker, a noticeable decrease in viability is still observed. This could be attributed to the high culture density produced by the bioreactors. It has long been suggested that relatively high proportions of non-viable cells are produced when the cultures are incubated to very high cell densities [51]. The observation of a lower viability from bioreactor cultures compared to traditional growth in flask could be due to the high biomass created. Furthermore, in a batch bioreactor system there is no change or enrichment of the media, leaving the individual *Mtb* cells to compete with the high concentration of other *Mtb* cells. In a chemostat bioreactor system there is a continuous exchange of fresh media added. In the case of

cultures grown under normoxic conditions, perhaps using a chemostat bioreactor system would alleviate some of the observed die off.

As for reactor replicates N2 and H2, which both showed 1.24% or less viability (Table 3.2), was not anticipated nor agreed with the viability trends of the replicates one and three. Looking back at the culture conditions (Supplemental Material) no discrete issues were seen. Replicate N2 was maintained at 35% DO concentration without deviation, and the same went for pH, agitation and temperature. No significant oddities were observed from the gas flow either as the concentration consisted of 80% filtered breathing air and 20% CO_2 with a flow rate not exceeding 0.8 SLPM. Replicate H2 also followed this same trend, however it is worth noting that this hypoxic vessel required little to no gas flow into the vessel to maintain hypoxic conditions (Supplementary Material). Considering the banding observed during the discontinuous density gradient centrifugation was consistent with the other replicates (Figure 3.5), it could be suggested that this oddity of little or no viability would be attributed to human error. As mentioned previously, accurate direct counts of *Mtb* are very difficult and subject to a degree of inaccuracies when no detergent is used in the media to prevent cording and clumping of the bacilli. Furthermore, CFU and P-H counting methods are done by direct observation by the researcher and thus are correlated to the researchers own perception.

Some questions still arise from the fractionations observed from the *Mtb* replicate cultures grown in bioreactors described in chapter 2. The bioreactor replicates did not show any visible band or fractions pertaining to dead cells as shown from the test culture where the fraction in the highest density was shown to be only 1.44% viable (Table 3.1). Aside from culture conditions, the test culture contained Tween which would disrupt the characteristic clumping of the tubercle bacilli and allow it to be more readily suspended in the media. The GAS media used in the bioreactor vessels did not contain Tween and therefore a very high degree of cording took place. The tendency for *Mtb* to form clumps may have an effect on the efficiency of density gradient centrifugation to enrich for viability by retaining a degree of non-viable cells by cording together. However, this notion may not be accurate according to Hunter *et al.* (2006) where they characterize the cord factors role in pellicle formation of virulent mycobacteria. They describe from their study that cord factor, or trehalose dimycolate (TDM) may act as a free mycolic acid that is not covalently bonded to the cell wall and thus most likely are not retained by non-viable bacilli. However, the work done by Hunter and colleagues (2006) does not directly address this conundrum [52].

Certainly, the results shown in this study still warrant further investigation. Investing in more accurate methods to quantitate the total number of bacilli present and the number of viable bacilli would deliver a more accurate enumeration of viability. One method to obtain accurate cell counts could be done by flow cytometry (FCM) with SYTO9 and propidium iodide (PI) staining. In a relatively recent study, FCM-SYTO9/PI methods were used to distinguish between live and dead *Mtb* as SYTO9 is able to penetrate into the bacilli and form covalent bonds with the genome, however PI is only able to penetrate dead cells as the membrane permeability has been lost. Soejima *et al.* (2009) were also able to distinguish between injured-viable cells with the addition of ethidium monoazide (EMA) and UV light [43]. The draw back to this method in the case of the bioreactor culture described here is that in order to perform FCM, the culture must be evenly suspended which again would require Tween media.

In addition to utilizing alternative means to quantitate live and dead bacilli, a more sensitive Percoll gradient may also be applied to give more apparent separation of the *Mtb* propagated in cultures with and without oxygen tension. Optimizing a continuous Percoll density gradient to be more discrete around the densities of 1.08 g/ml and 1.12 g/ml, as observed in this study (see Appendix 7.1), could be generated via high speed ultra-centrifugation. One opposition to this method would be whether or not the tubercle bacilli would be able to withstand such incredible centrifugation forces. A publication in the American Society of Microbiology Journal offers a depiction of the cell surface damage due to centrifugation. This gives evidence that with increasing centrifugation speeds cause compaction of the cells and those collisions against each other result in shear forces that damage the bacterial cell surface [53]. Even though the mentioned study did not include mycobacteria, the same principle could be insinuated, especially taking into account the ultra-high speeds needed to generate such a specific Percoll gradient. Nonetheless the specific optimized Percoll gradient could be generated first without the addition of the *Mtb* culture overlaid onto the already prepared gradient and samples centrifuged at 400xg for 15 minutes as performed in this study. That would alleviate the compaction forces of ultra-centrifugation.

In conclusion, here we describe a method of separating *Mtb* H_{37}Rv metabolic phenotypes propagated in bioreactors via a discontinuous Percoll density gradient centrifugation. The evidence provided in this study shows promise towards the enrichment of viable culture by separation by buoyancy, as well as a means to observe different metabolic states of *Mtb* such as active and dormant phenotypes. Viable enrichment of the final *Mtb*

culture product could provide more accuracy in downstream applications by providing a more consistent population without the mask of contaminating dead bacilli.

4.0 Ch.4 Aim 3 Viability assessment and Viable but Non-Culturable cells

4.1 Introduction

4.2 Methods

4.3 Results

4.4 Discussion

4.1 Introduction

Several methods have been proposed in the past to investigate viable but non-culturable (VBNC) *Mtb*. As touched on in chapter 1, Wayne *et. al.* (1996) utilized the concentration of ATP and growth dynamics to hypothesize the VBNC phenotype [24]. However, in the case of this study, an ATP luciferase assay did not deliver data in real time as the temporal cell samples were lysed for total ATP concentration analysis. Furthermore, quantitative PCR methods were also attempted to determine the extent of the VBNC phenomenon as investigators found enough nucleic transcripts to insinuate several logs of bacilli to be present in tissue homogenates even though they were determined to be culture negative [23]. As sensitive as qPCR may be, this method was unable to distinguish between live, dead or treatment-injured cells since it measures amplified DNA. Finally, much more recently, methods of fluorescent staining have been able to distinguish between live, dead and injured cells. Using traditional methods of fluorescent staining by SYTO9 and PI to stain live and dead bacteria, an addition of ethidium monoazide and UV light was also able to differentially stain sub-populations of live cells due to the active transport of ethidium monoazide out of the metabolically active cell while ethidium monoazide is retained in live metabolically dormant cells where it can crosslink with the DNA by the UV light [11]. However, with this method, expensive fluorescent microscopy equipment is required. What is needed is a low cost assay that can detect the metabolic rates of cellular respiration in real time and be able to distinguish between not only live and dead bacilli, but metabolically altered phenotypes as well.

The Alamar Blue dye viability assay is an effective means to test for viability of a culture of *Mtb* subjected to a treatment [54]. The assay is much faster, taking only three to four days, rather than the traditional means of streaking on LJ slants which takes over two weeks. Active viable and VBNC cells both carry out metabolic processes for respiration, even though the latter is described to be very minimal, the reactions can still be detected by

sensitive assays. One particular assay utilizes the dye p-iodonitrotetrazoliom (INT) violet that is based on the electron transport system activity. The dye is a soluble tetrazolium salt that competes with oxygen as the final electron acceptor and is reduced to the insoluble compound formazan. INT is a blue color, however when it is reduced to formazan it becomes pink [55]. The reduction of the dye causes a colorimetric change from blue to pink by the reduction of INT to formazan that can be read for absorbance by spectrophotometry. The Alamar Blue dye also reacts to redox reactions produced by active cellular respiration. Alamar blue is the commercial name for resazurin (7-Hydroxy-3*H*-phenoxazin-3-one 10-oxide), which is also a tetrazolium salt and in the same manner is reduced to resorufin that is a pink insoluble compound [56]. Here we used the Alamar blue dye assay to interrogate the level of viability of *Mtb* produced in the bioreactor system and enriched for cell viability as discussed previously.

Alamar blue has an absorbance wavelength of 570nm, so by analyzing the value of absorbance at 570nm from the dye over the absorbance at 630nm from the cells, the amount of resazurin can be relatively quantitated. By plotting the absorbance over time the rate of respiration can be obtained. When the rate of respiration is analyzed in frame with colony forming units (CFU) and Petroff-Hausser (P-H) counts of the culture, this could shed some light on understanding the extent of VBNC *Mtb* present [54]. However, first a standard curve needs to be generated from active *Mtb* in order to develop a standard rate of respiration of healthy untreated cells. Utilizing a standard rate of respiration should give an expression that can bridge the gap between the rate of respiration of a treated sample and the number of CFUs that can be expected. The difference between the estimated number of CFUs and the observed number of CFUs for a treated sample may give an indication of a VBNC population.

4.2 Materials and methods

4.2.1 Generation of standard curve control

First a standard curve must be made from active *Mtb*. This was done using *Mtb* H_{37}Rv. Briefly, a 1ml frozen glycerol stock was thawed, transferred to a 1.7ml microcentrifuge tube and centrifuged at 14K RPM for 10 minutes in a microcentrifuge to pellet the cells. The supernatant was discarded and the pellet was washed with 1ml PBS, spun down to pellet at 14K RPM for 10 minutes in a microcentrifuge. The supernatant was discarded and the washed pellet was resuspended in 1ml of 7H9 media. The washed and resuspended cells were transferred to

3ml of 7H9 media containing OADC and 0.05% Tween in a 15ml conical tube and incubated for 24 hours at 37°C on an orbital shaker. Using the activated 4ml cell culture, 1ml samples were made at a concentration of optical density (OD_{600}) 1.0, 0.6, 0.4, and 0.1. Each of the four *Mtb* concentrations were serially diluted and were plated in triplicate on 7H11 agar, incubated for 16 days at 37°C for CFU counts, and analyzed via microscopy for P-H counts via a hemocytometer.

4.2.2 Preparation of standard curve Alamar Blue assay

200ul of each of the four OD_{600} concentrations were taken (in triplet), transferred to a 96-well flat bottom plate and serially diluted 1000-fold in 7H9 media with OADC and 0.05% Tween. Alamar blue dye (ThermoFisher) was added to each well at a 1:10 dilution and the plate was wrapped in foil and incubated at 37°C. Absorbance reading of 570nm and 630nm were taken at 24 hour intervals for 3 days.

4.2.3 Preparation of Alamar Blue assay of bioreactor paired cultures

Secondly, 200ul of each bioreactor sample, as described in chapter 2 (in quadruplet), obtained from the density gradient separated extracts N1-N3 and H1-H3 from a discontinuous density centrifugation in a 15ml conical tube, as described in chapter 3, were transferred to a 96-well flat bottom plate and serially diluted 1000-fold in 7H9 media with OADC and 0.05% Tween. Alamar Blue was added to each well at a 1:10 dilution, the plate was wrapped in foil and incubated at 37°C, and absorbance readings of 570nm and 630nm were taken at 24 hour intervals over 3 days as above.

4.3 Results

4.3.1 Standard rate of respiration

In order to generate a standard curve of the rate of respiration of *Mtb* $H_{37}Rv$, the absorbance ratio of 570nm/630nm was determined by spectrophotometry at 24 hour intervals of standard samples at an OD_{600} of 1.0, 0.6, 0.4 and 0.1. The rate of absorbance was plotted in respect to time (Figure 4.1). By generating a trend line for each OD_{600} of *Mtb*, an OD_{600} of 1.0 gave a respiration rate of 0.695, while an OD of 0.6, 0.4 and 0.1 gave respiration rates of 0.100, 0.0515 and -0.0387, respectively.

From here, a relationship can be determined between the rate of respiration, total number of cells via P-H methods and number of viable cells via plating for CFUs. At an OD_{600} of 1.0, the rate of respiration was determined

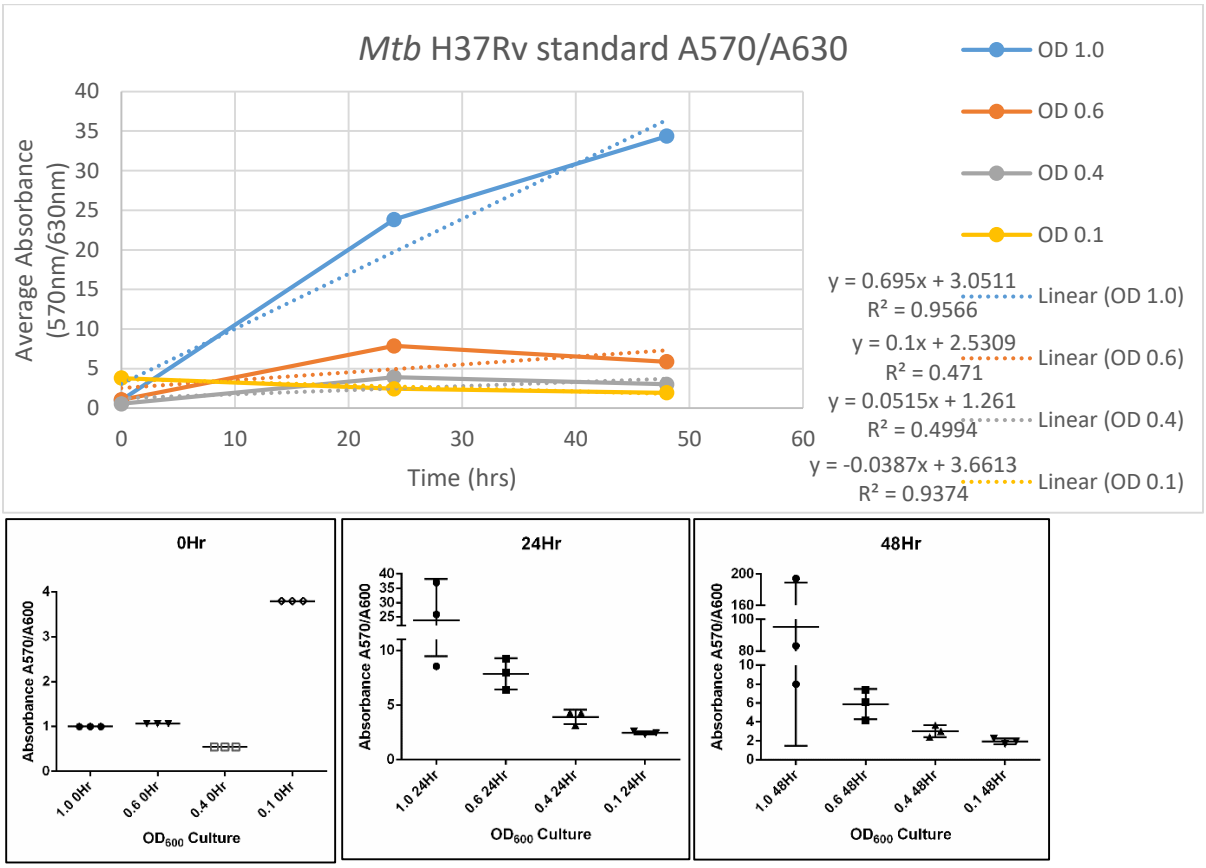

Figure 4.1

Mtb $H_{37}Rv$ standard rate of respiration. Alamar Blue dye assay was used to measure the rate of resazurin reduction due to active respiration. The absorbance of A570/A630 was taken at 24 hour time points. For the standard deviations: raw values presented as diamonds, circles, squares and triangles; horizontal bars indicate average; vertical bars indicate standard deviation.

to be 0.695, while the P-H and CFU counts showed $1.12x10^9$ cells/ml and $2.61x10^8$ CFU/ml, respectively. This gave a viability of 23.3%, a 4.29-fold difference between the total number of cells and viable cells. At an OD_{600} of 0.6, the rate of respiration was determined to be 0.100, while the P-H and CFU counts showed $1.83x10^8$ cells/ml and $1.37x10^8$ CFU/ml, respectively. This gave a viability of 74.86%, a 1.34-fold difference between the total number of cells and viable cells. At an OD_{600} of 0.4, the rate of respiration was determined to be 0.0515, while the P-H and CFU counts showed $1.00x10^8$ cells/ml and $9.12x10^7$ CFU/ml, respectively. This give a viability of 91.2%, a 1.10-fold difference between the total number of cells and viable cells. Finally, at an OD_{600} of 0.1, the rate of respiration was

determined to be -0.0387, while the P-H and CFU counts showed $4.38x10^7$ cells/ml and $2.43x10^7$ CFU/ml, respectively. This gave a viability of 55.48%, a 1.80-fold difference between the total number of cells and viable cells (Table 4.1).

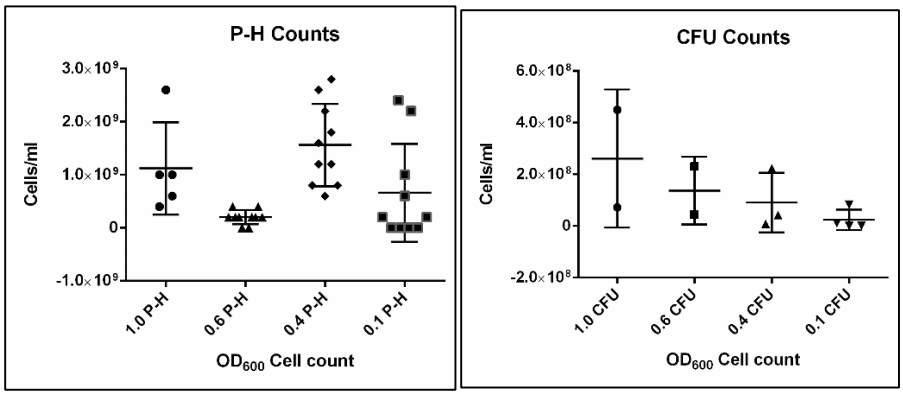

Figure 4.2

The averages of the replicates increase in viability are summarized in the Table 4.1. For these counts: raw values presented as diamonds, circles, squares and triangles; horizontal bars indicate average; vertical bars indicate standard deviation.

Table 4.1

Relationship between the rate of respiration, total number of cells and number of viable cells of *Mtb* $H_{37}Rv$.

Table 4.1 Standard rate of respiration and culture viability				
OD_{600}	Rate of respiration	Petroff-Hausser (cells/ml)	Colony Forming Units (CFU/ml)	Percent viability
1	0.695	$1.12x10^9$	$2.61x10^8$	23.30%
0.6	0.1	$1.83x10^8$	$1.37x10^8$	74.86%
0.4	0.0515	$1.00x10^8$	$9.12x10^7$	91.20%
0.1	-0.0387	$4.38x10^7$	$2.43x10^7$	55.48%

4.3.2 Relationship between standard rate of respiration and expected CFUs

Using the number of total cells obtained by P-H methods to create a relationship between the rate of respiration and the number of viable cells, the P-H counts for total number of cells were plotted on an x-axis with both the rate of respiration and the CFU counts for number of viable bacilli on the y-axis (Figure 4.3). Adjusting the trend lines to the rate of respiration in regards to total number of cells and the number of CFUs in regards to total

number of cells, defined the following relationship:

Expected CFU=0.1827((rate of respiration+0.0347)/7x10^{-10})+6x10^{7}

Using this relationship, the number of expected CFUs can be determined based on the rate of respiration from a treated sample. In this study the treated samples were *Mtb* grown in bioreactors with dissolved oxygen

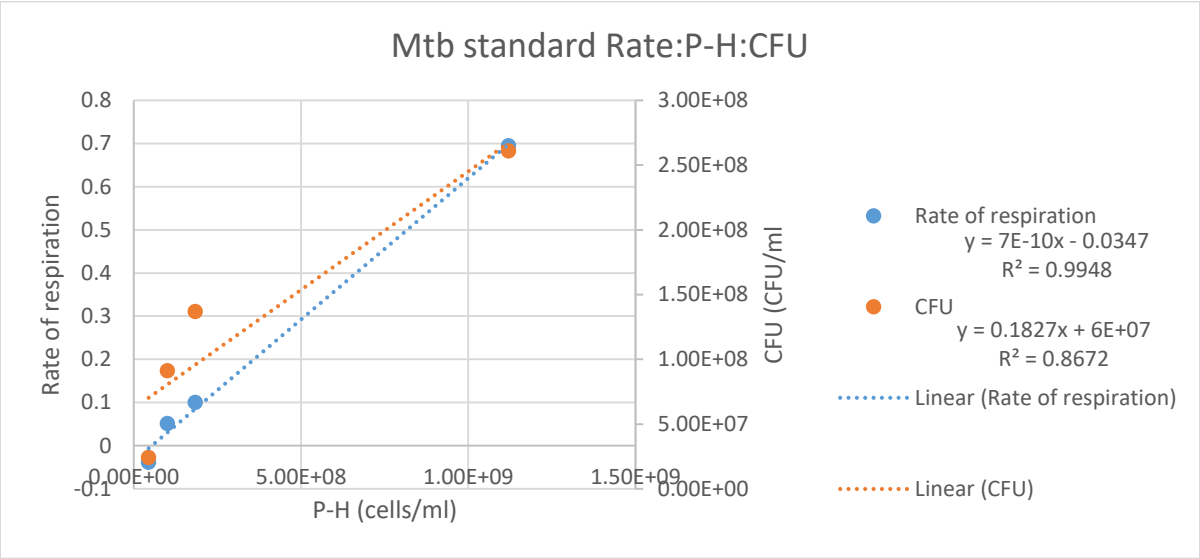

Figure 4.3

The relationship between the rate of respiration and expected number of CFUs. Plot of respiration rate and CFUs over total number of cells of *Mtb* $H_{37}Rv$ at OD_{600} 1.0, 0.6, 0.4 and 0.1.

concentration as the variable and enriched for viability via a discontinuous density gradient centrifugation. By comparing the expected number of CFUs, based on the standard curve, to the actual CFUs observed from the treated sample, we hypothesize that the difference between expected and actual CFU represents the number of VBNC cells present in the sample.

4.3.3 Respiration rate of bioreactor pairs enriched for viability

Using the Alamar blue dye assay, the rate respiration was determined for the normoxic and hypoxic cell products produced as described in chapter 2. The assay was performed after each bioreactor product was separated by a discontinuous Percoll density gradient centrifugation in a 15ml conical tube, as described in chapter 3 (Figure 4.4). The enriched cell products harvested from the normoxic vessels N1, N2 and N3 show a rate of respiration of 0.0638, 0.0035 and 0.0498, respectively. The enriched cell products harvested from the hypoxic vessels H1, H2 and H3 show a rate of respiration of 0.3349, 0.2307 and 0.1878, respectively.

4.3.4 Estimation of VBNC population

From here, using the relationship established by the *Mtb* standard control, the rate of each of the replicates can be inserted into the equation to produce the expected number of CFUs based on the rate of

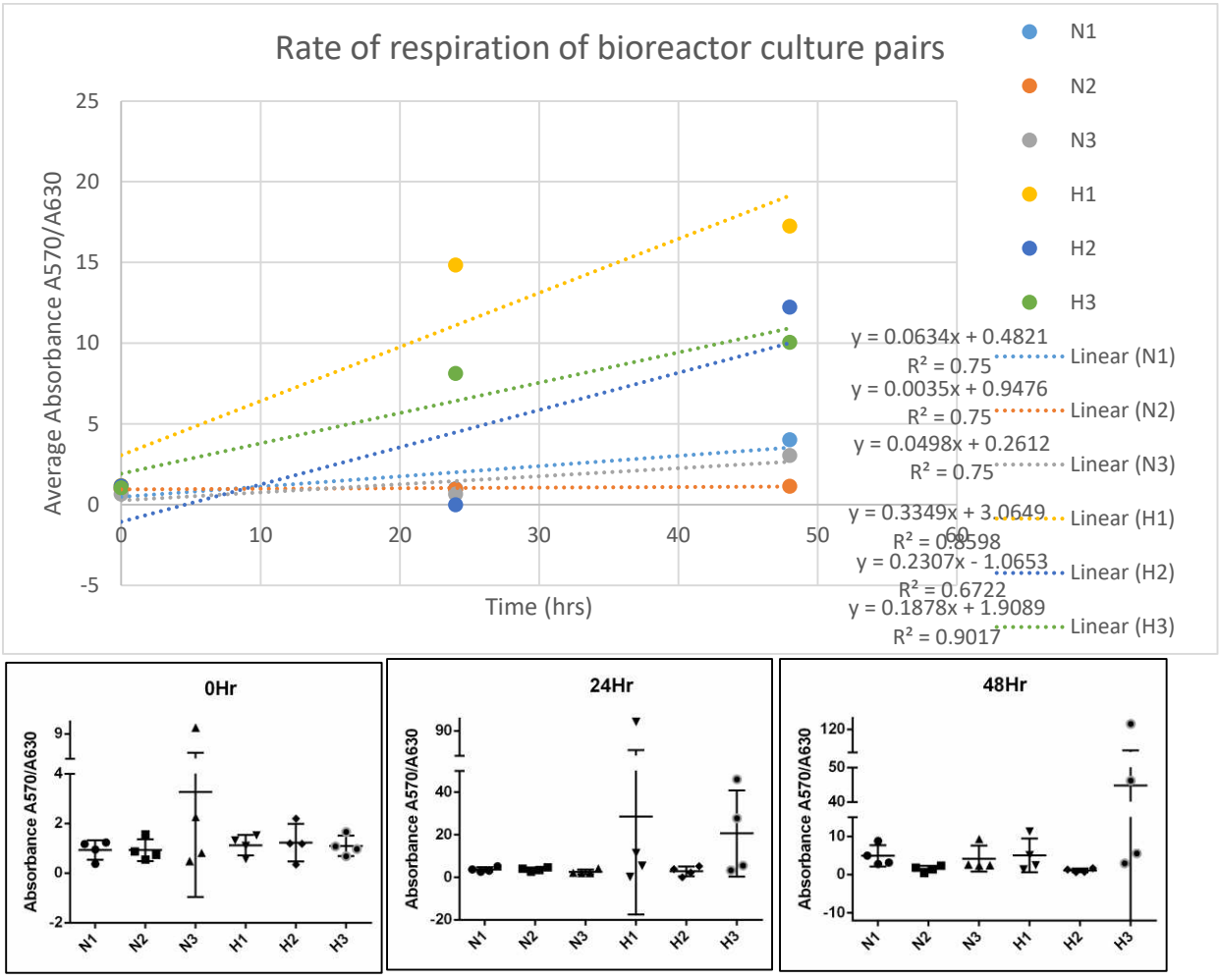

Figure 4.4

Rate of respiration of the extracted fractions from the discontinuous Percoll density gradient centrifugation of 1ml of *Mtb* $H_{37}Rv$ cells produced in bioreactors with oxygen availability as the variable. Replicates N1, N2 and N3 were propagated under normoxic conditions. Replicates H1, H2 and H3 were propagated under hypoxic condition. For the standard deviations: raw values presented as diamonds, circles, squares and triangles; horizontal bars indicate average; vertical bars indicate standard deviation.

respiration (Table 4.2). Replicate N1 had a rate of 0.0634, which would estimate $8.56x10^7$ CFU/ml, compared to the observed number of $2.46x10^8$ CFU/ml. This would give a difference of $-1.60x10^8$ CFU/ml. Replicate N2 had a rate of 0.0035, which would estimate $7.00x10^7$ CFU/ml, compared to the observed number of $1.08x10^7$ CFU/ml. This would give a difference of $5.92x10^7$ CFU/ml. Replicate N3 had a rate of 0.498, which would estimate $8.21x10^7$

CFU/ml, compared to the observed number of $6.05x10^7$ CFU/ml. This would give a difference of $2.16x10^7$ CFU/ml. Replicate H1 had a rate of 0.3349, which would estimate $1.56x10^8$ CFU/ml, compared to the observed number of $8.79x10^7$ CFU/ml. This would give a difference of $6.86x10^7$ CFU/ml. Replicate H2 had a rate of 0.2307, which would estimate $1.29x10^8$ CFU/ml, compared to the observed number of $9.67x10^6$ CFU/ml. This would give a difference of $1.20x10^8$ CFU/ml. Replicate H3 had a rate of 0. 1878, which would estimate $1.18x10^8$ CFU/ml, compared to the observed number of $6.03x10^7$ CFU/ml. This would give a difference of $5.78x10^7$ CFU/ml.

Table 4.2

The rate of resazurin reduction was measured by Alamar Blue assay for three replicates of paired cultures of *Mtb* $H_{37}Rv$ propagated in bioreactors and enriched for viability. Replicates N1, N2 and N3 represent normoxic cultures. Replicates H1, H2 and H3 represent hypoxic cultures. CFUs were determined by plating on 7H11 agar and P-H counts were determined by microscopy. The estimated number of CFUs was determined by the standard curve of respiration relationship. The difference is in terms of the difference in observed CFUs and the expected CFUs based on the rate of respiration.

Table 4.2 Estimated population of Viable but non-culturable *Mtb*

Replicate	Rate of Respiration	Petroff-Hausser (cells/ml)	Colony Forming Units (CFU/ml)	Percent Viable	Estimated CFU/ml	Difference	Percent VBNC
N1	0.0634	$1.44x10^9$	$2.46x10^8$	17.08%	$8.56x10^7$	*	**
N2	0.0035	$1.33x10^9$	$1.08x10^7$	0.81%	$7.00x10^7$	$5.92x10^7$	4.49%
N3	0.0498	$3.33x10^8$	$6.05x10^7$	18.17%	$8.21x10^7$	$2.16x10^7$	7.91%
H1	0.3349	$6.67x10^8$	$8.79x10^7$	13.18%	$1.56x10^8$	$6.86x10^7$	11.84%
H2	0.2307	$7.78x10^8$	$9.67x10^6$	1.24%	$1.29x10^8$	$1.20x10^8$	15.57%
H3	0.1878	$5.56x10^8$	$6.03x10^7$	10.85%	$1.18x10^8$	$5.78x10^7$	11.65%

* The difference was negative and thus the VBNC formula could not be applied.
** Indeterminate.

Given the difference between the estimated number of CFUs that should be seen based on the rate of respiration, and the actual observed CFUs, an estimated percentage of VBNC can be determined. Using the number of perceived dead cells by the difference of observed CFUs and total number of bacilli via P-H, and the difference of how many more viable cells should be present based on the rate of respiration, the percentage of the perceived dead cells that are actually VBNC is described. Replicates N1, N2 and N3 produced under normoxic conditions and enriched for viability show that 4.49% and 7.91% (n=2, average 6.35%), respectively, of the

perceived dead cells are actually VBNC. Replicates H1, H2 and H3 produced under hypoxic conditions and enriched for viability show that 11.84%, 15.57% and 11.65% (n=3, average 13.02%), respectively, of the perceived dead cells are actually VBNC.

4.4 Discussion

Here, *Mtb* H_{37}Rv was propagated under defined oxygen conditions in bioreactors and enriched for viability via density gradient centrifugation. Alternatively, the control culture was generated by traditional *Mtb* propagation in 7H9 media with OADC and Tween and grown to late-mid log phase in an Erlenmeyer flask with gentle shaking at 37°C. In this study, an Alamar Blue assay was used to develop a standard rate of respiration of *Mtb* H_{37}Rv grown to mid-log phase by traditional culture methods. Using a series of optical densities, the results of the rates of respiration were as one would expect, where a standard rate OD_{600} of 1.0 gave the highest rate of resazurin reduction per hour while the lowest OD_{600} of 0.1 was relatively undetectable (Figure 4.1). Interesting enough the standard OD_{600} of 1.0 also showed to have to lowest viability of 23.3%. With that said, the viability across the OD_{600} range of 1.0, 0.6, 0.4 and 0.1 was quite variable (Table 4.1) even though they were diluted from the same culture containing Tween in the growth media. This may again represent error in the dense cultures.

Deriving a linear relationship between the rate of respiration and the total number of cells, then intercalating the total number into the linear relationship between the total number of cells and the number of viable CFUs, delivers a simplified means to estimate the expected number of viable CFUs that would be expected based on the rate of resazurin reduction from the Alamar Blue assay (Figure 4.3). This method uses the number of total cells, live and dead, as a bridge to calculate the number of expected CFUs based on the rate of respiration of the treated culture, using the standard rates derived from the standard curve of actively growing *Mtb*. In this study the treated cultures were propagated in bioreactors in an environment rich in oxygen and devoid of oxygen. Based on the calculations given in chapter 2 and chapter 3, it can be reasonable to say the treated cultures represent active and dormant *Mtb* populations, and thus should maintain differential populations of VBNC *Mtb*.

It is important to note, that counting colony forming units only gives an accurate estimation of the number of viable bacilli, especially when no detergent is used to break up the serpentine cording of the *Mtb in vitro*. Furthermore, this estimation is most likely an underestimation due to a suspected population of VBNC *Mtb*

that are viable but have lost the ability to grow by standard culture methods. Therefore, when taking the difference between the total number of bacilli and the number of colony forming units to inquire a number of dead, non-viable bacilli, a fraction of the perceived dead bacilli is actually of the VBNC phenotype.

It is satisfactory to observe that hypoxic cultures demonstrate a greater number of VBNC as previous literature indicates this phenotype is induced under environmental stress. Also, the percent of VBNC bacilli for each replicate does not seem to be conditional to the initial viability as seen from replicates N2 and H2. Based on the standard relationship of respiration and expected CFUs, using the rates of respiration form the bioreactor pairs derived from the Alamar Blue assay, the expected number of CFUs were determined for each replicate. The expected number of CFUs were all higher than the observed number of CFUs for each replicate except N1 (Table 4.2). This indicating that there are more viable bacilli that were not able to grow on standard 7H11 agar, whereas replicate N1 indicated a higher number of observed CFUs contradictory to its rate of resazurin reduction. However, the difference of how many more viable bacilli present in the sample, based on its rate of respiration, can be interrogated over the number of perceived non-viable bacilli. This interrogation equates to a percentage of the perceived dead bacilli that are actually viable but non-culturable.

It was very interesting to see that the replicates grown under oxygen tension that seem to be indicative of *Mtb* in a bacteriostatic state would have a higher rate of respiration as compared to the actively growing replicates harvested at late-mid log phase (Table 4.2). It has been previously hypothesized that *Mtb* grown in the presence of sufficient oxygen *in vitro* have a higher rate of respiration than *Mtb* grown under hypoxia to NRP stage 1 [57], due to the evidence of a transcriptional down-regulation of the ATP synthase operon and significantly lower cellular ATP levels during dormancy [58]. These results may have been confounded by the number of dead bacilli in the culture. This is contradictory to the observations in this study where the hypoxic bioreactor cultures have over a 4-fold increase in the rate of respiration than the normoxic bioreactor cultures. The possibility may arise that this observation is respiration bias as dormant *Mtb* quickly reactivate once fresh media becomes available as in the case we enriched for viable *Mtb* by density centrifugation and that thin population of the Alamar Blue assay. Reports have indicated that *Mtb* subject to hypoxia for up to seven days are able to regain logarithmic growth in as little as 24 hours' post-reaeration [59]. Perhaps it could be hypothesized that the reactivation of *Mtb* from NRP stage 1 employs a vigorous rate of respiration to regain normal metabolic systems. In dormant mycobacteria, there

is a considerable remodeling of the respiratory chain. Studies have also shown very compelling data that there is a shift and up-regulation of alternative respiration machinery during NRP stage 2 other than NDH-1. In the case of *Mtb*, ATP synthase is required for optimal growth as revealed by high-density mutagenesis [60]. These findings suggest that mycobacterium cannot gain enough energy by substrate level phosphorylation and need respiratory ATP synthase for maintenance during dormancy. Instead NADH is oxidized by a non-proton translocating type-II NADH dehydrogenase (NDH-2) using menaquinone as an electron acceptor [54]. Furthermore, NDH-2 and *Mtb* cytochrome bd oxidase are upregulated during NRP stage 2, and the cytochrome bd oxidase displays a greater affinity for oxygen at low oxygen tension due to a greater number of monomers per subunit c oligomer to facilitate the synthesis of ATP under low proton motive force conditions [61]. The maintenance of an energized membrane during dormancy is critical as *Mtb* has been shown to be able to persist in NRP stage 2 cultures that are not supplemented with the usual external terminal electron acceptors for respiration [28].

Detailed in this study is a simplified method to estimate the fraction of VBNC that may be present in *Mtb* culture based on the rate of resazurin reduction. This method is beneficial as it can help to narrow the underestimation of the number of viable bacilli present in a culture. This is important when interrogating murine or macrophage models with a defined infectious dose. Furthermore, the Alamar Blue assay is a rather inexpensive way to estimate the altered-metabolic phenotype induced by hypoxia, as compared to methods requiring sensitive equipment such as flow cytometry. Here we used the Alamar Blue dye assay to generate a relationship to estimate the number of expected viable colony forming units based on the cultures rate of respiration, then using the expected number of colony forming units, the number of viable but non-culturable *Mtb* present can be reliably estimated.

5.0 Ch. 5 Discussion

Mycobacterium tuberculosis is a global issue, not just in developing countries but for first world countries as well. *Mtb* is the leading cause of death by an infectious agent worldwide with 1.5 million deaths reported in 2014 [1]. The scientific community needs to address novel systems of propagation to generate the reagent materials necessary to expedite the development of novel cost effective diagnostic and treatment means. We need new drugs, or a combination of new and current drugs, etc. to reduce the toxicity and longevity of the current drug treatment. The aspect of safer drug cocktails would also promote the adherence of drug treatment and benefit in the protection of incurring the spread of multiple or extensively drug resistant *Mtb* [6]. The increasing prevalence of drug resistant strains of *Mtb* would also be hindered by the development of novel antibiotics that are capable to assaulting the dormant state of the pathogen where drug susceptibility is observed [25]. The reservoir of latency of *Mtb* within the human population ensures the pathogens continued spread and existence of the deadly pathogen in our communities.

The immunopathogenesis of tuberculosis infection is centered around the formation of the granuloma within the lung. Granuloma formation is induced by the inability of the host immune response to control the proliferation of the bacilli. As the granuloma lesion matures, the center becomes caseous and necrotic. The breakdown of the damaged granulomatic tissue releases dormant tubercle bacilli that reactivate replication and cause active disease [9]. Studies show that the core of the evolved granuloma is an environment of high oxygen tension, in and around the necrotic center [15]. Thus, novel propagation systems capable of maintaining an environment depleted of oxygen are warranted in order to further our understanding of the survivability of *Mtb* under such environmental stress.

Animal models have long been used to study the latent disease state of *Mtb*; attempts to mimic the dormant *Mtb* phenotype *in vitro* have also been proposed [27]. The pioneering literature give irrefutable evidence that *Mtb* can enter into a bacteriostatic state and persist within the granuloma for years or decades, only to reactivate at a later time to cause active disease and continued transmission of the pathogen [17]. The dormant phenotype of *Mtb* is the cause of disease latency, where it survives in a non-replicating persistent state [24], unabated by the harsh environment induced by the lesion [25]. In addition to oxidative stress and acidic pH,

oxygen tension is also prominent inside the granuloma and has been shown to be intimately associated with the induction of the transcriptional shift necessary to enter into the altered metabolic state of *Mtb* during latency [45]. The physiology of the latent bacilli has been incredibly difficult to appropriately study due to an additional phenotypic population of *Mtb* that are still considered viable but have lost the ability to grow *in vitro*, and this sub-population of viable but non-culturable bacilli is characteristic of latent TB [18].

Several *in vitro* models have been characterized to provide a culture environment of oxygen stress, known as hypoxia, with the Wayne model of hypoxia being the most popular [26]. The method of propagation introduced by Wayne in the late 1970s and later expanded on in the mid '90s relies on a self-generated oxygen gradient to induce hypoxic conditions as the bacilli naturally deplete the available oxygen through natural respiration. Hypoxic conditions of one percent or less were shown to induce the non-replicating persistent phenotype congruent to dormant *Mtb* seen *in vivo* [24] giving rise to using *in vitro* culture conditions rather than animal models to interrogate dormant *Mtb*.

Use of animal models for the study of *Mtb* infection has been well documented and has a lengthy historical background, while *in vitro* culture methods have remained relatively unchanged. However, *in vivo* studies require an incredibly high degree of expenses and well as regulation. They also carry a great deal of time restraint, as it takes weeks to grow the *Mtb* to be used in infection, qualify the *Mtb* to be suitable for infection, and then observe the pathogenesis *in vivo*. Thus the procedure takes months to conduct [62]. This becomes further challenging due to the need for specialized equipment, multiple laboratory spaces including biosafety level-3 (BSL-3) space, multiple highly trained personnel and constant monitoring of the animals. This can be extremely laborious when to goal is to extract and interrogate the physiology of the bacilli rather than the immunological response. With a method, as proposed in this study, equipment and reagent cost as well as time is still required, however it carries the need for reduced laboratory space inside the BSL-3 as well as the reduced need for multiple personnel. Furthermore, very little processing of the final product is needed as compared to methods of extracting *Mtb* from tissue [18]. The amount of insult delivered to mycobacteria during extraction from tissue has been questioned for some time. In one study, it was found that *Mycobacterium leprae* purified from armadillo liver only retained approximately 10% of the features of typical mycobacterial cells including a three-layer cell wall, regular cytoplasmic membrane with inclusions, and a granulated cytoplasmic membrane with observed 14nm ribosomes

[16]. This study was done using SEM and the comparative mycobacterial model was *M. avium* that was able to retain 95% of the typical observed characteristics as it was grown by culture methods. Therefore, a method of *Mtb* propagation that can induce the metabolic phenotypes of *Mtb* seen *in vivo* would be an ideal product for investigation as the bacillary product is left unharmed.

One of the major challenges to traditional culture methods to target the differential metabolic state of latent TB is the inability of existing models to observe the full range of phenotypes as *Mtb* are shown to exist in single micro-environments [11]. Bioreactors have been previously used to generate reproducible cultures of BCG with high viability [40]. Bioreactor systems provide direct control and consistency of the culture environment and thus could be ideal to induce the differential metabolic phenotypes characteristic to non-replicating dormant *Mtb*.

In this study, we used the Bioflo 115 bioreactor system with 5L CelliGen Blue vessels to culture three replicates of *Mtb* H_{37}Rv pairs grown in GAS media, one in normoxic conditions of 35% DO and the pair in hypoxic conditions of 1% or less DO. Each culture was propagated for ten-days in their respective culture conditions. Using western blot analysis, we were able to show a relative increase in abundance of the hypoxia marker, Acr, from hypoxic culture lysates, indicating induction of *Mtb* to a dormant state.

It has been expressed that the environment inside the granuloma is not only hypoxic, but nutrient starved as well [27]. This had led investigators to try and understand how *Mtb* are able to survive and persist. Transcriptional studies indicate that during environmental stress, *Mtb* upregulate the production of an array of lipids including mycolic acids. It is suggested that they are used as energy stores during dormancy [49]. Previous evidence shows an increase in buoyancy of *Mtb* due to an increase in lipid load during the temporal adaptation to hypoxia [27]. This led to the assumption that the active and dormant phenotypes of *Mtb* could be separated based on their buoyant nature when subject to a density gradient. Furthermore, on the same principle, it could also be assumed that a density gradient based centrifugation method could also remove the non-viable dead bacilli present in the culture, or at the very least enrich the culture for viability [50]. This would allow for higher accuracy in downstream interrogations that might be masked by an over abundancy of dead bacilli.

As described earlier, there is a high degree of die off as the bacilli that are not fit enough to fully adapt to hypoxia succumb to the environmental stress as the level of oxygen is limited. The temporal range of non-viable bacilli fastened to their transcriptional profile could skew the true transcriptional profile of the bacilli able to enter

into true bacteriostasis. Enriching the cell culture for viable bacilli under hypoxia could bear higher accuracy when the transcriptome is questioned.

In this study, we used a discontinuous Percoll density gradient centrifugation method to enrich the final bacillary biomass for viability that was generated from *Mtb* grown in normoxic and hypoxic environments using the bioreactor system. This method resulted in a marked increase of over 4-fold in viability with the normoxic bioreactor cultures and over a 2-fold increase in viability with the hypoxic bioreactor cultures. However, this increase did not show a higher viability than *Mtb* cultures grown by traditional means in an Erlenmeyer flask incubated with gentle shaking.

The benefit to applying a gradient capable of fractioning culture sub-populations by buoyancy also provided a means of observing the different physiology of the metabolic states of *Mtb* under normoxic and hypoxic conditions. In this study we were able to show a distinct increase in buoyancy of the hypoxic *Mtb* grown in bioreactors as compared to their paired normoxic cultures. The observation of an increase in cell wall lipids of dormant *Mtb* has been readily characterized [48], however here we were able to fractionate three distinct populations of *Mtb* at notably different densities, from the same test culture, further corroborating that *Mtb* can exist in multiple populations within the same relative micro-environment [11].

The concept of the viable but non-culturable phenotype of *Mtb* has troubled researchers for decades [22]. The arduous task to evaluate this population is critical when defined infection models are required. Traditional techniques of determining viable bacilli by counting colony forming units give an underestimation of the true number of viable units, as even the non-culturable sub-population is able to cause disease as shown in *in vivo* murine models [18]. However, just because VBNC bacilli are not able to grow on traditional 7H11 agar for counting, that does not mean that they do not carry out metabolic processes that can be evaluated by their electron transport chain activity.

In this study, we developed an Alamar Blue assay as a means to resolve the probable burden of VBNC *Mtb* in normoxic and hypoxic cultures propagated in bioreactors and enriched for viability through density gradient centrifugation. The molecule resazurin of the Alamar Blue dye acts as a final electron acceptor in the electron transport chain and is reduced to resorufin, causing a colorimetric change that can be detected by spectrophotometry. Here we were able to devise a relationship between the rate of respiration of a culture and

the number of viable colony forming units using a standard curve of *Mtb* grown by traditional means in an Erlenmeyer flask incubated with gentle shaking. This relationship, when used to solve for CFUs based on the rate of resazurin reduction of the normoxic and hypoxic cultures propagated in bioreactors and enriched for viability by density gradient centrifugation, produced a number of CFUs that would have been expected based on their respiration rate. The difference between the expected number of CFUs and the observed number of CFUs indicate a population of VBNC *Mtb*. Interestingly enough, in this study we observed a 2 to 4-fold increase in the percent of VBNC *Mtb* from the hypoxic bioreactor cultures over the normoxic bioreactor cultures. This observation is supported by studies that show compelling evidence that the VBNC phenotype is indicative to disease latency and non-replicative persistence [24].

The WHO's End TB Strategy contains a call out for intensified research and innovation in order to stop the global burden of TB in our lifetime. They ask for innovation in discovery, development and rapid uptake of new tools, interventions and strategies. They want research to optimize implementation and impact, and promote further innovations [63]. It can be said that our efforts thus far have not been able to meet these goals of controlling TB in the next fifty years. Thus we need to expand the availability of quality *Mtb* reagents and materials for research purposes. Procuring a method to produce large scale cellular materials of *Mtb* that can mirror the alternative physiological states described during infection will expedite the accuracy of our analysis to develop novel drugs, vaccines and diagnostics.

In the presence of this study, it is promising to narrate a novel method of producing high quality cultures of *Mtb* in a wide range of observed phenotypes. Despite the limitations of this study, the proposed method may lay the foundation to promote novel research needed to meet the goals set forth by the End TB Strategy, such as novel, non-invasive point of care diagnostics like a breathalyzer to detect TB infection (see Appendix 7.2). Due to the novelty of this approach, certainly further interrogation of continued replicates is required for confidence. Furthermore, it would be interesting to see how the *Mtb* products produced by the method in this study would correlate in downstream *in vivo* or systems biology approaches, as these studies have yet to be investigated.

In conclusion, here we developed a novel method of propagation of *Mtb* in bioreactors under variable oxygen tension to produced cultures enriched for viability to remove transcriptional bias, and interrogated the abundance of VBNC *Mtb* for increased accuracy of infectious dose. This approach may lead to higher quality

research products that could further our understanding of the mechanisms of TB infection and the development of improved diagnostics, vaccines, and treatment procedures.

6.0 References

[1] WHO TB Report (2015).

[2] Castelnuovo, B. (2010) A review for compliance to anti tuberculosis treatment and risk factors for defaulting treatment in Sub Saharan Africa. African Health Sciences. 10(4): 320-324.

[3] WHO, Media centre. Tuberculosis: factsheet. March 2016. http://www.who.int/mediacentre/factsheets/fs104/en/.

[4] Gulbay, B., *et al.* (2006) Side effects due to primary antituberculosis drugs during the initial phase of therapy in 1149 hospitalized patients for tuberculosis. Respiratory Medicine. 100: 1834-1842.

[5] Comstock, G. W. (2000) How Much Isoniazid Is Needed for Prevention of Tuberculosis among Immunocompetent Adults? In Reply. *International Journal of Tuberculosis and Lung Disease.* 4: 485–86.

[6] Garner, P., *et al.* (2007) Promoting adherence to tuberculosis treatment. *Bull World Health Organ*. 85: 404-6.

[7] Centers for Disease Control and Prevention. The role of BCG vaccine in the prevention and control of tuberculosis in the United States: a joint statement by the Advisory Council for the Elimination of Tuberculosis and the Advisory Committee on Immunization Practices. MMWR 1996; 45 (No. RR-4).

[8] Deuffic-Burban, S., *et al.* (2010) Cost-effectiveness of QuantiFERON-TB test vs. tuberculin skin test in the diagnosis of latent tuberculosis infection. Int. J. Tuberc. Lung Dis. 14(4): 471-481.

[9] Guirado, E., *et al.* (2013) Modeling the *Mycobacterium tuberculosis* granuloma- the critical battlefield in host immunity and disease. Frontiers in Immunology. April, vol. 4, article 98. DOI: 10.3389/fimmu.2013.00098.

[10] Canetti, G. (1955) The Tubercle Bacillus in the Pulmonary Lesion of Man; Histobacteriology and its bearing on the therapy of pulmonary tuberculosis. New York: Springer Publishing Company, Inc.

[11] Ryan, G. J., *et al.* (2010) Multiple *M. tuberculosis* phenotypes in mouse and guinea pig lung tissue revealed by a dual-staining approach. PLoS ONE. 5: e11108.

[12] Dharmadhikari, A. S., *et al.* (2008) What Animal Models Teach Humans about Tuberculosis. American Journal of Respiratory Cell and Molecular Biology. 39(5): 503-508. DOI: 10.1165/rcmb.2008-0154TR.

[13] Hoft, D. R., *et al.* (2011) Location of Intra- and Extracellular *M. tuberculosis* Populations in Lungs of Mice and Guinea Pigs during Disease Progression and after Drug Treatment. PLoS ONE. 6(3): e17550. DOI:10.1371/journal.pone.0017550.

[14] Turner, O. C., *et al.* (2003) Immunopathogenesis of pulmonary granulomas in the guinea pig after infection with *Mycobacterium tuberculosis*. Infect Immun. 71: 864–871.

[15] Lenaerts, A. J., *et al.* (2007) Location of persisting mycobacteria in a Guinea pig model of tuberculosis revealed by r207910. Antimicrob Agents Chemother. 51: 3338–3345.

[16] Rastogi, N., *et al.* (1982) Comparative ultrastructure of *Mycobacterium leprae* and *M. avium* grown in experimental hosts. Ann Microbiol. 133(B): 109-128.

[17] Saviola, B., *et al.* (2013) *Mycobacterium tuberculosis* adaptation to survival in a human host. Tuberculosis-Current Issues in Diagnosis and Management. DOI: 10.5772/54956.

[18] Mccune, R. M., *et al.* (1966) Microbial persistence. II. Characteristics of the sterile state of tubercle bacilli. J Exp Med. 123:469–486.

[19] Kell, D.B., *et al.* (1998) Viability and activity in readily culturable bacteria: a review and discussion of the practical issues. Antonie van Leeuwenhoek. 73: 169-187.

[20] Paul, S., *et al.* (1996) Comparable growth of virulent and avirulent *Mycobacterium tuberculosis* in human macrophages *in vitro*. J. Infect. Dis. 174: 105-112.

[21] Biketov, S., *et al.* (2000) Culturability of *Mycobacterium tuberculosis* cells isolated from murine macrophages: a bacterial growth factor promotes recovery. FEMS Immunology and Medical Microbiology. 29: 233-240.

[22] Li, L., *et al.* (2014) The importance of the viable but non-culturable state in human bacterial pathogens. Frontiers in Microbiology, Review Article. June 2, 2014. DOI: 10.3389/fmicb.2014.00258.

[23] de Wit, D., *et al.* (1995) The bacterial DNA content of mouse organs in the Cornell model of dormant tuberculosis. Tuberc. Lung Dis. 76: 555-562.

[24] Wayne, L., *et al.* (1996) An in-vitro model for sequential study of shiftdown of *Mycobacterium tuberculosis* through two stages of non-replicating persistence. Infection and Immunity. June 64(6) 2062-2069.

[25] Rustad, T., *et al.* (2006) Microreview, Hypoxia: a window into *Mycobacterium tuberculosis* latency. Cellular Microbiology. 11(8), 1151-1159. DOI: 10.1111/j.1462-5822.2009.01325.x.

[26] Wayne, L. G. (1977) Synchronized replication of *Mycobacterium tuberculosis*. Infect. Immun. 17: 528–530.

[27] Deb, C., *et al.* (2009) A novel *in vitro* multiple-stress dormancy model for *Mycobacterium tuberculosis* generates a lipid-loaded, drug-tolerant, dormant pathogen. PLoS ONE. June, 4(6).

[28] Adler, J. J., *et al.* (1996) Transmission and pathogenesis of tuberculosis. In *Tuberculosis*. Rom, W.N. and Garay, S.M. (eds). Boston: Little, Brown, pp. 129–140.

[29] Medlar, E. M., *et al.* (1936) A study of the pathology of experimental pulmonary tuberculosis in the rabbit. Am Rev Tuberc. 34: 456-476.

[30] Ivanovic, Z. (2009) Hypoxia or *in situ* normoxia: the stem cell paradigm. J. Cell. Physiol. 219:271-275.

[31] Wayne, L. G., *et al.* (1982) Glyoxylate metabolism and adaptation of *Mycobacterium tuberculosis* to survival under anaerobic conditions. Infect. Immun. 37:1042–1049.

[32] Sherman, D. (2001) Regulation of the *Mycobacterium tuberculosis* hypoxic response gene encoding α-crystallin. PNAS. June, 98(13): 7534-7539. DOI: 10.1073.

[33] Fang, X. *et al.* (2012) Modeling Phenotypic Metabolic Adaptations of *Mycobacterium tuberculosis* H_{37}Rv under Hypoxia. PLoS Comput Biol. 8(9): e1002688. DOI:10.1371/journal.pcbi.1002688.

[34] Betts, J., *et al.* (2006) Miniature bioreactors: current practices and future opportunities. Microbial Cell Factories. 5:21. DOI: 10.1186/1475-2859-5-21.

[35] San, K. Method title: Bioreactors in biochemical and metabolic engineering. RICE University, Institute of bioscience and bioengineering, NIH biotechnology research training program. Available from: http://www.bioc.rice.edu/bios576.nih_bioreactor/NDL_Bioreactor%20Page.htm.

[36] Brecht, R. (2009) Disposable bioreactors: Maturation into pharmaceutical glycoprotein manufacturing. Adv Biochem Engin/biotechnol. 115: 1-31. DOI: 10.1007/10_2008_33.

[37] Paek, K., *et al*. (2001) Applications of bioreactors for large scale micropropagation systems of plants. In Vitro Cell. Dev. Biol.-Plant. 37: 149-157. DOI: 10.1079/IVP2000149.

[38] Schiigerl, K., *et al.* (1987) Bioreactors. In: Preile, P.; Faust, U.; Sittig, W.; Sukatsch, D. A., eds. Basic biotechnology. 179-224.

[39] Hooker, B. S., *et al.* (1990) Cultivation of plant cells in a stirred vessel: effect of impeller design. Biotechnol. Bioeng. 35: 296-304.

[40] Dietrich, G., et al. (2002) Cultivation of *Mycobacterium* bovis BCG in bioreactors. Journal of Biotechnology. 96: 259-270.

[41] Leathers, R. R., *et al.* (1995) Automation of the bioreactor process for mass propagation and secondary metabolism. In: Aiken-Christie, J.; Kozai, T.; Smith, M. A. L., eds. Automation and environmental control in plant tissue culture. Dordrecht: Kluwer Academic Publishers. 187-214.

[42] Wolfe, L. *et al.* (2010) Proteomic Definition of the cell wall of Mycobacterium tuberculosis. Journal of Proteome Research. 9: 5816-5826. DOI: 10.1021/pr1005873.

[43] Soejima, T., *et al.* (2009) Discrimination of live, anti-tuberculosis agent-injured, and dead *Mycobacterium tuberculosis* using flow cytometry. FEMS Microbiol Lett 294: 74-81. DOI: 10.1111/j.1574-6968.2009.01549.x.

[44] Cho, S. (2006) ICAT-based comparative proteomic analysis of non-replicating persistent *Mycobacterium tuberculosis*. Tuberculosis. 86: 445-460.

[45] Rustad, T. R., *et al.* (2008) The Enduring Hypoxic Response of *Mycobacterium tuberculosis*. PLoS ONE. 3(1): e1502. DOI:10.1371/journal.pone.0001502.

[46] Julian, E., *et al.* (2010) Microscopic cords, a virulence-related characteristic of *Mycobacterium tuberculosis*, are also present in nonpathogenic mycobacteria. Journal of Bacteriology. April, 192(7): 1751-1760.

[47] Masaki, S., *et al.* (1990) Effects of Tween 80 on the growth of *Mycobacterium avium* Complex. Microbiol. Immunol. 34(8): 653-663.

[48] Cunningham, A., *et al.* (1998) Mycobacterial stationary phase induced by low oxygen tension: Cell wall thickening and localization of the 16-kilodalton alpha-crystallin homolog. J. Bacteriol. 180(4): 801.

[49] Galagan, J., *et al.* (2013) The *Mycobacterium tuberculosis* regulatory network and hypoxia. Nature. 499(178) DOI:10.1088/nature12337.

[50] Lewis, C., *et al.* (2014) Mass and density measurements of live and dead gram-negative and gram-positive bacterial populations. Appl Environ Microbiol. June, 80(12): 3622-3631. DOI: 10.1128/AEM.00117-14.

[51] Clynes, M. M. (1979) Effect of culture conditions on the survival of mammalian cells without medium change. Biochem. Soc. Trans. 7: 30-32.

[52] Hunter, R., *et al.* (2006) The role of trehalose dimycolate (cord factor) on morphology of virulent *M. tuberculosis in vitro*. Tuberculosis. 86: 349-356.

[53] Peterson, B., *et al.* (2012) Bacterial cell surface damage due to centrifugation compaction. Applied and Environmental Microbiology. Jan., 78(1): 120-125.

[54] Rampersad, S. (2012) Multiple applications of alamar blue as an indicator of metabolic function and cellular health in cell viability bioassays. Sensors. 12(9): 12347-12360. DOI: 10.3390/s120912347.

[55] Rahman, I., *et al.* (1994) Methionine uptake and cytopathogenicity of viable but nonculturable *Shigella dysenteriae* type 1. Appl. Envirion. Microbiol. 60: 3573-3578.

[56] Riss T. L., *et al*. Cell Viability Assays. 2013 May 1 [Updated 2015 Jun 29]. In: Sittampalam GS, Coussens NP, Nelson H, et al., editors. Assay Guidance Manual [Internet]. Bethesda (MD): Eli Lilly & Company and the National Center for Advancing Translational Sciences; 2004-. Available from: http://www.ncbi.nlm.nih.gov/books/NBK144065/.

[57] Hartman T., *et al.* (2014) Succinate Dehydrogenase is the Regulator of Respiration in *Mycobacterium tuberculosis*. PLoS Pathog. 10(11): e1004510. DOI: 10.1371/journal.ppat.1004510.

[58] Koul A., *et al.* (2008) Diarylquinolines are bactericidal for dormant mycobacteria as a result of disturbed ATP homeostasis. J Biol Chem. 283: 25273–25280.

[59] McGillivray, A., *et al.* (2015) The *Mycobacterium tuberculosis* Clp gene regulator is required for *in vitro* reactivation from hypoxia-induced dormancy. Journal of Biological Chemistry. 290(4): 2351-2367. DOI: 10.1074/jbc.M114.615534.

[60] Sassetti C. M., *et al.* (2003) Genes required for mycobacterial growth defined by high density mutagenesis. Mol Microbiol. 48: 77–84.

[61] Meier T., *et al.* (2007) A tridecameric c ring of the adenosine triphosphate (ATP) synthase from the thermoalkaliphilic Bacillus sp. strain TA2.A1 facilitates ATP synthesis at low electrochemical proton potential. Mol Microbiol. 189: 5895–5902.

[62] Ordway, D., *et al.* (2001) Animal models of *mycobacterium* infection. Curr. Protoc. Immunol. chapter: unit-19.5. DOI: 10.1002/0471142735.im1905s30.

[63] The global plan to stop TB. WHO. Available from: http://www.stoptb.org/global/plan/.

[64] Graham, J. (2013) Bacterial volatiles and diagnosis of respiratory infection. Advances in Applied Microbiology. 82: 29-52. DOI: 10.1016/B978-0-12-407679-2.00002-8.

[65] Mann, F., *et al.* (2009) Edaxaditene: a new bioactive diterpene from *Mycobacterium tuberculosis*. Journal of American Chemical Society. 131: 17526-17527.

[66] Weetjens, B., *et al*. (2009) African pouched rat for the detection of pulmonary tuberculosis in sputum samples. Int J Tuberc Lung Dis. 13: 737-743.

[67] McNerney, R., *et al.* (2012) Production of volatile organic compounds by mycobacteria. FEMS Microbiol Lett. 328: 150-156.

[68] Fu, X., *et al.* (2011) A novel microreactor approach for analysis of ketones and aldehydes in breath. Analyst. 136: 4662-4666. DOI: 10.1039/c1an15618g.

[69] Li, M., *et al.* (2012) Preconcentration and analysis of trace volatile carbonyl compounds. Anal Chem. 84: 1288-1293. DOI: 10.1021/ac2021757.

[70] Uragami, T., *et al.* (2001) Removal of dilute volatile organic compounds in water through graft copolymer membranes consisting of poly(alkylmethacrylate) and poly(dimethylsiloxane) by pervaporation and their membrane morphology. Journal of Membrane Science. 187: 255-269.

[71] Laaks, J., *et al.* (2011) Solvent-free microextraction techniques in gas chromatography. Anal Bioanal Chem. 402: 565-571. DOI: 10.1007/s00216-011-5511-4.

7.0 Appendix I

7.1 Continuous density gradient centrifugation of normoxic and hypoxic cultures

We wanted to determine separation efficiency when up-scaling to larger cellular biomass products harvested from the bioreactors. This was done using a continuous Percoll density gradient formed with greater separation surface area in a 50ml conical tube. Using a Hoeffer SG30 density gradient maker, the gradient column was formed to a final volume of 30mls at 0.15M saline using 15mls each of the stock Percoll as the heavy solution and 0.3M saline as the light solution (Figure 7.1.1). Again, 1ml of cell suspension from each of the bioreactor replicates was carefully overlaid on to the top of the gradient column and centrifuged at 400xg for 15min in a table top centrifuge and the banded cell fractions extracted by pipetting and transferred to a 1.7ml microcentrifuge tube and spun down to pellet at 14K RPM for 10 minutes in a microcentrifuge. The supernatant was decanted and the

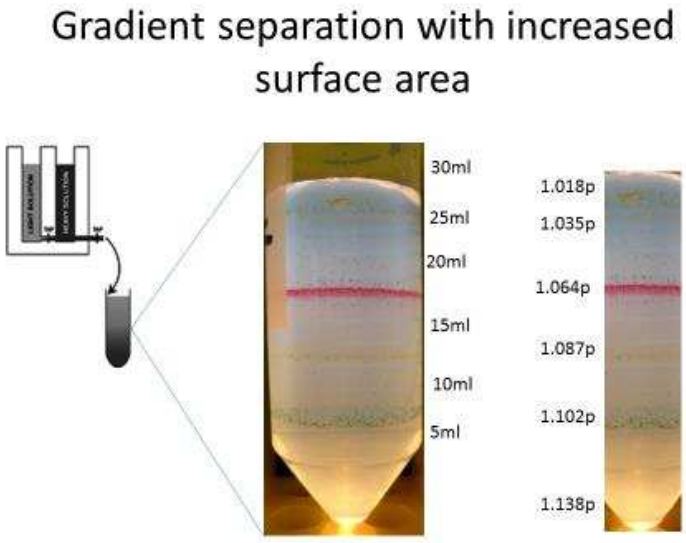

Figure 7.1.1

Continuous density gradient. Using a Hoeffer SG30 density maker, 30mls of a continuous gradient was prepared from 15mls each of Percoll SIP and 0.3M saline. Density marker beads were added at the top of the gradient and centrifuged at 400xg for 15 minutes in a table top centrifuge for density equilibrium.

pellet was washed with 1ml of PBS media and spun down to pellet at 14K RPM for 10 minutes in a microcentrifuge. The supernatant was decanted and the washed pellet was re-suspended in 1ml of GAS media, serially diluted and plated in triplicate for CFU and counted via the P-H method.

In order to interrogate the efficiency of a density gradient separation for use of separating larger sample sizes, 1ml of each of the three replicate pairs, three Biological replicates of normoxic and three replicates of hypoxic culture were overlaid onto the top of a 30ml continuous gradient and spun down by a soft centrifugation of 400xg for 15 minutes. All six samples showed the same trend of forming a loose band at around the 10ml mark of the 50ml conical tube. This region equates to about a density of 1.095 g/ml Percoll solution (Figure 7.1.2 A). A 1ml extract was carefully taken by pipetting around the core of the loose band, of each sample, and transferred to a 1.7ml Eppendorf tube. The extracts were then centrifuged via a microcentrifuge at 14K RPM for 10 minutes in

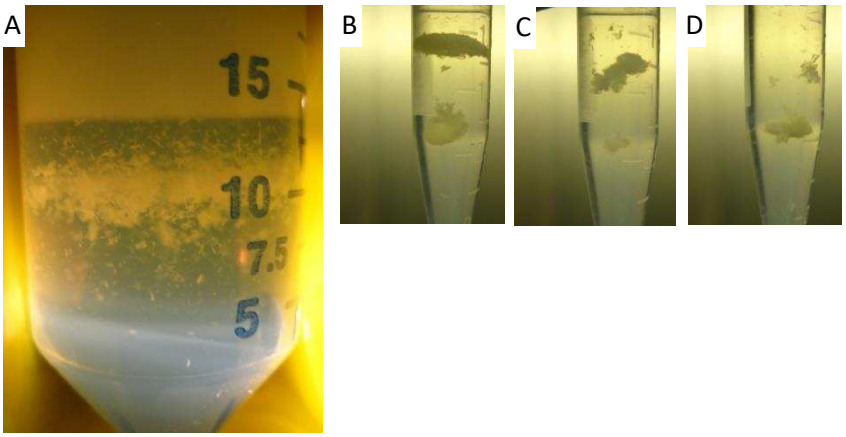

Figure 7.1.2

Continuous density centrifugation of *Mtb* $H_{37}Rv$ propagated in bioreactors with and without oxygen tension. A) Primary centrifugation of 1ml of cells obtained from bioreactor products, laid onto the top of a 30ml continuous Percoll density gradient. The 10ml mark of the 50ml conical tube represents 1.095 g/ml Percoll solution. B) Secondary centrifugation from 1ml of cells extracted from the primary centrifugation. This fractionation contains a neat uniform band of cells and a globular form of cells in the upper and lower regions of the tube. C) Secondary centrifugation from 1ml of cells extracted from the primary centrifugation. This fractionation contains a globular formation of cells and an irregular globular form of cells in the upper and lower regions of the tube. D) Secondary centrifugation from 1ml of cells extracted from the primary centrifugation. This fractionation contains an irregular globular of cells and a globular formation form of cells in the upper and lower regions of the tube.

order to pellet the cell extract to prepare for washing. However, after centrifugation, a secondary cell fractionation took place (Figure 7.1.2 B, C and D). Each of the six samples formed two additional fractions. This observation did not seem to be conditional to the growth conditions the cells originated from. Each fraction being either a nice tight band to an irregular globular shape. Also, all fractions seemed to be unique in size as according to the other. Of each of the six samples, now containing an upper and lower fraction, each were carefully extracted by pipetting

and washed with PBS. Each of the twelve cell extracts were resuspeded in 1ml GAS and plated for CFUs and counted via P-H method.

P-H counting was performed using a cell counting hemocytometer and 100x oil immersion light microscopy. Here the P-H cell counts between the normoxic and hypoxic samples were pooled together and the upper extracts of the secondary fractionation contained an average of $4.57x10^9$ cells/ml, while the lower extracts of the secondary fractionation contained $1.15x10^8$ cells/ml (Table 7.1.1). CFU counting was performed after 16 days of incubation at 37°C on 7H11 agar. Here the CFU counts between the normoxic and hypoxic replicates were pooled together and the upper extracts of the secondary fractionation contained an average of $1.11x10^7$ CFU/ml, while the lower extracts of the secondary fractionation contained $2.24x10^7$ CFU/ml (Table 7.1.1). This equates to the upper extracts only being 0.24% viable on average, and the lower extracts coming in at 19.7% viable on average, as compared to the unseparated bioreactor control with 4.20% viability with $1.73x10^8$ cells/ml and $7.28x10^6$ CFU/ml (Table 7.1.1).

Table 7.1.1

Viability of upper and lower secondary fractions obtained through continuous density centrifugation of cell extracts of the primary density centrifugation of *Mtb* $H_{37}Rv$ propagated in bioreactors with and without oxygen tension. Each fraction and unseparated control is the average of the pooled viability data of both normoxic and hypoxic cultures.

Fraction	Petroff-Hausser (cells/ml)	Colony Forming Units (CFU/ml)	Percent Viability	FOLD
Upper extract	$4.57x10^9$ (StDev $2.95x10^9$)	$1.11x10^7$ (StDev $9.8x10^6$)	0.24%	411.71
Lower extract	$1.15x10^8$ (StDev $5.08x10^7$)	$2.24x10^7$ (StDev $2.12x10^7$)	19.48%	5.13
Unseparated Control	$1.73x10^8$ (StDev $1.28x10^8$)	$7.28x10^6$ (StDev $5.76x10^6$)	4.21%	23.76

Using a continuous density gradient in an effort to upscale our efforts for the enrichment of viable cells did not provide reproducible banding results as compared to using a discontinuous gradient. Here the banding was

confluent through all six replicates, regardless of culture conditions (Figure 7.1.2). Furthermore, the phenomenon of a secondary fractionation was observed entirely by accident. Once the cellular fractions were extracted from the gradient column for each sample, the 1ml extract was transferred to a 1.5ml Eppendorf tube and centrifuged in a micro centrifuge at 14k RPM for ten minutes. This is always done to pellet the cells and remove the supernatant to wash the cells with PBS in order to remove residual Percoll solution. However, it was only the extracts from the larger continuous gradient column that formed this pattern. No extracts from the discontinuous gradient columns formed a secondary fractionation. From the discontinuous columns, the extracts pelleted tightly to the bottom of the tube.

From the continuous density gradient column extracts, the phenomenon of the secondary fractionation showed an increase in variability between the upper and lower extracts seemingly regardless of culture conditions or replicate reactor run. However, they did show consistency in that the lower fractions were almost 100-fold higher than the upper fraction in terms of viability (Table 7.1.1). In this case, the unseparated control is the pooled data of viability between the three replicate pairs and is consistent with the viability of the test culture control; roughly 3-4% viable (Table 7.1.1). Only this fractionation trend is in reverse as to what was seen by the test culture. Specifically, the upper fractions contained higher viability and the bottom fraction was barely viable at all, comparatively. Thus, we conclude that the discontinuous density gradient method is more ideal for viability enrichment of a culture of *Mtb*.

7.2 Volatile organic compound analysis

Perhaps the most intuitively appealing approach to rapid point of care diagnosis of specific bacterial infections is the analysis of patient breath, especially for respiratory infections [64]. It has been shown previously that it is possible to identify infecting microorganisms based on the volatile metabolites they are known to produce. Our knowledge of the volatile organic compounds (VOC) produced by bacteria is relatively limited, however a great amount of groundwork is being paved to identify the bacterial “fingerprints” that can establish a novel and rapid diagnostic technique [64]. Recently specific volatiles including three diterpenes have been described for tuberculosis, one of which is called Iso-tuberculosinol that was shown to block phagosome maturation in infected macrophages and is only produced in standard media when magnesium levels are reduced [65]. Furthermore, olfactory sensing by African pouch rats suggest that animals conditioned to detect headspace

gases from *Mtb* can identify infected sputum samples taken from patients with pulmonary tuberculosis [66]. McNerney and colleagues (2012) sought out to determine a potential VOC fingerprint of BCG. In their work, BCG grown on LJ slants were incubated inside nalophan sampling bags, and the headspace analyzed via selected ion flow tube mass spectrometry (SIFT-MS) and thermal desorption gas chromatography mass spectrometry (TD-GC-MS). Using this method, they were able to determine potential markers that were only found from the LJ slants inoculated with BCG and were absent in the LJ controls. However, the compounds detected were not unique to mycobacteria [67].

Solid phase micro extraction (SPME) techniques have been a popular preconcentration method introduced over a decade ago as a rapid extraction technique for analysis of VOCs, overcoming the issue of ultra-trace compounds too diluted using gas bags during collection. However, the surface area of the SPME absorbent polymer is very small and may have limitations when sampling from human breath and distinguishing specific trace compounds from the host VOC profile [68]. In an effort to increase sensitivity by increasing the absorbent surface area, Micro-electro-mechanical-systems (MEMS) were designed. These preconcentration microreactors are fabricated from silicon wafers approximately half an inch in square length. Ion etching is used to create thousands of micropillars, 50umx50umx250um in dimension [69]. The micropillars of the MEMS chips are coated with poly-dimethylsyloxane (PDMS). PDMS membranes have been studied as a VOC-permselective membrane due to its high selectivity for organic compounds in water [70].

VOC sampling was collected from bioreactor cultures of *Mtb* H37Rv propagated as described in chapter 2. A MEMS wafer chip was placed inside a glass storage vial. At day 8 of incubation for both the normoxic and the hypoxic vessels, an extension tube was attached to the exhaust filter of the vessel and the outlet of the tube was placed inside the glass storage vial to expose the MEMS wafer to the exhaust gas of the vessel. The wafer was exposed to the exhaust for 5 minutes. After exposure, 1ml of 200 proof molecular grade ethanol was added to the vial. The vial was quickly closed with a screw cap, sealed with parafilm and the sample was stored at -20°C. A GAS media only blank was also sampled using the same method, one blank each of normoxic media conditions at 35% DO and hypoxic conditions of less than 6% DO, and stored same as above. A third blank was also sampled by simply opening the storage vial containing the MEMS chip and exposing the wafer to ambient room air and stored same as above. The treated MEMS wafers were then shipped to Dr. James Graham of the University of Louisville

for analysis via gas chromatography- mass spectrometry (GC-MS). However, the results of the analysis were less than ideal as no VOC compounds were detected. We hypothesized that perhaps the VOCs given off in the exhaust from the bioreactors were becoming trapped in the 0.2um exhaust filter of the CelliGen vessel. Thus we sought to perform VOC sampling from unfiltered bioreactor exhaust.

In order to expose the MEMS chip to unfiltered exhaust gas, a custom VOC collection tube was constructed in house (Figure 7.2.1). This was done using an Amicon Ultra centrifugal 15ml capacity, 50ml conical tube (Millipore). First, the filter insert was removed from the conical and the filter portion was cut off using a

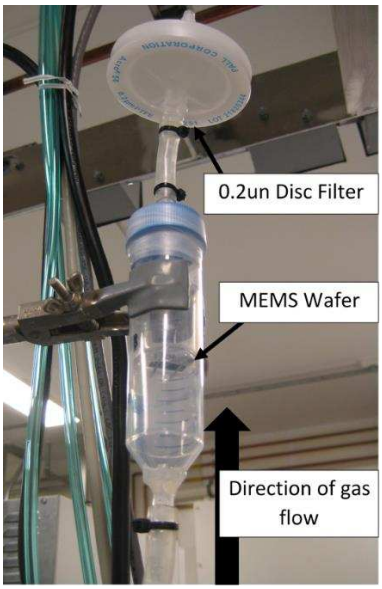

Figure 7.2.1

VOC sampling tube. The VOC sampling apparatus was constructed in house at Colorado State University. This was done using an Amicon Ultra 50ml conical, where the inner membrane filter was modified to create a basket that would hold a MEMS wafer in the direct flow of exhaust given off by the culture propagated in a sealed bioreactor.

Dremel tool with a rotary cutter. The rough edges were smoothed using the sander adaptor of the Dremel tool. This revealed a direct opening through the insert. Second, two 1cm lengths were cut from a paper clip and glued to the opening of the insert using a hot glue gun to create a “basket”. This was done to prevent the wafer from falling through the opening of the insert that was cut previously. Next, using a drill, a hole was created in the center of the 50ml conical screw cap and at the very bottom of the conical. A 1000ul graduated pipet tip (GeneMate) was then fitted through each opening, with the graduated ends pointing outward. Again a hot glue gun was used to glue the pipet tips to the conical and screw cap. Finally, the basket was inserted into the 50ml conical VOC

collection tube. Tubing was attached to the protruding pipet tips and sealed tight using small zip ties to allow gas flow to pass directly through the opening of the basket and exhaust out the top of the collection chamber. For a safety control check, the upper exhaust tube was closed with a clamp and the gas inlet line was attached to a compressor where the sampling chamber was lightly pressurized to detect any gas leaks. Any detected gas leaks around the glued junctions were then re-heated using the hot glue gun, smoothed and sealed, to ensure no unfiltered gas would escape the device.

The custom VOC sampling tube was washed in a shallow bath of 70% ethanol and allowed to air dry. A 0.2um filter was attached to the upper line on the screw cap lid. The lower gas inlet line was then attached to the regulator of a nitrogen gas tank and the sampling chamber was washed with a low flow of nitrogen gas to purge the room air from the chamber. Using a finger to close the exhaust port of the filter, the sampling chamber was again checked for gas leaks, in which none were detected. The gas inlet line was closed using a clamp and the sampling chamber disconnected from the nitrogen gas. The gas inlet line was attached to the overlay liquid addition port of the bioreactor and clamped to a stand positioned above the Bioflo 115 control unit to allow any condensation to fall back into the vessel. The screw cap of the sampling chamber was quickly removed and the MEMS chip carefully dropped into the basket inside the conical. The screw cap was reapplied and sealed with parafilm. The clamp on the inlet line was released and the main exhaust lines on the bioreactor were closed with clamps. This allowed for 100% of the exhaust gas from the bioreactor culture to be re-routed through the VOC sampling chamber and expose the MEMS wafer to unfiltered culture exhaust. The MEMS wafers were exposed to exhaust gas for 5 minutes. After exposure was complete, the clamps on the main bioreactor exhaust lines were opened and the VOC sampling line was closed using a tube clamp. The VOC sampling tube was removed from the stand and the screw cap quickly removed. Without touching the wafer, the basket was removed and the MEMS chip was dropped into a glass storage vial containing 200 proof molecular grade ethanol. Two inoculated GAS media only blank samples were also taken using the VOC sampling tube during normoxic and hypoxic conditions as previously stated. The storage vials containing the treated MEMS wafers were stored as described above and shipped to Dr. James Graham of the University of Louisville for analysis via GC-MS. However, again the VOCs were either absent for analysis or the concentration of the VOCs were too trace to be detected. Thus we sought to determine a different method for direct VOC sampling.

The method of SPME features a fused-silica fiber core coated with a 100um film of PDMS as the extraction phase. This method can be used for sampling from the liquid phase by direct immersion of the fiber or by headspace analysis. One major advantage to SPME is that no processing to elute the VOC sample is necessary, as the needle casing around the fiber can be directly inserted into the thermal desorption unit of the GC-MS analyzer [71]. The VOC sampling chamber, described previously, was modified to accept VOC collection via SPME (Sigma). Again, a drill was used to create an opening approximately 1in from the top of the of the 50ml conical, on its side. A rubber stopper was then taken from the crimp cap (Kimble-Chase) of a glass syringe vial and inserted into the opening as a re-sealable septum for the SPME needle to penetrate (Figure 7.2.2). The septum was then glued to the conical using a hot glue gun. A safety control check was performed as previously described.

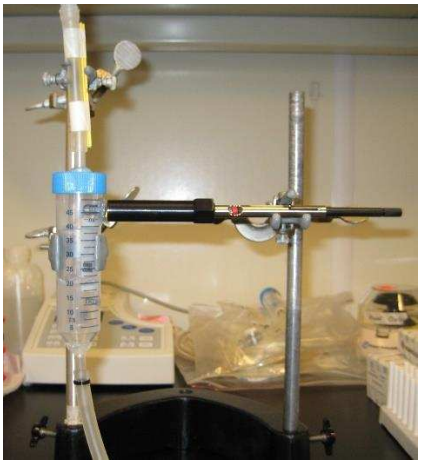

Figure 7.2.2

VOC-SPME sampling tube. The VOC sampling apparatus was modified by the addition of a septum to accept the insertion of a SPME needle for direct sampling of the exhaust given off from the bioreactor culture.

To condition the SPME fiber, the fiber assembly was loaded into the manual holder (Sigma) with the depth gage set to 2.5cm. After removing the AOC-20i auto injector unit from the injection port of a GC-2014 Gas Chromatography analyzer (Shimadzu), the SPME needle was inserted into the injection port and the PDMS coated fiber was protruded into the thermal desorption unit for conditioning at 250°C for 15 minutes. Once conditioning was complete, the fiber was retracted and removed from the GC and the fiber assembly was removed from the manual holder and placed in a 15ml conical for storage.

Prior to sampling, each fiber was protruded into 200 proof methanol for 15 minutes to elute and clean the PDMS coating (Figure 7.2.3). In addition, the SPME needle casing of the fiber was cleaned with filter paper soaked

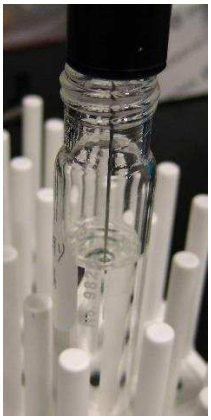

Figure 7.2.3

PDMS fiber cleaning. Prior to SPME insertion into the VOC sampling apparatus, the PDMS coating of the fiber is washed with 200 proof methanol. This cleaning elutes any compounds from the fiber and readies the coating for VOC saturation of the direct exhaust given off by the bioreactor culture.

in 70% ethanol immediately before needle penetration through the septum and into the sampling chamber. Using a stand adjacent to the VOC collection apparatus to stabilize the SPME holder, the PDMS coated fiber was protruded from the needle and locked into place with the fiber in the direct flow of the exhaust from the vessel culture. Three exposure times of 5 minutes, 4 hours, and 16 hours were taken from both the normoxic and hypoxic culture conditions as described above, as well as an unimmolated GAS media blank with DO conditions of 35% and less than 6%. VOC sampling was performed at day 8 of incubation, same as before (Figure 7.2.4). When the exposure time was complete, the PDMS fiber was retracted into the SPME needle, and the needle was removed from the sampling chamber while immediately cleaning the needle casing with filter paper soaked in 70% ethanol as it passed through the septa. The SPME needle containing the VOC treated PDMS coated fiber was removed from the manual holder assembly, placed in a 15ml conical and stored at -20°C. GC-MS analysis was performed by the Proteomics and Metabolomics (PMF) core facility at Colorado State University by Dr. Corey Broeckling.

To perform the data analysis, first all AIMDS data reports were imported into an Excel workbook and the features for each sampling were sorted by CAS number. Second, all duplicate features found between the GC blank report and the GAS media blank report were identified and removed from the list, leaving all suspected GAS media

only features. Finally, the same process was done to remove duplicate features between the GAS media blank and the exposure time points of both the normoxic and hypoxic culture conditions, leaving only suspected *Mtb* VOC features for each condition.

Figure 7.2.4

VOC-SPME sampling apparatus. During VOC sampling, the stabilizing stand holding the VOC sampling chamber is positioned above the vessel during VOC collection. The overhead positioning allows for any condensation that may build up within the tube to condense and drain back into the reactor vessel, preventing liquid splashing within the chamber and blockage of the exhaust flow.

For the normoxic bioreactor culture, the GC-MS results of the 5 minute exposure produced 887 features and after removing the reduced normoxic GAS media blank features, 229 features remained. The 4 hour exposure produced 2013 features and after removing the reduced normoxic GAS media blank features, 126 features remained. The 16 hour exposure produced 2651 features and after removing the reduced normoxic GAS media blank features, 115 features remained. For the hypoxic bioreactor culture, the 5 minute exposure PDMS coating on the SPME fiber was found to be damaged and stripped from the fiber prior to analysis, and thus deemed unusable. However, the 4 hour exposure produced 2558 features and after removing the reduced hypoxic GAS media blank features, 521 features remained. The 16 hour exposure produced 3028 features and after removing the reduced hypoxic GAS media blank features, 322 features remained. When interrogating the peak intensities of the remaining features between the three exposure periods, no direct differences were observed between exposure

time. However, looking at only the normoxic culture features, the 5 minute exposure time produced the greatest number of unique features once the blank features were removed. Perhaps indicating that a longer exposure time drowns out the low abundance features as the volatile equilibrium takes place. Therefore, all features from the normoxic cultures were analyzed, same as previously stated, by identifying features found in all three exposure times. This was also done for the hypoxic culture features from the 4 hour and 16 hour exposure times. This produced 3 unique features found in the normoxic culture, and 188 unique features found in the hypoxic culture. Of the 3 normoxic features, 2 of them were shared by the hypoxic features (Figure 7.2.5).

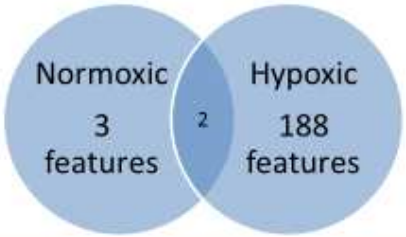

Shared Norm features	Shared Norm and Hypo features	Absent features in Hypoxia
Formamide, N-cyclohexyl-	Formamide, N-cyclohexyl-	
Cyclohexane, 1123-tetramethyl	Cyclohexane, 1123-tetramethyl	
5- Undecene, 2-methyl (Z)		5- Undecene, 2-methyl (Z)

Figure 7.2.5

GC-MS *Mtb* hypothesized unique features. After the removal of all blank features from the AIMDS reports, the exposure time points for each the normoxic and hypoxic vessel were pooled together. Any non-duplicate features were removed from the normoxic and hypoxic compound pools. The normoxic pools contained 3 unique features while the hypoxic pool contained 188 unique features, at which both pools shared 2 of the 3 normoxic features. Here the solitary unique feature present in only the normoxic pool is proposed as 5- Undecene, 2- methyl (z), which was not found in the hypoxic pool.

Of the unique features proposed in this study, these proposed compounds may be hypothesized VOC markers that may have their roots as intermediates in lipid biosynthesis and degradation. For instance, N-cyclohexyl formamide, according to the KEGG database, is an intermediate in the caprolactam degradation pathway of mycobacterium as an alcohol dehydrogenase involved in energy production and conversion. Here, we were able to describe a novel method of VOC sampling from *Mtb* propagated in bioreactors using oxygen tension as the variable. The advantage of using this system for VOC sampling is that the total flow of exhaust from the

sealed vessels can be re-routed to fully expose the gas to the VOC sampling method desired. Further interrogation of this technique may provide insight to the generation of a VOC profile of *Mtb* to be used in the development of a rapid, non-invasive, point of care breathalyzer diagnostic tool for the detection of TB infection, as well as perhaps even the detection of active and latent TB.

8.0 Supplemental Material

Vessel N1, Normoxic culture conditions.

The DO concentration (blue trend line) begins at 100% saturation decreases almost exponentially for approximately 65 hours. After approximately 55 hours the agitation (red trend line) begins to increase from 25 RPM to max 65 RPM at approximately hour 65 where it remains consistent for the remainder of the culture period. After approximately 65 hours, the DO concentration is maintained at 40% until approximately hour 110 where it drops to 35% and remains consistent for the remainder of the culture period. Temperature (green trend line) is kept constant at 37°C and the pH (pink trend line) starting at 6.6 remained relatively consistent, only rising slightly after approximately 180 hours. At the end of the monitoring trends after approximately 250 hours, the shutdown of the vessel via the control unit can be seen by an abrupt decrease in agitation and drastic increase of DO concentration.

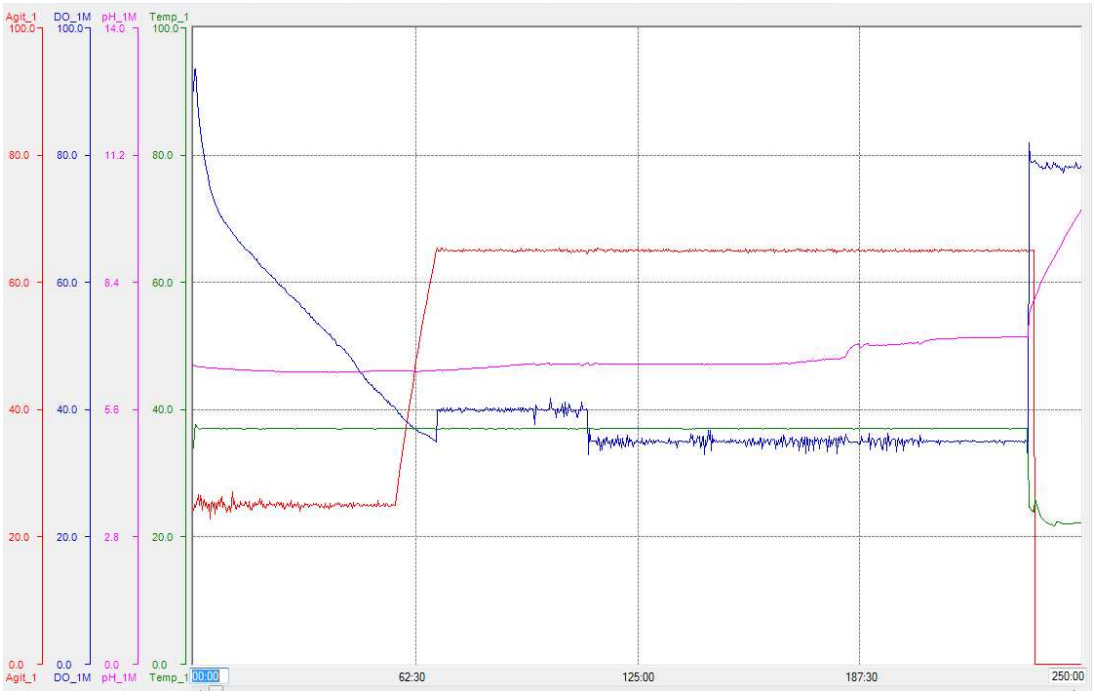

The CO_2 concentration (blue trend line) was not needed to maintain pH at 6.6 until approximately 90 hours. After approximately 70 hours the gas flow (red trend line) begins to increase and peaks after approximately 150 hours at 0.6 SLPM where it then decreses slightly and remains relatively consistent. No nitrogen (green trend line) was supplemented into the gas flow and the air (pink trend line) was seen to dramatically increase to 100% after 60 hours only to decrease to 60% until approximately 150 hours were another decrease is seen to about 30% where it remained. At the end of the monitoring trends after approximately 250 hours, the shutdown of the vessel via the control unit can be seen by an abrupt decrease in gas flow and breathing air concentration.

Vessel N2, Normoxic culture conditions.

The DO concentration (blue trend line) begins at 100% saturation decreases almost exponentially for approximately 67 hours. During this reactor run, the control unit had to be shut down and restarted due to pH probe issues as seen by the drastic increase of pH well beyond 14. The second half of the monitoring trend lines can be seen in the following graph. After approximately 67 hours the agitation (red trend line) begins to increase from 25 RPM to max 65 RPM at approximately hour 65 where it remains consistent for the remainder of the culture period. After approximately 65 hours, the DO concentration is maintained at 40% until approximately hour 110 where it drops to 35% and remains consistent for the remainder of the culture period. Temperature (green trend line) is kept constant at 37°C and the pH (pink trend line) starting at 6.6 remained relatively consistent.

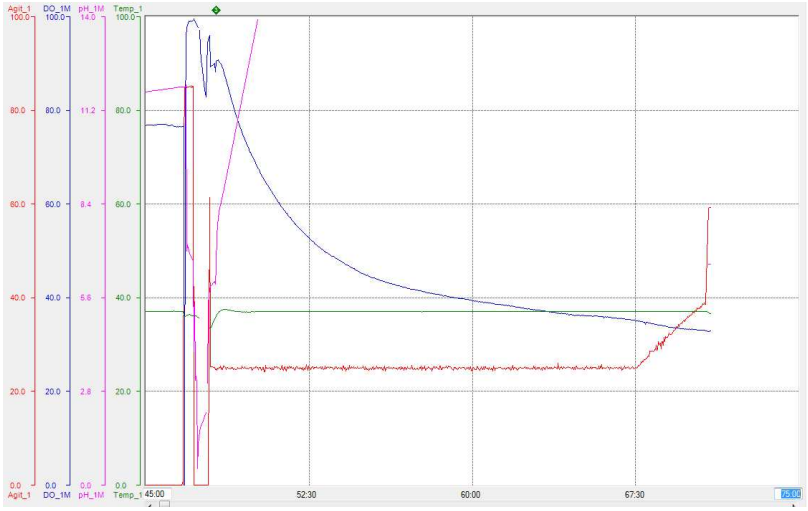

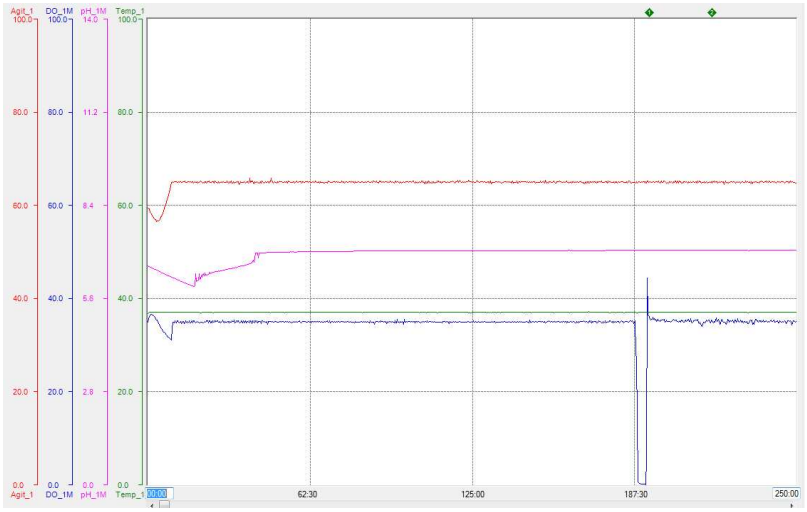

The CO_2 concentration (blue trend line) was maintained constant at 20%. After approximately 70 hours the gas flow (red trend line) begins to increase and peaks after approximately 150 hours where it then spikes high to approximately 3.2 and 3.5 SLPM at hour 190 and 220 and remains relatively consistent at 0.8 SLPM. No nitrogen (green trend line) was supplemented into the gas flow (even though 80% nitrogen can be seen over the first 70 hours, the gas flow was not initiated by the cascade control at that time) and the air (pink trend line) was seen to dramatically increase to 100% after 70 hours only to decrease to 60% until approximately 150 hours were another decrease is seen to about 30% where it remained. At the end of the monitoring trends after approximately 250 hours, the shutdown of the vessel via the control unit can be seen by an abrupt decrease in gas flow and breathing air concentration.

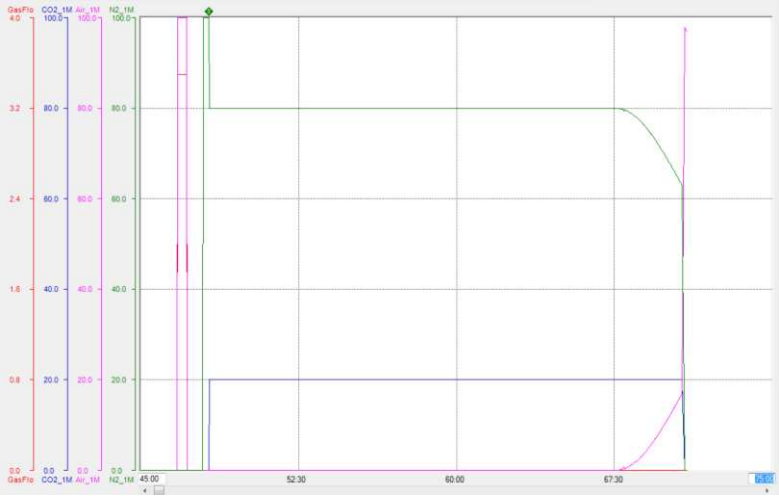

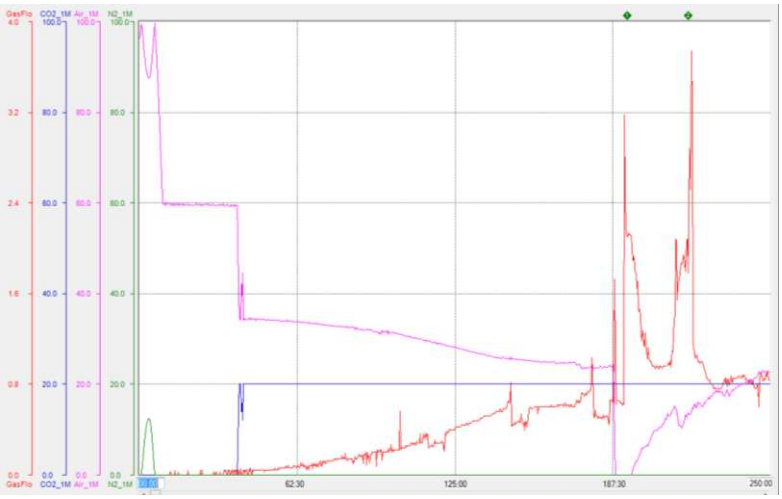

Vessel H1, Hypoxic culture conditions.

The DO concentration (blue trend line) begins at 100% saturation and rapidly decreases initially and almost linearly for approximately 180 hours. The agitation (red trend line) remained relatively constant at 25 RPM for the remainder of the culture period. After approximately 200 hours, the DO concentration spiked upward to approximately 60% (during this period the nitrogen gas tank ran empty and switched with a full spare nitrogen tank) where it then decreased to less than 20% and into hypoxic conditions by the end of the culture period. Temperature (green trend line) is kept constant at 37°C and the pH (pink trend line) starting at 6.6 remained relatively consistent. At the end of the monitoring trends after approximately 360 hours, the shutdown of the vessel via the control unit can be seen by an abrupt end of the trend lines.

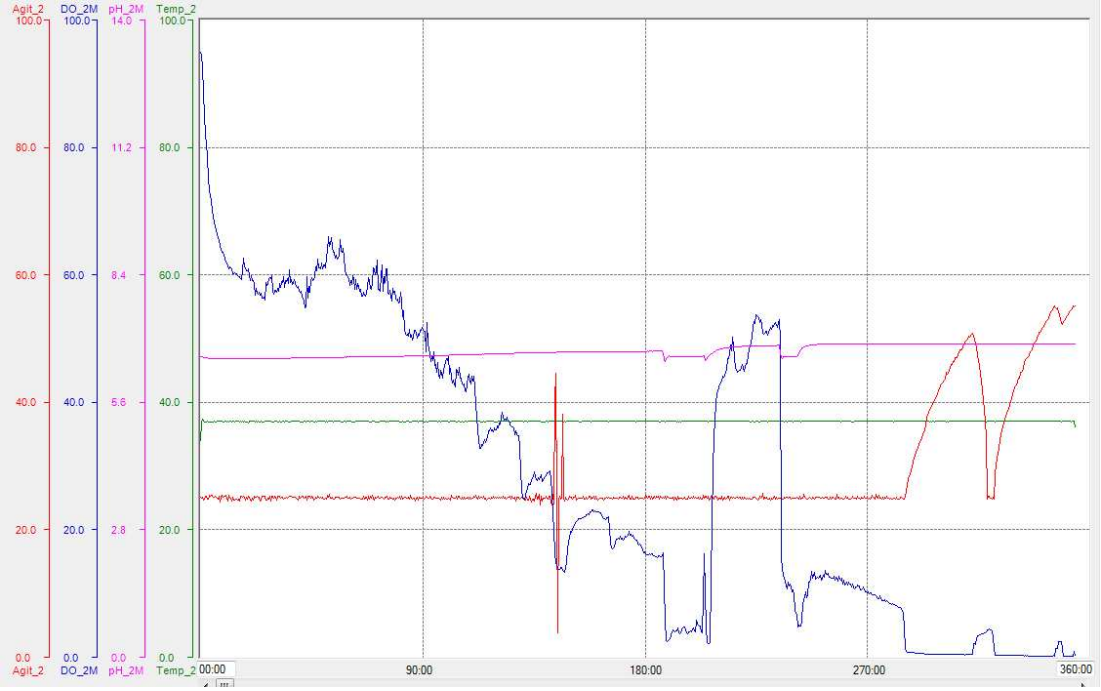

The CO_2 concentration (pink trend line) was not needed to maintain pH at 6.6 until approximately 80 to 180 hours and then again 200 hours for the remainder of the run, using 20% concentration in the gas flow. After approximately 190 hours the gas flow (red trend line) begins to increase and remain relatively consistent at 0.1 and 0.2 SLPM. Nitrogen (green trend line) was supplemented into the gas flow at 80% corresponding with the addition of CO_2 at the same time periods, and the air (blue trend line) was not seen until approximately 300 hours where it switches inversely with the nitrogen concentration for the remaining 60 hours of incubation. At the end of the monitoring trends after approximately 360 hours, the shutdown of the vessel via the control unit can be seen by an abrupt decrease in gas flow and breathing air concentration.

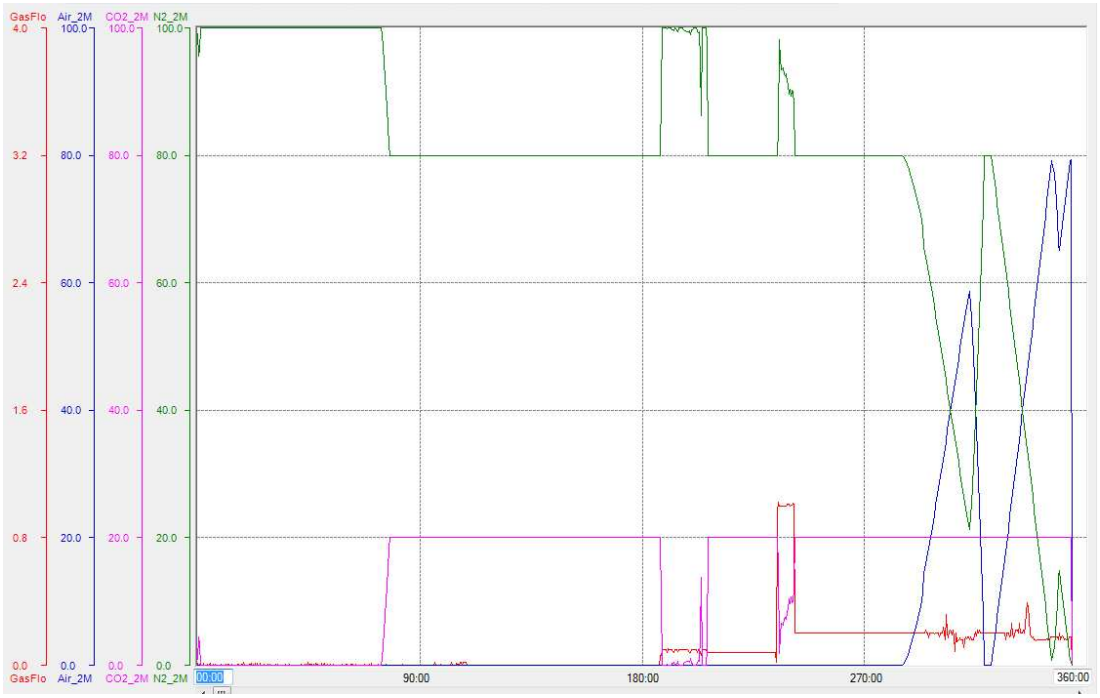

Vessel H2, Hypoxic culture conditions.

No DO concentration (blue trend line) can be seen initially during the first approximately 70 hours, however the DO concentration was initially 100%. During this reactor run, the control unit had to be shut down and restarted due to pH and DO probe issues as seen by absence of the trends. The second half of the monitoring trend lines can be seen in the following graph. After approximately 67 hours the agitation (red trend line) begins to increase from 25 RPM to max 65 RPM at approximately hour 65 where it remains consistent until approximately 90 hours where it decreased abruptly to 25 RPM for about 100 hours and then gradually increased for the remainder of the culture period. After approximately 65 hours, the DO concentration is maintained at 40% until approximately hour 90 where it rapidly drops to less than 1% and remains consistent for the remainder of the culture period. Temperature (green trend line) is kept constant at 37°C and the pH (pink trend line) starting at 6.6 remained relatively consistent.

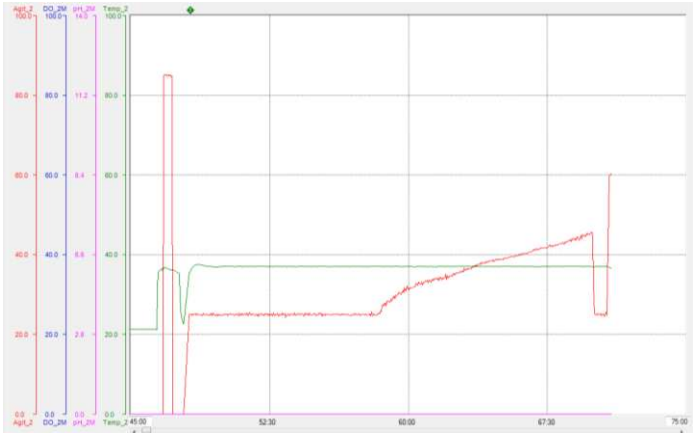

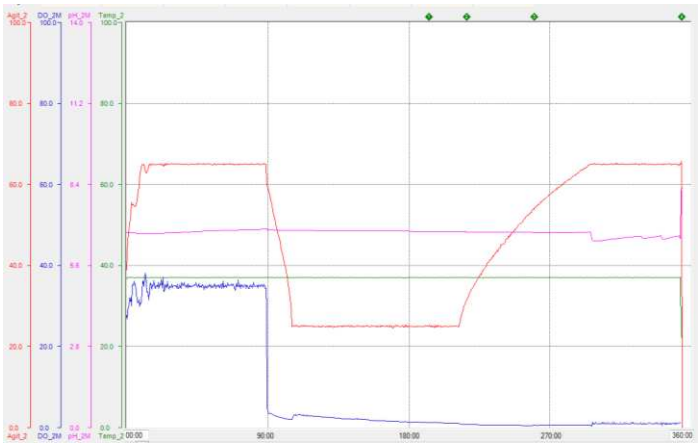

The CO_2 concentration (pink trend line) was not needed to maintain pH at 6.6 until approximately 90 hours where is remained constant at 20% of the gas flow. After approximately 70 hours the gas flow (red trend line) begins to increase very slightly but remain at less than 0.1 SLPM. No nitrogen (green trend line) was supplemented into the gas flow while the gas flow was implemented and the air (blue trend line) was also not supplemented into the gas flow while the gas was initiated. At the end of the monitoring trends after approximately 360 hours, the shutdown of the vessel via the control unit can be seen by an abrupt decrease in gas flow and breathing air concentration.